Pharmacological Research 79 (2014) 34–74

Contents lists available at ScienceDirect

Pharmacological Research

journal homepage: www.elsevier.com/locate/yphrs

Invited Review

The ErbB/HER family of protein-tyrosine kinases and cancer

Robert Roskoski Jr.*

Blue Ridge Institute for Medical Research, 3754 Brevard Road, Suite 116, Box 19, Horse Shoe, NC 28742, USA

ARTICLE INFO

Article history:
Received 7 November 2013
Accepted 8 November 2013

This paper is dedicated to the memory of Dr. John W. Haycock (1949–2012) who prompted the author to write a review on the treatment of malignant diseases with targeted protein kinase inhibitors.

Chemical compounds studied in this article:
Afatinib (PubChem CID: 10184653)
Docetaxel (PubChem CID: 148124)
Doxorubicin (PubChem CID: 31703)
5-Fluorouracil (PubChem CID: 3385)
Erlotinib (PubChem CID: 176870)
Gefitinib (PubChem CID: 123631)
Lapatinib (PubChem CID: 208908)
Oxaliplatin (PubChem CID: 5310940)
Pemetrexed (PubChem CID: 446556)
Regorafenib (PubChem CID: 11167602)

Keywords:
Breast cancer
Colorectal cancer
Monoclonal antibody therapy
Non-small cell lung cancer
Small molecule protein kinase inhibitor
Targeted cancer therapy

ABSTRACT

The human epidermal growth factor receptor (EGFR) family consists of four members that belong to the ErbB lineage of proteins (ErbB1–4). These receptors consist of a glycosylated extracellular domain, a single hydrophobic transmembrane segment, and an intracellular portion with a juxtamembrane segment, a protein kinase domain, and a carboxyterminal tail. Seven ligands bind to EGFR including epidermal growth factor and transforming growth factor α, none bind to ErbB2, two bind to ErbB3, and seven ligands bind to ErbB4. The ErbB proteins function as homo and heterodimers. The heterodimer consisting of ErbB2, which lacks a ligand, and ErbB3, which is kinase impaired, is surprisingly the most robust signaling complex of the ErbB family. Growth factor binding to EGFR induces a large conformational change in the extracellular domain, which leads to the exposure of a dimerization arm in domain II of the extracellular segment. Two ligand-EGFR complexes unite to form a back-to-back dimer in which the ligands are on opposite sides of the aggregate. Following ligand binding, EGFR intracellular kinase domains form an asymmetric homodimer that resembles the heterodimer formed by cyclin and cyclin-dependent kinase. The carboxyterminal lobe of the activator kinase of the dimer interacts with the amino-terminal lobe of the receiver kinase thereby leading to its allosteric stimulation. Downstream ErbB signaling modules include the phosphatidylinositol 3-kinase/Akt (PKB) pathway, the Ras/Raf/MEK/ERK1/2 pathway, and the phospholipase C (PLCγ) pathway. Several malignancies are associated with the mutation or increased expression of members of the ErbB family including lung, breast, stomach, colorectal, head and neck, and pancreatic carcinomas and glioblastoma (a brain tumor). Gefitinib, erlotinib, and afatinib are orally effective protein-kinase targeted quinazoline derivatives that are used in the treatment of ERBB1-mutant lung cancer. Lapatinib is an orally effective quinazoline derivative used in the treatment of ErbB2-overexpressing breast cancer. Trastuzumab, pertuzumab, and ado-trastuzumab emtansine, which are given intravenously, are monoclonal antibodies that target the extracellular domain and are used for the treatment of ErbB2-positive breast cancer; ado-trastuzumab emtansine is an antibody-drug conjugate that delivers a cytotoxic drug to cells overexpressing ErbB2. Cetuximab and panitumumab are monoclonal antibodies that target ErbB1 and are used in the treatment of colorectal cancer. Cancers treated with these targeted drugs eventually become resistant to them. The role of combinations of targeted drugs or targeted drugs with cytotoxic therapies is being explored in an effort to prevent or delay drug resistance in the treatment of these malignancies.

Contents

Abbreviations: ADCC, antibody-dependent cellular cytotoxicity; ado-trastuzumab emtansine, ado-trastuzumab-DM1; AL, activation loop; AR, amphiregulin; BTC, betacellulin; C-spine, catalytic spine; CAQ, 4-(3-chloroanilino) quinazoline; CDK, cyclin-dependent kinase; CNS, central nervous system; CRC, colorectal cancer; EC, extracellular; EGFR, epidermal growth factor receptor; EPG, epigen; EPR, epiregulin; FDA, United States Food and Drug Administration; FISH, fluorescent *in situ* hybridization; HB-EGF, heparin-binding epidermal growth factor-like growth factor; Nrg, neuregulin; JM, juxtamembrane; mAb, monoclonal antibody; LE, ligand efficiency; LipE, lipophilic efficiency; NSCLC, non-small cell lung cancer; PI3K, phosphatidylinositol 3-kinase; PK, protein kinase; PLC, phospholipase C; PTEN, phosphatase and tensin homolog; R-spine, regulatory spine; TGFα, transforming growth factor α; TM, transmembrane; VEGFR, vascular endothelial growth factor receptor; MW, molecular weight.

* Tel.: +1 828 891 5637; fax: +1 828 890 8130.
E-mail address: rrj@brimr.org

1043-6618/$ – see front matter © 2013 Elsevier Ltd. All rights reserved.
http://dx.doi.org/10.1016/j.phrs.2013.11.002

1. Introduction

The ErbB/HER protein-tyrosine kinases, which include the epidermal growth factor receptor, are among the most studied cell signaling families in biology [1]. Cohen initiated this line of investigation and described epidermal growth factor (EGF), its receptor (EGFR), and its biochemical actions [2]. He discovered that the EGF receptor was a protein-tyrosine kinase, which was a revolutionary finding at the time (see Ref. [3] for a historical review). Cohen et al. found that a solubilized 170 kDa polypeptide contains both EGF binding activity and protein kinase activity [4]. EGFR was also the first receptor that provided evidence for a relationship between receptor overexpression and cancer [5]. EGFR is among the most studied receptor protein-tyrosine kinases owing to its general role in signal transduction and in oncogenesis.

The human protein kinase family consists of more than 500 members thereby making it one of the largest gene families [6]. These enzymes catalyze the following reaction:

$$MgATP^{-1} + protein{-}OH \rightarrow Protein{-}OPO_3^{2-} + MgADP + H^+$$

Based upon the nature of the phosphorylated —OH group, these proteins are classified as protein-serine/threonine kinases (385 members), protein-tyrosine kinases (90 members), and tyrosine-kinase like proteins (43 members). Moreover, there are 106 protein kinase pseudogenes. Of the 90 protein-tyrosine kinases, 58 are receptor and 32 are non-receptor kinases. A small group of dual-specificity kinases including MEK1 and MEK2 catalyze the phosphorylation of both tyrosine and threonine in target proteins; dual-specificity kinases possess molecular features that place them within the protein-serine/threonine kinase family. Protein phosphorylation is the most widespread class of post-translational modification used in signal transduction. Families of protein phosphatases catalyze the dephosphorylation of proteins thus making phosphorylation–dephosphorylation an overall reversible process [7].

Protein kinases play a predominant regulatory role in nearly every aspect of cell biology [6]. They regulate apoptosis, cell cycle progression, cytoskeletal rearrangement, differentiation, development, the immune response, nervous system function, and transcription. Moreover, dysregulation of protein kinases occurs in a variety of diseases including cancer, diabetes, and autoimmune, cardiovascular, inflammatory, and nervous disorders. Considerable effort has been expended to determine the physiological and pathological functions of receptor protein-kinase signal transduction pathways during the past 30 years.

2. Overview of the ErbB/HER protein kinase family and their ligands

2.1. ErbB protein kinases

The human EGF receptor family consists of four members (HER1–4) that belong to the ErbB lineage of proteins (ErbB1–4). This family of receptors is ubiquitously expressed in epithelial, mesenchymal, and neuronal cells and their cellular progenitors. The

gene symbol, *ERBB*, is derived from the name of the avian viral erythroblastosis oncogene to which these receptors are related. Human gene symbols generally are italicized with all letters in uppercase (*EGFR*). Italics are not necessary in gene catalogs or lists. Protein designations are the same as the gene symbol, but are not italicized with the first letter in uppercase and the remaining letters in lowercase (Egfr). Gene names often possess synonyms. Those for *EGFR* include *ERBB*, *ERBB1*, and *HER1*. *ERBB1* refers to the erythroblastosis virus, and *HER1* refers to the human *EGFR* receptor 1. For mice and rats, gene symbols generally are italicized, with only the first letter in uppercase and the remaining letters in lowercase (*Egfr*). Protein designations are the same as the gene symbol, but they are not italicized (Egfr). See Ref. [8] for human, Ref. [9] for mouse, and Ref. [10] for rat gene nomenclature guidelines.

For the four members of the human epidermal growth factor receptor gene family, we have the following designations: (i) *EGFR*/*ERBB1*/*HER1*, (ii) *ERBB2*/*HER2*/*NEU*, (iii) *ERBB3*/*HER3*, and (iv) *ERBB4*/*HER4*. The HER designation is commonly, but not exclusively, used in clinical papers and reports. Schechter et al. found that the *Neu* oncogene, which was induced in rats by ethylnitrosourea, is related to the rat *Erbb2* gene of the EGF receptor family [11]. This finding provided another clue on the potential role of the ErbB family of receptors in the pathogenesis of cancer, and *NEU* is occasionally used in human gene nomenclature. Although these recommendations are not universally followed, the correct meanings are generally unambiguous. For example, the human epidermal growth factor receptor protein is most often written as EGFR and not Egfr.

The human *ERBB* genes are found on four different chromosomes. Null mutations of any of the *Erbb* genes in mice result in embryonic or perinatal lethality [12–14]. Knockout of the *Erbb1* gene results in gastrointestinal, skin, and lung defects [15]. Threadgill et al. reported that the nature of the defects in *Erbb1* null mice depends upon the genetic background [16]. On a 129/Sv background, homozygous mutants died at mid-gestation due to placental defects; on a CD-1 background, the mutants lived for up to three weeks and showed abnormalities in skin, kidney, brain, liver, and gastrointestinal tract. Rajagopalan et al. reported that selective disruption of adult cardiac ErbB1 receptor-mediated signaling in mice, along with compromised ErbB2 function, leads to compromised cardiac function at rest and during stress [14]. Hearts of *Erbb2*- or *Erbb4*-mutant mice [17,18] fail to develop normally and the mice exhibit an irregular heart beat. Cardiac development most likely involves an inductive signal from Nrg-1 to the ErbB2 and ErbB4-expressing myocardium that initiates ventricular differentiation. *Erbb3* knockout mice exhibit dilated and thinned atrioventricular valves leading to death by embryonic day 13.5 [19]. As noted later, one of the adverse effects of ErbB-targeted treatments is cardiotoxicity, which is most likely related to the expression of these receptors in the heart.

Based upon the cDNA analysis and the primary amino acid structure of EGFR, Ulrich et al. hypothesized that the receptor consisted of an extracellular domain, a single hydrophobic transmembrane segment, and an intracellular domain with protein kinase activity [20]. This hypothesis has stood the test of time and fundamentally applies to all receptor protein kinases. The ErbB family of protein kinases consists of an extracellular domain that is divided into four parts: domains I and III, which are related leucine-rich segments that participate in ligand binding, and domains II and IV, which contain numerous cysteine residues that participate in disulfide bond formation. Domain II participates in homo and heterodimer formation with ErbB family members. The extracellular domain is followed by a single transmembrane segment of 19–25 amino acid residues and an intracellular portion of about 550 amino acid residues that contains (i) a juxtamembrane segment, (ii) a protein kinase domain, and (iii) a carboxyterminal tail (Fig. 1).

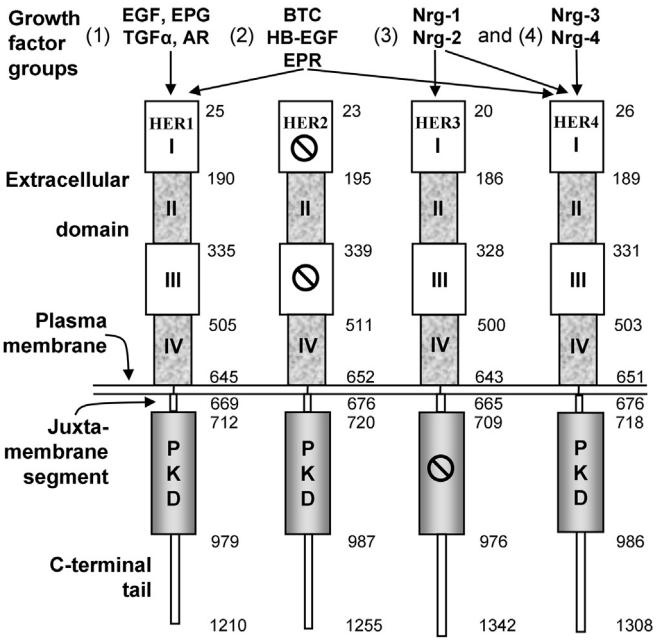

Fig. 1. Organization of the human ErbB/HER receptors. The extracellular segment of each receptor consists of four domains (I–IV). Domains I and III participate in ligand binding (except for those of HER2, which are marked with the stop symbol ⊘), and domain II participates in dimer formation. The carboxyterminal tail contains several tyrosine residues that can be phosphorylated. The kinase domain of HER3, which is marked with the stop symbol, is kinase-impaired. The numbers in the figure correspond to amino acid residues of the nascent protein containing the signal peptide (which is not depicted); each number corresponds to the initial residue of the adjacent segment except for (i) the last residues of the extracellular domains and (ii) the end of the proteins. The growth factor groups (1–4) that bind to the receptors are indicated. JM, juxtamembrane; PKD, protein kinase domain; EGF, epidermal growth factor; EPG, epigen; TGFα, transforming growth factor-α; AR, amphiregulin; BTC, betacellulin; HB-EGF, heparin-binding epidermal growth-factor like growth factor; EPR, epiregulin; Nrg-1/2/3/4, neuregulin-1/2/3/4.

There are two widely used numbering systems for the ErbB family amino acid residues. The system used in the Uniprot knowledge base includes the signal peptide yielding numbers that correspond to the nascent receptor. The system employed by Ullrich et al. [20] for ErbB1 excludes the 24-residue signal peptide and corresponds to the mature protein. Similarly, there are two numbering system for the other family members, one of which corresponds to the nascent protein while the second excludes the signal peptide and corresponds to the mature protein. To parallel usage in specific papers, both systems are used in this review and care is taken to specify whether the nascent or mature protein residue numbers are employed. Although the use of the mature protein numbering system is ingrained in the literature, it is easier to use the nascent protein numbers when going from DNA to RNA and then to protein.

2.2. ErbB ligands

Fig. 1 enumerates the ligands that bind to each of the monomeric receptors. The term neuregulin refers to the *NEU* gene and is synonymous with heregulin. Note that seven growth factors bind to EGFR/HER1, none bind to ErbB2/HER2, two bind to ErbB3/HER3, and seven ligands bind to ErbB4/HER4. The ErbB3/HER3 receptor is kinase impaired. Like all protein-tyrosine kinase receptors, the ErbB family functions as dimers or higher oligomers. There is one chief isoform of ErbB1/HER1, two full-length isoforms of ErbB2/HER2 that differ slightly owing to alternative mRNA splicing, and two full-length isoforms of ErbB3/HER3, one of which is missing residues 1–59. There are two different extracellular juxtamembrane versions (JMa and JMb), and there are two different versions

Table 1
ErbB receptor dimers, their ligands,[a] and the number of possible combinations of ligands with each dimer.

Receptor dimers	Ligands	Combinations[b,c,d,e]
ErbB1–ErbB1	EGF, EPG, TGFα, AR, BTC, HB-EGF, EPR (groups 1 and 2)	28
ErbB1–ErbB2	See above	7
ErbB1–ErbB3	EGF, EPG, TGFα, AR, BTC, HB-EGF, EPR, Nrg-1, Nrg-2 (groups 1, 2, and 3)	14
ErbB1–ErbB4JMa/CTa	EGF, EPG, TGFα, AR, BTC, HB-EGF, EPR, Nrg-1, Nrg-2, Nrg-3, Nrg-4 (groups 1, 2, 3, and 4)	49
ErbB1–ErbB4JMa/CTb	See above	49
ErbB1–ErbB4JMb/CTa	See above	49
ErbB1–ErbB4JMb/CTb	See above	49
ErbB2–ErbB2	None	0
ErbB2–ErbB3	Nrg-1, Nrg-2 (group 3)	2
ErbB3–ErbB3	Nrg-1, Nrg-2 (group 3)	3
ErbB2–ErbB4JMa/CTa	BTC, HB-EGF, EPR, Nrg-1, Nrg-2, Nrg-3, Nrg-4 (groups 2, 3, and 4)	7
ErbB2–ErbB4JMa/CTb	See above	7
ErbB2–ErbB4JMb/CTa	See above	7
ErbB2–ErbB4JMb/CTb	See above	7
ErbB3–ErbB4JMa/CTa	BTC, HB-EGF, EPR, Nrg-1, Nrg-2, Nrg-3, Nrg-4 (groups 2, 3, and 4)	14
ErbB3–ErbB4JMa/CTb	See above	14
ErbB3–ErbB4JMb/CTa	See above	14
ErbB3–ErbB4JMb/CTb	See above	14
ErbB4JMa/CTa–ErbB4JMa/CTa	BTC, HB-EGF, EPR, Nrg-1, Nrg-2, Nrg-3, Nrg-4 (groups 2, 3, and 4)	28
ErbB4JMa/CTa–ErbB4JMa/CTb	See above	28
ErbB4JMa/CTa–ErbB4JMb/CTa	See above	28
ErbB4JMa/CTa–ErbB4JMb/CTb	See above	28
ErbB4JMb/CTa–ErbB4JMa/CTb	See above	28
ErbB4JMb/CTa–ErbB4JMb/CTa	See above	28
ErbB4JMb/CTa–ErbB4JMb/CTb	See above	28
ErbB4JMa/CTb–ErbB4JMa/CTb	See above	28
ErbB4JMa/CTb–ErbB4JMb/CTb	See above	28
ErbB4JMb/CTb–ErbB4JMb/CTb	See above	28

[a] Group 1: EGF, EPG, TGFα, AR; group 2: BTC, HB-EGF, EPR; group 3: Nrg-1, Nrg-2; group 4: Nrg-3, Nrg-4.
[b] There are 28 combinations of receptor dimers. Assuming that ErbB2–ErbB2 and ErbB3–ErbB3 are inactive, this indicates that there are 26 possible combinations of active receptor dimers.
[c] There are 614 combinations of ligand–receptor complexes and 611 potential ligand-activated dimers (excluding ErbB2–ErbB2, which has no ligand, and ErbB3–ErbB3, which lacks protein kinase activity.
[d] For ErbB2–ErbB1/3/4 heterodimers, the number of ligand–receptor complexes is the number of ligands that bind to ErbB1/3/4 since ErbB2 lacks a ligand.
[e] As an example of the calculation of the number of combinations that a given homo or heterodimer and its ligand binding partners can make, consider the ErbB3–ErbB4JMa/CTa heterodimer with seven different ligands, two of which can bind to ErbB3 (group 3) and seven of which can bind ErbB4 (groups 2, 3, and 4). When ErbB4 binds BTC, ErbB3 can bind Nrg-1 or Nrg-2 ($n = 2$). When ErbB4 binds HB-EGF, ErbB3 can bind Nrg-1 or Nrg-2 ($n = 2$), etc., for a grand total of $N = 7 \times 2 = 14$. Finally consider the ErbB1–ErbB4JMa/CTa dimer where ErbB1 can bind seven different ligands (groups 1 and 2) and ErbB4JMa/CTa can bind seven different ligands (groups 2, 3, and 4). When ErbB1 binds EGF, ErbB4 can bind any of seven of its ligands ($n = 7$). When ErbB1 binds EPG, ErbB4 can bind any of its seven ligands ($n = 7$), etc., so that the total number of combinations $N = 7 \times 7 = 49$. When ErbB4 binds BTC, ErbB1 can bind any of its seven ligands, but these have already been considered and do not add to the total.

of the carboxyterminal tail (CTa and CTb) of the ErbB4/HER4 receptor. Thus there are four full-length transmembrane isoforms of ErbB4/HER4 proteins that are produced by alternative mRNA splicing: JMaCTa, JMaCTb, JMbCTa, and JMbCTb. Using reverse transcription polymerase chain reaction (RT-PCR) methodologies, Elenius et al. demonstrated that the JMa isoform is expressed in the mouse kidney, whereas the JMb isoform is expressed in the mouse heart and adrenal [21]. Moreover, both forms are expressed in cerebellum, cerebral cortex, eye, and spinal cord.

The four ErbB family members are able to form 28 homo and heterodimers. With the 11 growth factors in the EGF-like family and 28 possible dimers, there are 614 possible combinations of receptors (Table 1). Including both full-length isoforms of ErbB2 and both isoforms of ErbB3 increases the number of possible combinations even further. Not all ligands are expressed near cells that possess the ErbB family of receptors so that the number of potential combinations in a given cell is reduced, but still appreciable.

Note that the ErbB2/ErbB2 and ErbB3/ErbB3 homodimers are apparently non-functional and omitting these combinations reduces the possible number of active combinations to 611. ErbB2 fails to bind to any growth factor so that induced homodimer formation is unlikely. However, unphysiological overexpression of ErbB2 leads to the formation of a functional homodimer [22]. ErbB3 is kinase impaired so that induced homodimer formation would fail to stimulate protein kinase activity and downstream signaling. However, kinase-impaired ErbB3 possesses 1/1000th the autophosphorylation activity of ErbB1 [23] and the possibility exists that the ErbB3 homodimer is functional. ErbB2 is the favored dimerization partner for all of the other ErbB family members [24,25], and the ErbB2 heterodimer combinations with ErbB1 or ErbB3 exhibit robust signaling activity [26].

All of the ligands of the ErbB receptor family are expressed as single-pass integral membrane proteins [27]. These ligand precursors possess an extracellular component, a transmembrane segment, and a small intracellular portion. The growth factor precursors occur in the extracellular segment and they are released by proteolysis by members of the ADAMs (A disintegrin and metalloproteases) family [28]. The proteolytic processing and release of membrane proteins function as a post-translational switch that regulates the activity of the growth factor. This process is called protein ectodomain shedding, and the proteolytic enzymes are sometimes referred to as sheddases. In addition to growth factor processing, the ADAMs family also processes growth factor receptors, cytokines, cytokine receptors, and cell adhesion molecules. The family contributes to various physiological processes including adipogenesis, fertilization, myogenesis, and neurogenesis [29].

The human ADAMs family consists of more than two dozen members [29]. These membrane-anchored proteins require zinc ion for their activity, hence their classification as metalloproteases. The ADAMs family contains an amino-terminal signal sequence, a pro-domain, a metalloprotease domain, a disintegrin domain, a cysteine-rich segment, and EGF-like domain, a transmembrane segment, and an intracellular portion [28]. The metalloprotease domain contains a conserved His-Glu-Xxx-Gly-His sequence that binds zinc ion and confers catalytic activity.

Table 2
ErbB family activating ligands/growth factors.

Ligand	Uniprot KB ID	Amino acids in precursor	Final size	Sheddase[a]
Amphiregulin	P15514	252	84	ADAM17
Betacellulin	P35070	178	80	ADAM10
EGF	P01133	1207	53	ADAM10
Epigen	Q6UW88	154	61	ADAM17
Epiregulin	O14944	169	49	ADAM17
HB-EGF	Q99075	208	86	ADAM17
TGFα	P01135	160	84	ADAM17
Nrg-1	Q02297	640	222	ADAM17
Nrg-2	O14511	850	293	?
Nrg-3	P56975	720	359	?
Nrg-4	Q8WWG1	115	61	?

[a] From Refs. [28,30].

Of the numerous family members, ADAM10 and ADAM17 participate in the processing and generation of the functional EGF ligand family (Table 2) [28,31]. Note that EGF consists of 53 amino acid residues. It and the other members of the growth factor family contain six cysteine residues that form disulfide bonds in the order 1–3, 2–4, and 5–6, where the number refers to the relative position of the cysteine residue in the growth factor. Neuregulins 1–3 contain the EGF-like domain within a larger polypeptide while that of Nrg-4 (64 residues) is about the same size as EGF (53 residues) (Table 2). The ErbB/HER ligands generally act over short distances from their sites of generation [28]. They may act in an autocrine fashion on the same cell from which they were released, in a juxtacrine fashion on an adjacent cell, or in a paracrine fashion on a nearby cell.

3. ErbB/HER protein-tyrosine kinase structure and function

3.1. The extracellular ligand-binding domains

Binding of growth factors to ErbB1/3/4 promotes dimerization of monomeric receptors and increases the tyrosyl kinase activity of the intracellular domains of ErbB1/2/4 [32]. Although ErbB2 lacks a soluble ligand or growth factor, it readily forms heterodimers. There are a number of possible ways that a growth factor or ligand can induce receptor dimerization. One possibility for growth-factor induced receptor dimerization involves a single ligand that interacts simultaneously with two receptor molecules and effectively cross links them to form a dimeric complex [1]. The dimerization of Eph receptors, Kit, and VEGFR1 occurs by this mechanism [1]. In each of these cases, the factor cross links the ligand-binding portions of the two receptor molecules. Another possibility results when both ligands and both receptors contribute directly to the dimerization interface. This mechanism occurs in the formation of the dimeric complex of the granulocyte colony-stimulating factor and its receptor [33].

In contrast to the above possibilities, the ErbB1/3/4 receptors employ a receptor-only mediated dimerization mechanism as illustrated in Fig. 2 [1,34,35]. The bivalent ligand, EGF [34] or TGFα [35], contacts two distinct sites in domains I and III within a single receptor molecule. The X-ray crystal structure of the extracellular segment of EGFR reveals that the leucine-rich domain I resembles domain III and that the cysteine-rich domain II resembles domain IV [34,36,37]. Domain III of EGFR forms a six-turn right-handed barrel-shaped β-helix that is capped at each end by an α-helix and a disulfide bond. Domain I has a similar structure. Domains II and IV, in contrast, form extended rod-like folds similar to those that occur in fibrous nuclear lamins that participate in the formation of nuclear lamina on the interior of the nuclear envelop.

Ligand binding promotes a large conformational change in the extracellular segment that opens the extracellular receptor domains and removes a β-hairpin-loop dimerization arm from a sleeve in domain IV (Fig. 2) [38]. Before the ligand binds, the arm is completely buried in domain IV, which stabilizes a closed or tethered receptor conformation that restricts its movement so that both ligand binding and dimerization are autoinhibited. Ligand binding breaks the intramolecular tether and allows the dimerization arm to enter a different sleeve in domain II of a second ligand-bound receptor molecule.

The structure of EGF in the complex with EGFR corresponds to the crystal structure of EGF itself [39]. Human EGF, a 53 amino-acid-residue growth factor, contains three disulfide bonds that divide the molecule into three loops: the A-loop (Cys6–Cys20), the B-loop (Cys14–Cys31), and the C-loop (Cys33–Cys42). The B-loop forms a two-stranded antiparallel β-sheet (Fig. 2). The B-loop interacts with residues in domain I and the A- and C-loops interact with residues in domain III. Note that the EGFR dimer stoichiometry is 2:2 (2EGF:2EGFR), which is in agreement with the analytical ultracentrifugation results of Domagala et al. [40].

Cho and Leahy determined the crystal structure of unliganded ErbB3 (PDF ID: 1M6B) [41] and Bouyain et al. determined the crystal structure of unliganded ErbB4 (PDF ID: 2AHX) [42]. The structure of both ErbB3 and ErbB4 resembles that of ErbB1. ErbB3 and ErbB4 possess a tethered and closed structure with a domain II/IV contact similar to that observed in ErbB1. In contrast, ErbB2 exists in an extended and open conformation and the dimerization arm is exposed and not buried (PDB ID: 1N8Y) [43]. Unliganded ErbB2 is thus ready for dimerization with other ErbB family members.

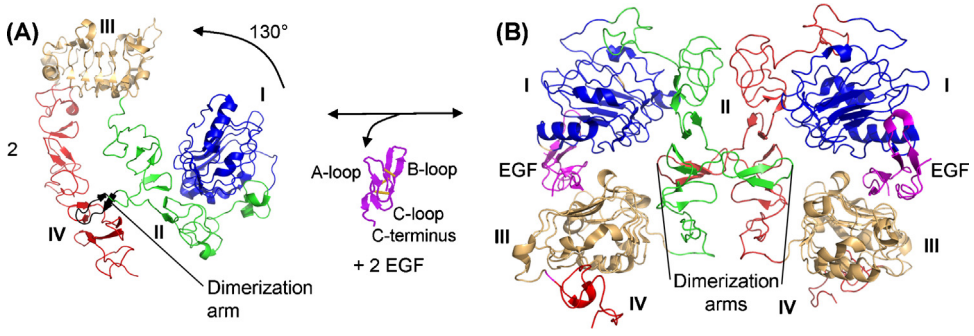

Fig. 2. Structures of the closed tethered extracellular segment of human EGFR and the growth-factor-induced open extended EGFR dimer. (A) The dimerization arm from domain II (black) of tethered EGFR interacts with domain IV (red) and is buried. Domains I (blue), II (green), and III (tan) are indicated. (B) Ligand binding induces a large conformational change that results in the exposure of the dimerization arm that allows EGFR back-to-back dimer formation. Note that the EGF ligands are far apart (≈80 Å) and that dimer formation involves contacts of domain II of the receptors. One dimerization arm (green) is close to the viewer and the second (orange) is partially hidden. Only a portion of domain IV is observed in the dimer owing to disorder in the X-ray crystal structure. The monomeric tethered form was prepared from PDB ID: 1NQL and the dimer was prepared from PDB ID: 1IVO using the PyMOL Molecular Graphics System Version 1.5.0.4 Schrödinger, LLC.

Cho and Leahy analyzed the residues in the dimerization arm and their contacts in domain IV of the ErbB family. ErbB1/3/4 contain Gly588/582/586 in the domain IV contact region whereas ErbB2 contains a proline (612) at this position in the nascent protein [41]. Furthermore, ErbB1/3/4 contain H590/H584/N588 in the domain IV contact region whereas ErbB2 contains a phenylalanine (614) at this position. These changes may be responsible for the inability of domain IV of ErbB2 to accept the dimerization arm to form the closed and tethered structure.

For the EGFR homodimer, Ogiso et al. reported that Tyr270, Pro272, and Tyr275 in receptor A interact with Phe287, Ala289, Tyr299, and Arg309 of receptor B using nascent protein residue numbers; reciprocal contacts from receptor B interact with receptor A of the EGFR homodimer [34]. There are four reciprocal hydrogen bond pairs that occur in the receptor dimer interface. All of these residues are conserved or replaced by homologous residues in the other ErbB family members. Accordingly, it is likely that a similar mechanism involving a dimerization arm is responsible for both homo and heterodimerization of the ErbB receptor family.

Garret et al. prepared a mutant of transmembrane EGFR with a deleted dimerization arm and stably expressed it in mouse bone-marrow derived BaF3 cells, which do not express any ErbB family members [35]. In contrast to the wild type receptor, the deletion mutant fails to show (i) EGF-induced dimerization, (ii) receptor autophosphorylation, or (iii) phosphorylation and activation of the downstream signaling ERK1/2. Taken together, these structural and functional studies indicate that a dimerization arm mediates the formation of EGFR complexes and most likely participates in the formation of homo and heterodimers involving the other ErbB family members.

Liu et al. reported that a single ligand is able to induce ErbB1 or ErbB4 homodimer formation and activation [44]. They prepared ErbB1 and ErbB4 mutants that were unable to bind a ligand or were kinase defective and expressed them in Chinese hamster ovary (CHO) cells. These mutants exhibited negligible ligand-dependent phosphorylation when expressed individually, but were able to mediate ligand-dependent phosphorylation when expressed together. These results indicate that ligand binding-deficient receptors are able to pair with kinase-deficient receptors to form active, singly ligated ErbB dimers.

Liu et al. noted that the X-ray crystal structure of the extracellular domains of ErbB/growth factor homo and heterodimers exhibit two different dimerization interfaces: a scissors-like 29° open or a 0° closed conformation [44]. They reported that ErbB1/EGF and ErbB4/Nrg-1β form a heterodimer with a scissors-like open (staggered) interface with the dimerization arms acting as a pivot. In contrast, truncated extracellular EGFR (lacking domain IV) bound to TGFα forms a homodimer with a scissors-like closed (flush) interface. The scissors-closed interface also occurs in the asymmetric homodimer of *Drosophila* EGFR in which only one receptor subunit possesses a high affinity ligand [44,45]. The absence of a high-affinity ligand in one subunit changes the relative orientation of the domain I/II and III/IV pairs and allows domain I and the amino-terminal region of domain II of the unliganded subunit to form a scissors-closed domain II interface with the ligand-containing subunit. Binding of the second ligand promotes the formation of a less-stable scissors-open dimer interface, which reduces the apparent affinity of the second receptor for the ligand relative to the first and explains the observed negative cooperativity [45]. Negative cooperativity occurs when the affinity of the second binding site for a ligand is decreased when compared with that of the first binding site after the first site is occupied by a ligand.

Although the extracellular segment of ErbB2 lacks a tether and occurs in an extended conformation, ErbB2 does not form active dimers unless it is overexpressed [22]. Like ErbB1/3/4, ErbB2 is autoinhibited, but by a mechanism not involving a buried dimerization arm. Domain II contains eight disulfide bonds (m1–m8) that make up distinct modules. In the autoinhibited state of ErbB2, these modules exist in a linear structure that fails to form dimers [45]. In the active state, domain II forms an 11° bend between m4 and m5 that facilitates dimerization.

Macdonald-Obermann et al. analyzed the interaction of EGFR, ErbB2, and ErbB3 by luciferase fragment complementation imaging [46]. Firefly luciferase can be split into amino-terminal and carboxyterminal fragments, neither of which exhibits enzyme activity alone, but they form a functional enzyme complex when they are brought together. This luciferase complementation strategy monitors the interaction of these receptors. They fused these fragments to the C-termini of the three receptors and stably expressed them in CHO cells. They found that Nrg-1β, which binds to ErbB3, leads to the following order of receptor pairing and stability: ErbB2/ErbB3 > EGFR/ErbB3 > ErbB3/ErbB3. They reported that EGF induces the formation of EGFR homodimers at the exclusion of EGFR/ErbB3 heterodimer formation when both are present in the cell. They found that EGF, which binds to EGFR, leads to the following order of receptor pairing and stability: EGFR/EGFR ≈ EGFR/ErbB2 ≫ EGFR/ErbB3. They also found evidence for the formation of pre-dimers of EGFR/ErbB2, EGFR/ErbB3, and ErB2/ErbB3 that exist in the plasma membrane prior to the addition of growth factor.

3.2. Catalytic residues in the amino and carboxyterminal lobes of the active and dormant ErbB1 protein kinase domains

Although the tertiary structure of catalytically active protein kinase domains are strikingly similar, Huse and Kuriyan reported that the crystal structures of dormant enzymes reveal a multitude of distinct inactive protein kinase conformations [47]. The practical consequence of this is that drugs targeting specific inactive conformations may be more selective than those targeting the active conformation. These authors noted that protein kinases usually assume their less active conformation in the basal or non-stimulated state, and the acquisition of their activity may involve several layers of regulatory control [47]. The three main regulatory elements within the kinase domain include the small lobe αC-helix (αC-in, active; α-C-out, inactive), the large lobe DFG-Asp (DFG-Asp in, active; DFG-Asp out, inactive), and the large lobe activation loop (AL open, active; AL closed, inactive). Taylor et al. refer to the process of going from the dormant to active conformation (and vice versa) as a dynamic switch [48].

The EGFR protein kinase domain has a small amino-terminal lobe and large carboxyterminal lobe that contains several conserved α-helices and β-strands, first described by Knighton et al. for PKA [49]. The small lobe is dominated by a five-stranded antiparallel β-sheet (β1–β5) [48]. It also contains an important regulatory αC-helix that occurs in active or inactive positions (Fig. 3A, C, and E). The small lobe contains a conserved glycine-rich (GxGxxG) ATP-phosphate-binding loop, sometimes called the P-loop, which occurs between the β1- and β2-strands. The glycine-rich loop, which is the most flexible part of the small lobe, helps position the β- and γ-phosphates of ATP for catalysis. The β1 and β2-strands harbor the adenine component of ATP. The glycine-rich loop is followed by a conserved valine (V726; nascent receptor residue numbers are used in Sections 3.2 and 3.3) that makes a hydrophobic contact with the adenine of ATP. The β3-strand typically contains an Ala-Xxx-Lys sequence, the lysine of which (K745) couples the α- and β-phosphates of ATP to the αC-helix. A conserved glutamate occurs near the center of the αC-helix (E762) in protein kinases. The presence of a salt-bridge between the β3-lysine and the αC-glutamate is a prerequisite for the formation of the activate state and corresponds to the "αC-in" conformation (Fig. 3A); by contrast the Lys745 and Glu 762 of the dormant form of EGFR fail to

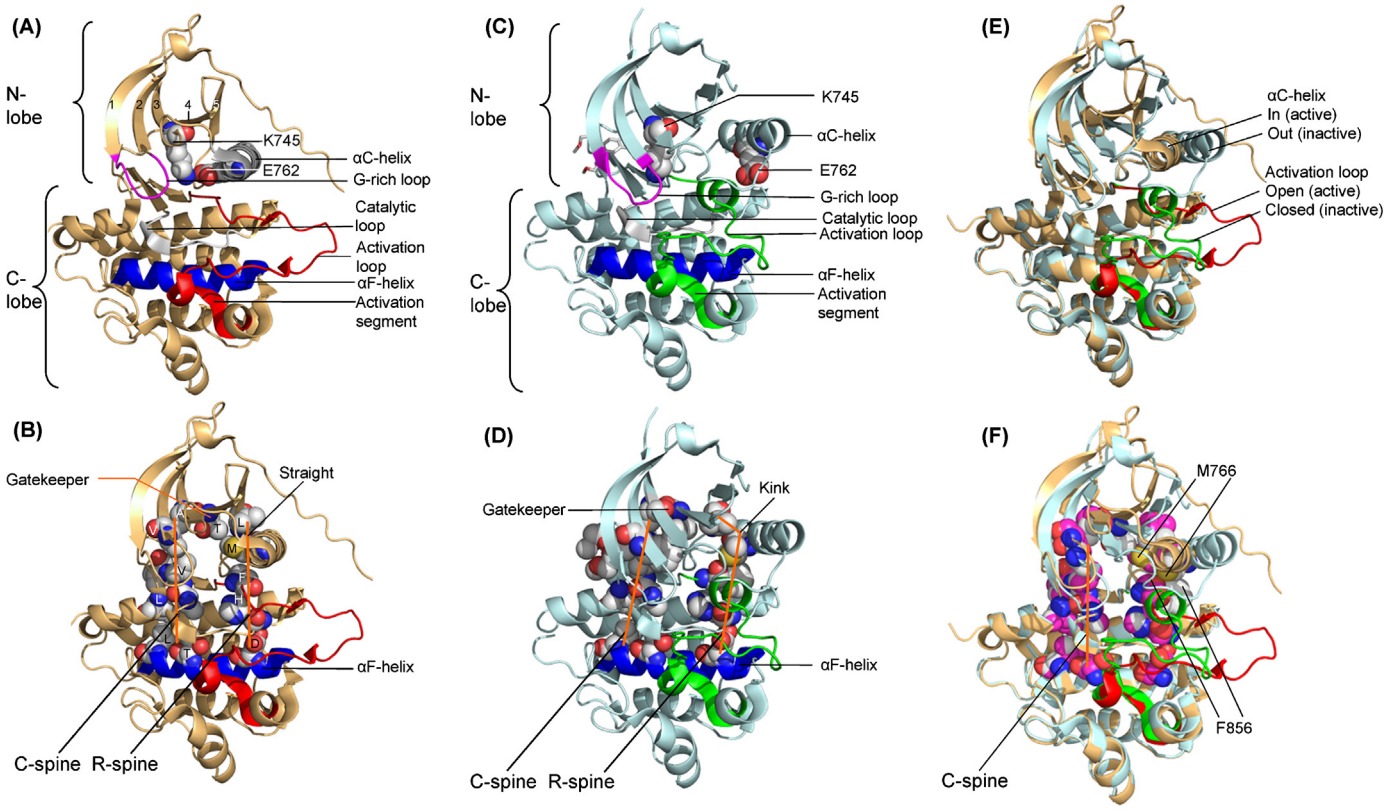

Fig. 3. Structures of active and inactive human EGFR protein kinase domains. (A) Active EGFR. Note that Lys745 and Glu762 are kissing and the activation loop is in its open conformation. (B) Spines of active EGFR, same view as in A. (C) Inactive EGFR. Note that Lys745 and Glu762 are not kissing and the activation loop is in its closed conformation. (D) Spines of inactive EGFR, same view as C. (E) Superposition of the active and inactive enzymes, (F) Superposition of the spines from the active and inactive enzymes. The active enzyme structure was prepared from PDB ID: 1M17 and the inactive enzyme structure was prepared from PDB ID: 4HJO using the PyMOL Molecular Graphics System.

make contact (Fig. 3C). The αC-in conformation is necessary, but not sufficient, for the expression of full kinase activity.

The large lobe of the EGFR protein kinase domain is mainly α-helical with six conserved segments (αD-αI) [48]. It also contains four short conserved β-strands (β6–β9) that contain most of the catalytic residues associated with the phosphoryl transfer from ATP to its substrates. The primary structure of the β-strands occurs between those of the αE- and αF-helices. The activation loop in the active state forms an open structure that allows protein/peptide binding. The activation loop in the less active state forms a closed, compact structure that blocks protein/peptide binding (Fig. 3E). The dormant and the active EGFR protein kinase domain contain an additional helix near the end of the activation segment.

Hanks et al. identified 12 subdomains (I–VIa, VIb–XI) with conserved amino-acid-residue signatures that constitute the catalytic core of protein kinases [50]. Of these, the following four amino acids, which define a K/E/D/D (Lys/Glu/Asp/Asp) signature, illustrate the catalytic properties of EGFR. An invariant β3-strand lysine (K745, the K of K/E/D/D) forms salt bridges with the αC-glutamate (the E of K/E/D/D) and with the α- and β-phosphates of ATP (Fig. 4). The catalytic loops surrounding the actual site of phosphoryl transfer are different between the protein-serine/threonine and protein-tyrosine kinases. This loop is made up of a YRDLKPEN canonical sequence in protein serine/threonine kinases and an HRDLAARN sequence in protein-tyrosine kinases including ErbB1/2/4. The catalytically impaired ErbB3 contains HRNLAARN with an asparagine (N) in place of aspartate (D). The catalytic aspartate (D837) in ErbB1, which is the first D of K/E/D/D serves as a base that accepts a proton from the tyrosyl —OH group. The AAR sequence in the catalytic loop represents a receptor protein-tyrosine kinase signature, and RAA represents a

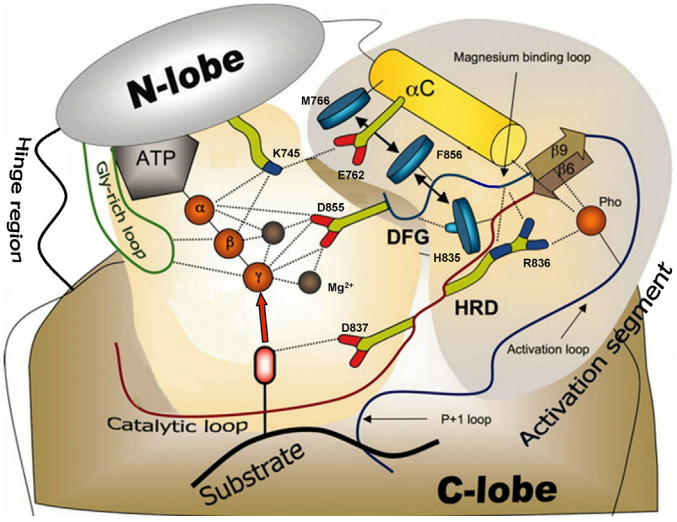

Fig. 4. Diagram of the inferred interactions between the human EGFR catalytic domain residues, ATP, and a protein substrate. Catalytically important residues that are in contact with ATP and the protein substrate occur within the light khaki background. Secondary structures and residues that are involved in regulation of catalytic activity occur within the gray background. Hydrophobic interactions between the HRD motif (the first D of K/E/D/D), the DFG motif (the second D of K/E/D/D), and the αC-helix are shown by the double arrows while polar contracts are shown by dashed lines. Pho is the phosphate that may be attached to Tyr869; residue numbers correspond to the nascent protein including the 24-residue signal peptide.

The figure is adapted from Ref. [52] copyright *Proceedings of the National Academy of Sciences of the United States of America.*

Table 3
Important residues in human ErbB receptors.

	EGFR	ErbB2	ErbB3	ErbB4
Number of residues	1–1210	1255	1342	1308
Signal peptide	1–24	1–22	1–19	1–25
Extracellular segment	25–645	23–652	20–643	26–651
Transmembrane segment	646–668	653–675	644–664	652–675
Intracellular segment	669–1210	676–1255	665–1342	676–1308
Protein kinase domain	712–979	720–987	709–966	718–985
Glycine-rich loop; GSGAFG	719–724	727–732	716–721	725–730
The K of K/E/D/D, or the β3-lysine	K745	K753	K742	K751
αC-Glu or His	E762	E770	H759	E769
Hinge residues	792–796; LMPFG	800–804; LMPYG	789–793; YLPLG	798–802; LMPHG
Gatekeeper residue	T790	T798	T787	T796
Catalytic HRD, the first D of K/E/D/D	837	845	N834	843
Activation segment DFG, the second D of K/E/D/D	855	863	852	861
Activation segment tyrosine phosphorylation sites	869	877	868	875
End of the activation segment	882–884	890–892	879–881	888–890
Molecular weight (kDa)	134	138	148	147
UniProt KB ID	P00533	P04626	P21860	Q15303

non-receptor protein-tyrosine kinase. See Ref. [51] for a general discussion of phosphorylation reactions and the enzymology of protein kinases.

The second aspartate of the K/E/D/D signature, D855, is the first residue of the activation segment. The activation segment of nearly all protein kinases begins with DFG (Asp-Phe-Gly) and ends with APE (Ala-Pro-Glu). The EGFR activation segment begins with DFG, but it ends with ALE (Ala-Leu-Glu). The DFG-Asp in configuration represents the active conformation. In contrast to many protein kinases, however, dormant EGFR exhibits the DFG-Asp in arrangement. DFG-Asp855 binds Mg^{2+}, which in turn coordinates the α-, β- and γ-phosphates of ATP. The primary structure of the catalytic HRD loop of EGFR, which occurs before the β7-strand, consists of His835, Arg836, and Asp837 (Fig. 4). Fig. 3E is the superposition of active and dormant EGFR kinase domains that illustrates the relative positions of the αC-helix and the activation loops. The primary structure of the activation segment occurs after that of the catalytic loop. Functionally important human ErbB1–4 residues are listed in Table 3. The large lobe characteristically binds the peptide/protein substrates.

The activation segment influences both substrate binding and catalytic efficiency [53]. The five-residue magnesium-positioning loop begins with the DFG of the activation segment. The activation loop in EGFR contains a phosphorylatable tyrosine. The loop is located close in the three-dimensional sense to the magnesium-binding loop, the amino-terminus of the αC-helix, and the conserved HRD component of the catalytic loop. The interaction of these three components is hydrophobic in nature, which is indicated by the double arrows in Fig. 4. Although phosphorylation of one or more residues in the activation segment of most protein kinases is required for activation [54], this phosphorylation is not required for EGFR activation [55,56].

The phosphorylation site of the peptide/protein substrate is numbered 0 (zero), the residue immediately after the phosphorylation site is P + 1, and the residue immediately before the phosphorylation site is P − 1 (P minus 1). The P + 1 binding site of protein kinases helps determine the substrate specificity of these enzymes by selecting amino acid residues in protein substrates that fit into this site. The P + 1 site is generally composed of the last eight residues of the activation loop within the activation segment.

All four members of the ErbB family of protein kinases possess a similar protein kinase domain. ErbB1/2/4 possess protein kinase activity while ErbB3 is catalytically impaired. The catalytically important residues within the kinase domain of ErbB1/2/4 are conserved (Table 3) and these three family members closely resemble one another in terms of overall protein kinase structure. The aspartate (D) in the catalytic loop HRD of ErbB3 is replaced by asparagine and the αC-glutamate is replaced by histidine. Furthermore, the αC-helix of ErbB3 is shortened when compared with those of ErbB1/2/4. ErbB1, ErbB2, and ErbB4 have been observed in both active (PDB ID: 1M14, 3PP0, 3BCE) and inactive (PDB ID: 4HJ0, 3RCD, 3BBW) conformations by X-ray crystallography. In contrast, the X-ray structure of ErbB3 occurs in an inactive conformation with the enzyme exhibiting the αC-out and activation loop closed orientation (PDB ID: 3KEX).

Guy et al. expressed human EGFR and bovine ErbB3 in insect cells and measured the ability EGFR or ErbB3 to catalyze the phosphorylation of exogenous substrates or to undergo autophosphorylation in immune complexes [57]. They reported that the ability of ErbB3 to catalyze the phosphorylation of exogenous substrates was at least two orders of magnitude less efficient than that of EGFR. Moreover, they observed only a low level of ErbB3 phosphorylation in the immune complexes that was not increased by the addition of neuregulin, an ErbB3 ligand. Such autophosphorylation was ascribed to endogenous insect cell protein kinases leading to the view that the ErbB3 protein kinase is inactive [58,59].

Later experiments, however, suggested that ErbB3 is not kinase dead, but kinase impaired. Using recombinant purified protein, Lemmon et al. reported that human ErbB3/ErbB3 is able to undergo autophosphorylation at a rate of about 1/1000th that of EGFR [23]. Although EGFR is able to catalyze the phosphorylation of exogenous protein substrates, these investigators reported that ErbB3 is unable to catalyze such reactions. They suggested that ErbB3 autophosphorylation plays an important role in signaling. However, additional experimentation will be required to verify this proposal.

In the ErbB2/ErbB3 heterodimer, both ErbB2 and ErbB3 become phosphorylated [24]. Zhang et al. performed experiments to address the mechanism of ErbB2 phosphorylation in ErbB2/ErbB3 heterodimers [60]. They used an RNA aptamer called A30 that targets the extracellular domain of ErbB3. A30 does not interfere with (i) ligand binding to ErbB3, (ii) receptor heterodimerization, or (iii) Akt signaling. The aptamer does not block the phosphorylation of ErbB3 by ErbB2 indicating that the allosteric activation of ErbB2 kinase activity, which is described in Section 3.4.1, is not inhibited. A30 blocks the formation of side-by-side ErbB2/ErbB3 heterodimers that facilitate the phosphorylation of one ErbB2 by the other ErbB2 within the dimer of dimers. Thus, ErbB2 catalyzes the phosphorylation of ErbB3 in a heterodimer and one ErbB2 catalyzes the phosphorylation of an adjacent ErbB2 in a heterotetramer. Accordingly, ErbB3 kinase activity is not required for ErbB2

Table 4
Human ErbB1–4 and murine PKA residues that form the R-spine and C-spine.

	ErbB1	ErbB2	ErbB3	ErbB4	PKA[a]
Regulatory spine					
C-helix (N-lobe)	Met766	Met774	Ile763	Met772	Leu95
β4-Strand (N-lobe)	Leu777	Leu785	Leu774	Leu783	Leu106
Activation loop (C-lobe) F of DFG	Phe856	Phe864	Phe853	Phe862	Phe185
Catalytic loop His or Tyr (C-lobe)[b]	His835	His843	His832	His841	Tyr164
F-helix (C-lobe)	Asp896	Asp904	Asp893	Asp902	Asp220
Catalytic spine					
β2-Strand (N-lobe)	Val726	Val734	Val723	Val732	Val57
β3-A/CXK motif (N-lobe)	Ala743	Ala751	C740	Ala749	Ala70
β7-Strand (C-lobe)	Leu844	Leu852	Leu841	Leu850	Leu173
β7-Strand (C-lobe)	Val843	Val851	Val840	Val849	Leu172
β7-Strand (C-lobe)	Val845	Val853	Val842	Val851	Ilele174
D-helix (C-lobe)	Leu798	Leu806	Leu795	Leu804	Met128
F-helix (C-lobe)	Thr903	Thr911	Thr900	Thr909	Leu227
F-helix (C-lobe)	Leu907	Leu915	Leu904	Leu913	Met231

[a] From Ref. [52].
[b] Part of the HRD (His-Arg-Asp) or YRD (Tyr-Arg-Asp) sequence.

phosphorylation. The authors note that higher order complexes may exist.

3.3. Structures of the hydrophobic spines in the active and dormant ErbB1 protein kinase domain

Taylor and Kornev [61] and Kornev et al. [52] analyzed the structures of active and dormant conformations of some two dozen protein kinases and determined functionally important residues by a local spatial pattern (LSP) alignment algorithm. This analysis revealed a skeleton of four non-consecutive hydrophobic residues that constitute a regulatory or R-spine and eight hydrophobic residues that constitute a catalytic or C-spine. Each spine consists of residues derived from both the small and large lobes. The regulatory spine contains residues from the activation loop and the αC-helix, whose conformations are important in defining active and dormant states. The catalytic spine governs catalysis by directing ATP binding. The two spines dictate the positioning of the protein substrate (R-spine) and ATP (C-spine) so that catalysis results. The proper alignment of the spines is necessary for the assembly of an active kinase.

The EGFR regulatory spine consists of a residue from the beginning of the β4-strand (Leu777), from the C-terminal end of the αC-helix (Met766), the phenylalanine of the activation segment DFG (Phe856), along with the HRD-histidine (His835) of the catalytic loop. Met766 and comparable residues from other protein kinases are four residues C-terminal to the conserved αC-glutamate. The backbone of His835 is anchored to the αF-helix by a hydrogen bond to a conserved aspartate residue (Asp896). The P + 1 loop, the activation loop, and the αH–αI loop bind to the αF-helix by hydrophobic bonds [52]. The regulatory spine of active EGFR is linear while that of dormant EGFR possesses a kink or dislocation between Met766 and Leu777 with the concomitant translocation of the αC-helix into its dormant configuration (Fig. 3B and D). The activation loop of the dormant enzyme possesses a short helix, which helps to restrain and hold the αC-helix in its inactive position. Table 4 lists the residues of the spines of human ErbB1–4 and the catalytic subunit of murine PKA, and Fig. 3B and D shows the location of the catalytic spines of active and dormant EGFR, respectively.

The catalytic spine of protein kinases consists of residues from the amino-terminal and carboxyterminal lobes that is completed by the adenine portion of ATP [52,61]. This spine mediates catalysis by directing ATP localization thereby accounting for the term catalytic. The two residues of the small lobe of the EGFR protein kinase domain that bind to the adenine component of ATP include Val726 from the beginning of the β2-strand and Ala743 from the conserved Ala-Xxx-Lys of the β3-strand. Furthermore, Leu844 from the middle of the β7-strand binds to the adenine base in the active enzyme. Val843 and Val845, hydrophobic residues that flank Leu844, bind to Leu798 at the beginning of the αD-helix. The αD-helix Leu798 binds to Thr903 and Leu907 in the αF-helix. Fig. 3F is the superposition of active and dormant EGFR that depicts the dislocation of Met766 and F856 in the dormant kinase regulatory spine.

Note that both the R-spine and C-spine are anchored to the αF-helix, which is a very hydrophobic component of the enzyme that is entirely within the protein and not exposed to the solvent. The αF-helix serves as a sacrum that supports the spines, which in turn anchors the protein kinase catalytic muscle. In contrast to the protein kinase amino acid signatures such as the DFG or the HRD, the residues that constitute the spine were not identified by sequence analyses *per se*. Rather, they were identified by their three-dimensional location based upon a comparison of the X-ray crystallographic structures of some twenty protein kinases in their active and dormant states [52,61].

Besides the hydrophobic interactions with the adenine group, the exocyclic 6-amino nitrogen of ATP characteristically forms a hydrogen bond with a backbone residue in the hinge that connects the N- and C-lobes of the protein kinase domain. The residues in the EGFR hinge include ^{792}Leu-Met-Pro-Phe-Gly^{796}. Most small-molecule inhibitors of protein kinases that compete with ATP binding also make hydrogen bonds with the backbone residues of the connecting hinge [62].

3.4. Activation of the ErbB protein kinases

3.4.1. Asymmetric dimer formation

In the general mechanism for the activation of receptor protein-tyrosine kinases, activating ligands or growth factors bind to the ectodomains of two receptors and induce the formation of an activated dimerization state [1]. The juxtaposed cytoplasmic kinase domains catalyze the phosphorylation of tyrosine residues, usually in the activation segment, that leads to protein kinase activation. The kinase domains also catalyze the phosphorylation of additional tyrosine residues that create docking sites for adaptor proteins or enzymes that result in downstream signaling. The docking proteins contain modular Src homology 2 (SH2) or phosphotyrosine binding (PTB) domains (or both) that recognize phosphotyrosine in sequence-specific contexts. This phosphorylation is accomplished in *trans*, i.e., the first member of the dimer mediates the

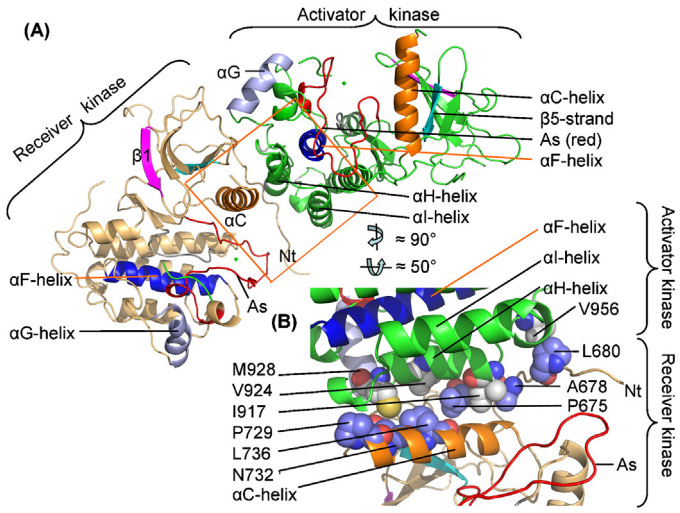

Fig. 5. Structure of the EGFR asymmetric dimer. (A) The asymmetric CDK/Cyclin-like dimer of the human EGFR kinase domain. Most of the activator kinase is colored green and most of the receiver kinase is colored khaki. (B) The EGFR dimer in (A) was rotated horizontally by ≈90° and vertically by ≈50° and magnified to illustrate the residue contacts enclosed within the orange rectangle that represent the interface between the activator and receiver kinase. As, activation segment; Nt, N-terminus. The pdb coordinates were provided by Prof. John Kuriyan, and the figure was prepared using the PyMOL Molecular Graphics System.

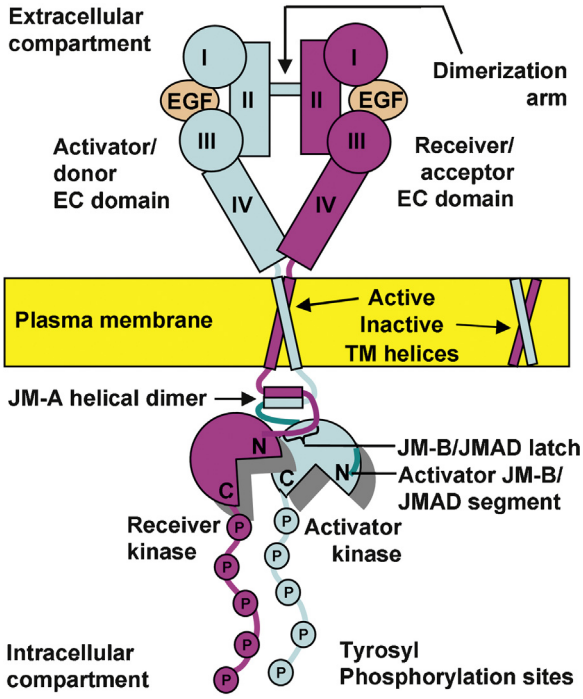

Fig. 6. Schematic of the structure of human EGFR. The activator receptor is colored cyan and the receiver is magenta. The dimerization arm of the activator obscures the view of the dimerization arm of the receiver. In the active state, the residues from domain IV from the receptor pair form a V-shape. The carboxyterminal portion of the activator kinase domain interacts with the amino-terminal portion of the receiver kinase domain. The transmembrane helices of the active receptor interact near their amino-termini by the extracellular compartment while those of the inactive receptor interact near their carboxytermini by the intracellular compartment. The figure is modified from Ref. [67].

phosphorylation of the second and the second member mediates phosphorylation of the first.

Although EGFR was the first receptor tyrosyl kinase to be discovered [3], its activation mechanism differs from that of other receptor kinases. Although phosphorylation of one or more residues in the activation segment of most protein kinases is required for activation [54] and phosphorylation of EGFR Tyr869 in the activation segment occurs [63], this phosphorylation is not required for activation [55,56]. Instead, ligand-activated EGFR kinase domains form an asymmetric homodimer that resembles the heterodimer formed by CDK2 and cyclin A, its activating protein [64]. In the EGFR asymmetric homodimer, one kinase domain plays the role of cyclin (the activator/donor) and the other kinase domain plays the role of CDK (the receiver/acceptor). Like other receptor kinases, the activated receiver kinase catalyzes the phosphorylation of tyrosine residues of the activator kinase, which then serve as docking sites for downstream signaling. A similar mechanism is responsible for the activation of the other homo and heterodimers of the ErbB family of enzymes.

The CDK/cyclin-like dimer interface is formed by the loop between the αG and αH-helices and the end of the αI-helix of the activator monomer and the N-terminal (Nt) extension (residues 672–685) of EGFR, the αC-helix, and the loop between strands β-4 and β-5 of the receiver monomer (Fig. 5A) [64] (EGFR residues in Sections 3.4.1–3.4.3 exclude those of the signal peptide). This dimer interface results in the burial of ≈2020 Å^2 of surface area [64]. The core of the asymmetric EGFR kinase domain dimer is dominated by interactions between the αH-helix of the activator kinase (Met928, Val924, Ile917) and the N-terminus of the kinase domain (Leu680, Ala678, Pro675) and the αC-helix (Pro729, Leu736, and Asn732) of the receiver kinase (Fig. 5B) [64].

Macdonald-Obermann et al. examined the mechanics of EGFR/ErbB2 kinase activation by luciferase fragment complementation imaging [65] as described in Section 3.1 [46]. They fused the N-terminal and C-terminal luciferase fragments to the C-termini of EGFR and ErbB2 and expressed them in CHO cells. In the basal state, the receptors existed as monomers in which no luciferase complementation occurs or as inactive pre-dimers in which complementation of the luciferase fragments results. Binding of EGF to EGFR induces dimerization of the receptor with ErbB2 and directs the kinase domain of EGFR to adopt the receiver position in the asymmetric dimer; recall that ErbB2 lacks a ligand. They reported that EGFR is activated first. If EGFR is catalytically competent, it mediates the phosphorylation of the C-terminal tail of ErbB2. This leads to a change in the position of the C-terminal tail of ErbB2 and results in the separation of the luciferase fragments and a decrease of luciferase activity. This phosphorylation-induced conformational change occurs prior to the formation of the reciprocal asymmetric dimer in which the kinase domain of ErbB2 is activated. If EGFR cannot phosphorylate its partner (kinase dead EGFR was used), the conformational change cannot occur and ErbB2 is never activated. These experiments indicate that EGFR functions as the first receiver kinase and ErbB2 is the initial activator kinase in cells expressing both receptors.

3.4.2. Role of the juxtamembrane segment and transmembrane helices in enzymatic activation

Red Brewer et al. [66] reported that the juxtamembrane (JM) segment of EGFR participates in protein kinase activation. Using alanine-scanning mutagenesis, they found that mutations of the C-terminal 19 residues (residues 664–682) of the JM region abolish EGFR activation. Mutations with the greatest inhibitory effect include Leu664, Val665, Pro667, Leu668, Pro670, Leu680, Arg681, and Ile682. These investigators dubbed this 19-residue component JMAD (for JM activation domain) (Fig. 6). They reported that the crystal structure of an inactive kinase domain mutant (Lys721Met, where Lys721 is the catalytic lysine of K/E/D/D) showed that the JM segment of the receiver kinase cradles or surrounds the C-lobe of the donor. They proposed that JMAD enhances the formation of

the asymmetric dimer and promotes the allosteric activation of the acceptor.

Jura et al. noted that the attachment of the JM domain (residues 645–671) to the EGFR protein kinase core (672–998) increases enzyme activity in solution by ≈70-fold [68]. They divided the JM segment into an N-terminal portion (residues 645–657) designated JM-A and a C-terminal portion (residues 658–671) designated JM-B and found that deletion of JM-A reduces catalytic efficiency 10-fold thereby indicating that the entire JM segment is required for full activation. Note that the JMAD residues (664–682) of Red Brewer et al. [66] overlap with the JM-A and JM-B residues [68]. Thus, in the absence of membranes or a lipid bilayer, the JM segment promotes EGFR protein kinase activity.

Jura et al. examined the ability of the JM-A segment to function on either the activator or the receiver kinase or both [68]. The Ile682Gln N-lobe mutant functions only as an activator kinase and the Val924Arg C-lobe mutant functions only as a receiver kinase. Both mutants containing the entire JM segment are inactive when expressed alone, but they exhibit ≈50% of the activity of the wild type enzyme when expressed together. Omission of JM-A on either the activator kinase mutant or the receiver kinase mutant reduces activity significantly indicating that both the JM-A and JM-B segments (Fig. 6) are required for full activation. These investigators showed by NMR studies of the isolated peptide corresponding to the JM segment of EGFR that the JM-A portion forms an antiparallel coiled-coil. They suggested that the formation of the coiled-coil by the JM segment stabilizes the asymmetric dimer of kinase domains and leads to the allosteric activation of the receiver kinase.

Based upon the X-ray crystal structure of the ErbB4 asymmetric dimer reported by Wood et al. [69], Jura et al. noted that the JM-B domain latches the receiver kinase to the surface of the C-lobe of the activator kinase [68]. Jura et al. performed experiments on EGFR and found that single mutations of Arg949, Asp950, Arg953, or Asn972 of the C-lobe of the activator kinase inhibit EGFR autophosphorylation in cell-based assays; these results are consistent with the notion that these residues anchor the JM-B region of the receiver kinase to the C-lobe of the activator kinase [68]. They found that mutation of Glu666 in the JM-B segment of the receiver kinase, which forms a salt bridge with Arg949 of the activator kinase, is also inhibitory. They reported that Leu664, Val665, and Leu668 of the JM-B region of the receiver kinase are also essential for EGFR activation.

Jura et al. introduced an Arg953Ala mutation into the C-lobe of full-length EGFR constructs, which disrupts the juxtamembrane latch [68], into (i) a mutant that can function only as a receiver kinase or (ii) into a mutant that can function only as an activator kinase. They found that the Arg953Ala mutation had no effect on EGFR activity when introduced into the receiver kinase in cotransfection experiments, but activation is reduced when introduced into the activator kinase. These results indicate that the juxtamembrane latch involves the C-lobe of the activator kinase domain, but not that of the receiver.

Bocharov et al. determined the structure of the TM segment (nascent residues 653–675) of ErbB2 by NMR in a lipid bilayer environment [70]. Their construct (641–684) contained additional residues on both sides of the transmembrane segment. They found that this peptide assembled into two transmembrane helices thereby forming a right-handed α-helical symmetric dimer with tight helical packing through an N-terminal Thr652-$(X)_3$-Ser656-$(X)_3$-Gly660 motif, leaving the C-terminal ends splayed apart. Mineev et al. of the same group found that the heterodimer of ErbB1 and ErbB2 formed a similar structure [71]. Significantly, neither ErbB1 nor ErbB2 homodimers formed in these experiments indicating the propensity for heterodimer formation.

The Thr652-$(X)_3$-Ser656-$(X)_3$-Gly660 motif is a member of the two glycine residues in the distance of four (GG4)-like motif – GxxxG – first described in glycophorin A [72]. In the case of ErbB2, the signature has a (Small residue)-$(X)_3$-(Small residue)-$(X)_3$-Gly sequence. All four ErbB family members possess an N-terminal GG4-like motif. Moreover, ErbB1/2/4 each possess a C-terminal GG4-like signature, which is lacking in kinase-impaired ErbB3. Escher et al. suggested that interaction of the N-terminal motifs of the transmembrane dimer corresponds to the active receptor while interaction of the C-terminal signatures of the transmembrane dimer corresponds to the inactive receptor (Fig. 6) [73].

The EGFR N-terminal GG4-like motif (residues 624–629) is Thr-Gly-Met-Val-Gly-Ala, which consists of two overlapping motifs (TGMVG and GMVGA). The C-terminal motif (residues 637–641) consists of Ala-Leu-Gly-Ile-Gly. Based upon cross-linking experiments, Lu et al. reported that the ligand-bound active EGFR dimer contains the N-terminal contacts [74]. Using molecular dynamics simulations, Arkhipov et al. concluded that the N-terminal dimer is stable whereas the C-terminal dimer is unstable [67]. The former may be more stable owing to the presence of the two overlapping GG4-like motifs.

Endres et al. determined the NMR structure of a fragment of EGFR spanning the transmembrane helix and the first 29 residues of the juxtamembrane segment (residues 618–673) in lipid bilayers [75]. They confirmed that the transmembrane helices formed a right-handed α-helical symmetric dimer as noted above [70,71]. They found that the transmembrane helices form a ≈44° angle with each other that results in the separation of the C-terminal ends of the helices by ≈20 Å, and this separation would provide the appropriate spacing for the antiparallel interaction between the JM-A helices. These investigators reported that their NMR analysis of the EGFR fragment supports the formation of antiparallel helices outside of the lipid bilayer by a ^{655}Leu-Arg-Arg-Leu-Leu^{659} motif in the JM-A segment [75]. The interface between the two helices is formed by the side chains of Leu655, Leu658, and Leu659.

Endres et al. reported that mutation of four small residues in the N-terminal transmembrane interface to isoleucine (Thr624/Gly625/Gly628/Ala629) results in significant inhibition of EGFR activation [75]. These results provide evidence for the importance of the N-terminal association between transmembrane helices in receptor activation. These workers found that an Ile640Glu mutation, which is present in and expected to stabilize the C-terminal dimerization motif, brings these residues together and disrupts the antiparallel JM-A interaction. Endres et al. reported that molecular dynamics computer simulations of the construct indicated that the formation of a C-terminal transmembrane interface is not compatible with the formation of the juxtamembrane dimer interface [75]. Furthermore, the introduction of the Ile640Glu mutation into the intact receptor impairs EGF-dependent activation. Accordingly, these results indicate that the interaction of the transmembrane helices through their N-terminal dimerization domain coupled to the formation of an antiparallel interaction of the JM-A helices is essential for the activation of the EGFR kinase domain.

The JM-A segment is rich in positively charged residues and Arkhipov et al. reported that they interact extensively with anionic lipids as determined by molecular dynamics simulations [67]. Moreover, the JM-A hydrophobic residues become buried in lipid bilayers. Their results support the notion that the JM-A regions exist as (i) an antiparallel helix dimer (the active state) or (ii) separated JM-A segments embedded in the membrane (the inactive state). The role that the plasma membrane plays in switching between the active and inactive states of receptor kinases, which is difficult to address structurally, represents an important new concept for our understanding of the regulation of receptor protein-tyrosine kinase activity *in vivo*. Bessman and Lemmon noted that a better appreciation of the interaction of the protein receptor and the

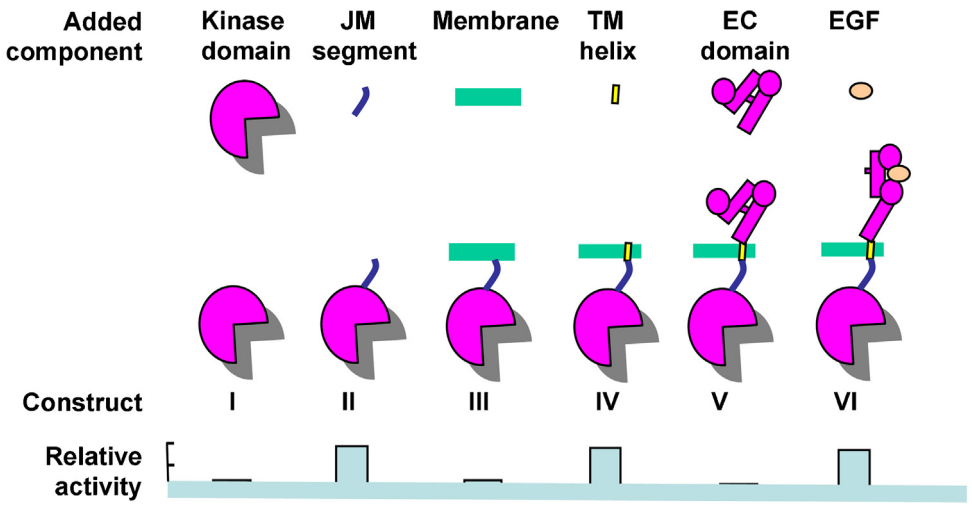

Fig. 7. Activity of various EGFR constructs. Although the active enzyme forms are dimers, they are shown as monomers for purposes of clarity. EC, extracellular; JM, juxtamembrane; TM, transmembrane.
Adapted from Ref. [67].

plasma membrane will be required to advance our comprehension of receptor-mediated signal transduction [76].

3.4.3. *A functional model of EGFR*

Arkhipov et al. combined the known and inferred structures of the separate parts of human EGFR into a blueprint or model of the complete receptor (excluding the carboxyterminal tail) [67]. The inactive monomeric EGFR extracellular domain exists in a tethered conformation attached to the transmembrane helix, with a portion of the intracellular JM-A segment embedded in the plasma membrane and with the JM-B segment connected to the inactive kinase domain. These investigators placed the kinase domain so that its two positively charged patches (Lys689, Lys690, Lys692, and Lys715 in one and Arg779, Arg817, Lys851, and Lys889 in the other) are in contact with the plasma membrane and interact with anionic lipid head groups. The postulated association of the kinase domain of a receptor protein-tyrosine kinase with membranes implicates yet another potential layer of receptor protein kinase regulation.

Although inactive EGFR is usually present as a monomer in normal cells, at higher levels of expression, inactive preformed dimers are observed. Chung et al. proposed that such preformed dimers are primed for ligand binding [77]. Using molecular dynamic simulations, Arkhipov et al. reported that the ligand-free extracellular dimer domains exhibit a bent domain IV along with rearrangement of domains I and III when compared with the ligand-free inactive monomer [67]. Instead of a V-shaped arrangement of domains IV in the two-ligand dimer (Fig. 6), they adopt an antiparallel arrangement resembling an equal sign with a distance of ≈45 Å between the two C-terminal ends. This distance disallows the formation of the active form of the transmembrane helices.

Arkhipov et al. assembled an inactive ligand-free EGFR extracellular domain dimer; their model included C-terminal transmembrane helices with the membrane-embedded JM-A segment attached to an inactive symmetric kinase dimer [67]. The symmetric kinase dimer is connected to a pair of separated juxtamembrane segments embedded in the membrane. They placed the symmetric dimer so that its positively charged patches face the membrane resulting in the occlusion of the substrate-binding sites by the membrane. The involvement of the symmetric dimer in inactive EGFR is consistent with the low-resolution visualization of a globular kinase dimer that differs from the rod-like asymmetric active kinase dimer [78]. The symmetric dimer may be readily connected to a pair of separated juxtamembrane segments embedded in the plasma membrane.

For their model of the active EGFR dimer, Arkhipov et al. assembled the ligand-activated extracellular domain symmetric back-to-back dimer with the N-terminal transmembrane helices connected to the antiparallel JM-A dimer and with the JM-B segment of the receiver kinase forming a latch with the C-lobe of the activator kinase (Fig. 6) [67]. In this situation, the peptide/protein substrate binding site of the allosterically activated receiver kinase faces the interior of the cell. Although not depicted in Fig. 6, the extracellular modules are flexible and may rest on the membrane surface, in agreement with measurements made by Kästner et al. [79].

In the assembly of intact EGFR, the kinase domain in solution exhibits low activity (Fig. 7). The addition of the JM segment promotes receptor dimerization via the JM-A coiled-coil and the formation of the JM latch, which leads to protein kinase activation. The addition of the membrane buries a portion of the JM-segment and disallows the formation of the (i) coiled-coil helix and the (ii) juxtamembrane latch, which stifles kinase activation. Addition of the transmembrane segment allows the N-terminal transmembrane helices to dimerize thereby promoting the formation of an activated dimer. When the extracellular domain is added, formation of the N-terminal transmembrane helices is disallowed, resulting in the formation of an inactive monomer or dimer. When EGF is added, the activated (i) receptor extracellular domain, (ii) N-terminal transmembrane helices, (iii) JM-A helices, (iv) juxtamembrane latch, and (v) the asymmetric dimer yield the allosterically activated receiver kinase. Owing to conservation of important regulatory amino acids in the entire ErbB family, it is likely that the same mechanism is operational in the formation of active homo and heterodimers taking into account the inability of ErbB2 to bind ligand and the impaired ability of ErbB3 to function as a protein kinase.

4. ErbB/HER signaling and receptor down regulation

4.1. *ErbB signaling*

The ErbB/HER signaling networks consist of several modules that are interconnected and overlapping [80]. These include the phosphatidylinositol 3-kinase (PI3K)/Akt (PKB) pathway, the Ras/Raf/MEK/ERK1/2 pathway, and the phospholipase C (PLCγ)

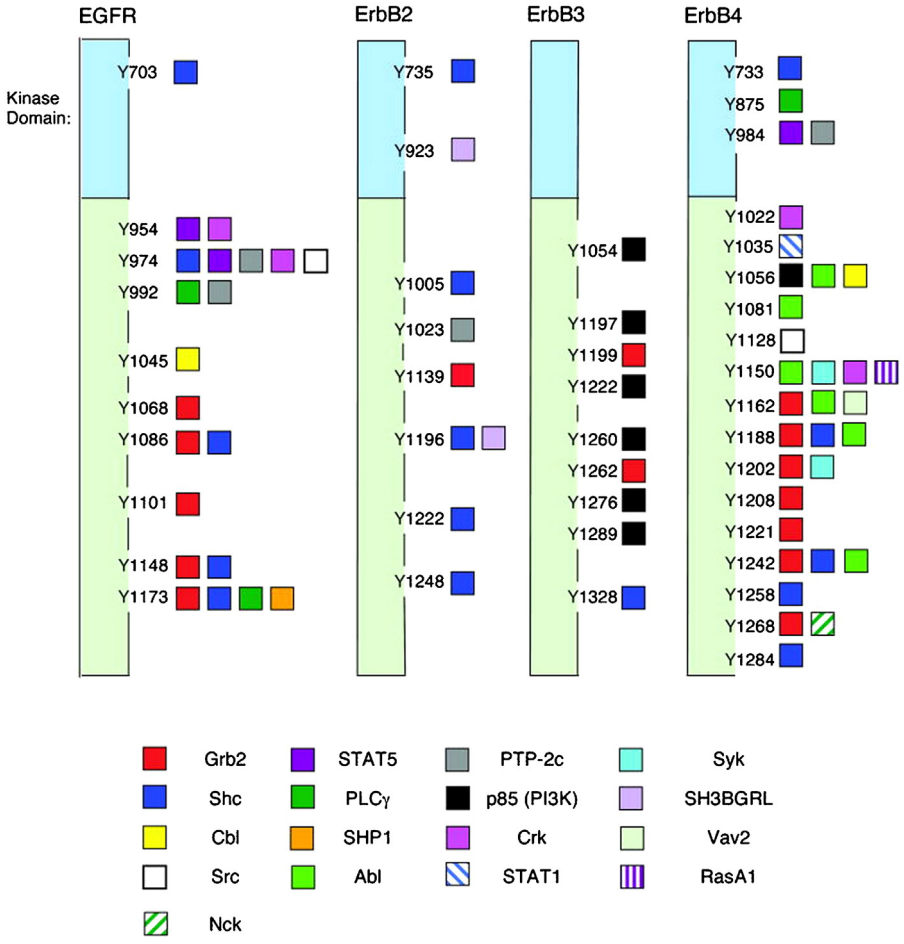

Fig. 8. Signaling by the ErbB/HER protein tyrosine kinases. The tyrosyl phosphorylation sites and their binding partners are depicted. The receptors are not drawn to scale. The residue numbers on EGFR correspond to the mature protein while those of ErbB2/3/4 correspond to the nascent protein including the signal peptides.
The figure is reproduced from Ref. [83] with copyright permission from Elsevier.

pathway. The PI3K/Akt pathway plays an important role in mediating cell survival and the Ras/ERK1/2 and PLCγ pathways participate in cell proliferation [81]. These and other ErbB signaling modules participate in angiogenesis, cell adhesion, cell motility, development, and organogenesis [82].

The ErbB3 receptor plays a major role in promoting cell survival. The regulatory subunit (p85) of PI3K binds potentially to a half dozen phosphotyrosines in ErbB3 that lead to the activation of PI3K activity (Fig. 8). This enzyme catalyzes the phosphorylation of membrane-bound phosphatidylinositol 4,5-bisphosphate (PIP_2) to form phosphatidylinositol 3,4,5-trisphosphate (PIP_3), which attracts Akt to the plasma membrane (Fig. 9A). Akt, which is also known as protein kinase B (PKB), is a protein-serine/threonine kinase that binds to phosphatidylinositol trisphosphate with high affinity [84,85]. PTEN catalyzes the hydrolysis of phosphatidylinositol 3,4,5-trisphosphate to form phosphatidylinositol 4,5-bisphosphate and inorganic phosphate; it negatively regulates the Akt/PKB pathway.

Phosphoinositide-dependent protein kinase 1 (PDK1) and mammalian target of rapamycin complex 2 (mTORC2) catalyze the phosphorylation of Akt Thr308 and Ser473, respectively, and the bisphosphorylated and activated Akt catalyzes the phosphorylation and activation of mTOR (mammalian target of rapamycin) [84]. mTOR is also a protein-serine/threonine kinase that has dozens of substrates and participates in many cellular processes including that of cell survival. Akt also catalyzes the phosphorylation and inhibition of Bcl2-associated death promoter (BAD); unphosphorylated BAD is pro-apoptotic [85].

The activation of the ERK1/2 MAP kinase pathway by the ErbB family is intricate. The adaptor protein Grb2, which is upstream from Ras, binds to several phosphotyrosine residues in ErbB1/2/3/4 [83]. The Shc adaptor protein has potential binding sites in ErbB1/2/3/4. The binding of Grb2 or Shc to phosphotyrosines in the ErbB family in sequence-specific contexts leads to the activation of the Ras/Raf/MEK/ERK1/2 signaling module (Fig. 9B) [86,87]. SOS is a Ras-guanine nucleotide exchange factor that mediates the exchange of GTP for GDP; SOS, or son of sevenless, was initially characterized in *Drosophila melanogaster* where it operates downstream of the *sevenless* gene and activates the Ras/MAP kinase pathway. ERK1/2 have several substrates including protein kinases and transcription factors that promote cell division [88]. Although Grb2 participates in many aspects of signal transduction involving numerous receptor protein-tyrosine kinases, its role in biology was initially established as a link between EGFR phosphorylation and Ras activation [89].

Nck1 (Uniprot ID: P16333) and Nck2 (Uniprot ID: O43639) are adaptor proteins that contain one SH2 and three SH3 domains and interact with dozens of signaling proteins [90]. They play a role in Ras activation. The SH2 and SH3 domains bind numerous cellular scaffolding and regulatory proteins within diverse multiprotein signaling modules. CrkI (SH2–SH3) and CrkII (SH2–SH3–SH3) are splicing isoforms of Crk that regulate transcription and cytoskeletal reorganization for cell growth and motility by linking tyrosine kinases to small G proteins [91]. CrkI shows substantial transforming or tumorigenic activity, whereas the transforming activity of CrkII is low. The molecular mechanisms underlying the distinct

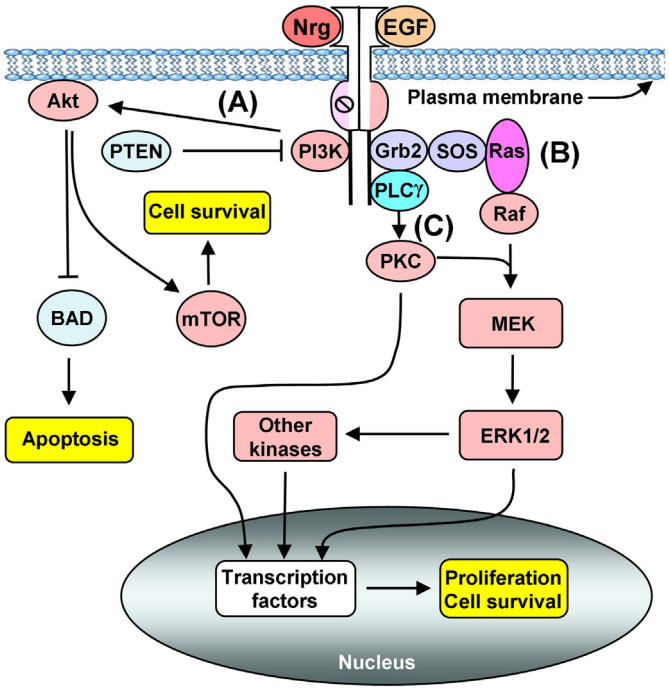

Fig. 9. Overview of ErbB family signaling. The main downstream signaling modules include (A) PI3K, (B) Ras/Raf/MEK/ERK1/2, and (C) PLCγ. PI3K, PLCγ, and Grb2 bind to phosphotyrosines in the carboxyterminal tail of the receptors to initiate the signaling process. Many of the arrows depict processes that require several steps. The PI3K regulatory subunit binds to kinase-impaired ErbB3, which is denoted by a stop symbol ⊘. PTEN, phosphatase and tensin homolog, the product of a tumor suppressor gene.

biological activities of the Crk proteins remain elusive. Vav2, a guanine nucleotide exchange factor for the Rho family of Ras-related GTPases, is expressed in a variety of cells [92]. Vav2 is a substrate for EGFR. EGF regulates Vav2 activity through PI3K activation, whereas tyrosine phosphorylation of Vav2 may be necessary for mediating protein-protein interactions. Vav2 is one of three members (Vav1/2/3) of the Vav family (vav is the sixth letter of the Hebrew alphabet).

STAT1 (UniProt ID: P42224) and STAT5 (UniProt ID: P42229) are transcription factors (signal transducers and activators of transcription) that contain a single SH2 domain and are implicated in tumor angiogenesis and cell survival. STAT1 is rapidly activated following EGF stimulation of human embryonic kidney 293 cells [93]. It then moves to the nucleus, where it is involved in the regulation of gene transcription. SH3BGRL is an SH3 domain-binding glutamic-acid-rich like protein that may play a role as a regulator of redox activity [94]. The protein is up regulated in glioblastoma [95]. RasA1 (UniProt ID: P20936) is one of six Ras GTPase activating proteins (RasGAPs) [96] that has two paradoxical activities. It mediates the hydrolysis of Ras-GTP to form inactive Ras, and its amino-terminal SH2–SH3–SH2 domain transmits mitogenic signaling to downstream binding partners [97].

ErbB1 and ErbB4 possess binding sites for the non-receptor protein-tyrosine kinase Src [83]. Src plays important roles in cell proliferation and survival and stimulation of EGFR leads to Src activation [98]. The Abl1 (Uniprot ID: P00519) and Abl2 (Uniprot ID: P42684) proto-oncogenes encode non-receptor protein-tyrosine kinases that are implicated in the response to genotoxic stress and in the regulation of the actin cytoskeleton [99]. Each contains one SH2 and one SH3 domain that work together to suppress kinase activation. Syk (spleen protein-tyrosine kinase where y is the one-letter abbreviation for tyrosine) is a non-receptor protein-tyrosine kinase (Uniprot ID: P43405) containing two SH2 domains and it plays a role in transmitting signals from receptor kinases including ErbB4 (Fig. 8). Syk has been implicated as both a positive and negative regulator in the pathogenesis of breast cancer, and the reason for these paradoxical results is unclear [100].

ErbB1, ErbB2, and ErbB4 possess several potential PLCγ phosphotyrosine binding sites [83]. PLC consists of six isoforms (β, γ, δ, ε, ζ, η) [101]. PLCγ1 and γ2, which are the product of two different genes, possess two tandem SH2 domains (nSH2, closer to the N-terminus and cSH2, closer to the C-terminus) and one SH3 domain; the other isoforms lack SH2 and PTB domains and are unable to bind to receptor protein-tyrosine kinases. PLCγ1 is widely expressed in many cell types, but PLCγ2 is expressed chiefly in immune cells. The nSH2 domain of PLCγ1 is responsible for its binding to the ErbB family phosphotyrosines. Activation of PLCγ1 requires its phosphorylation at Tyr783 by the ErbB receptors or other protein kinases. Following phosphorylation, the cSH2 domain binds to pTyr783 leading to a conformational change and PLCγ1 enzyme activation.

After its activation, PLCγ catalyzes the hydrolysis of phosphatidylinositol 4,5-bisphosphate to form inositol 1,4,5-trisphosphate (IP_3) and diacylglycerol (DAG) [101]. Inositol trisphosphate promotes the release of Ca^{2+} from the endoplasmic reticulum and diacylglycerol activates the protein-serine/threonine kinase C (PKC). PKC consists of eight homologous isoforms (α, βI, βII, γ, δ, ε, θ, η) that are the product of seven genes [102,103]. These isoforms are ubiquitously expressed in all tissues during and after development. PKCα, βI, βII, and γ are activated by Ca^{2+} and diacylglycerol, and PKCδ, ε, θ, and η are activated by diacylglycerol alone. PKC is activated by phorbol esters, which are co-carcinogens. PKCζ and ι are atypical isoforms not activated by diacylglycerol, Ca^{2+}, or phorbol esters [103].

PKC has broad substrate specificity and catalyzes the phosphorylation of dozens of proteins and has many divergent physiological effects [104]. These effects include angiogenesis, cell proliferation, cell death, increased gene transcription and translation, cell migration, and cell adhesion. One of the downstream effectors of PKC is the Raf/MEK/ERK1/2 pathway leading to cell proliferation in a process that bypasses Ras [88,105]. PKC also catalyzes the phosphorylation and activation of several transcription factors that lead to cell proliferation and survival (Fig. 9C). PKCε overexpression is observed in breast, colorectal, lung, and stomach cancers [103]. Furthermore, PKCη is implicated in the pathogenesis of non-small cell lung cancer (NSCLC) [106].

Human Shp1 and Shp2 (PTP-2C) are cytosolic protein-tyrosine phosphatases containing two tandem SH2 domains, a phosphatase domain, and a C-terminal inhibitory tail. Shp1 occurs primarily in hematopoietic cells, but it is moderately expressed in many other cell types, especially in malignant epithelial cells [107]. Shp2 is expressed in most cell types. Shp1 and Shp2 are non-membrane cytosolic protein-tyrosine phosphatases. Their N-terminal-SH2 domains block their catalytic domains and keep the enzyme in an inactive conformation [108]. One plausible notion for enzyme regulation entails the recruitment of these enzymes to a phosphotyrosine residue that binds to the N-terminal SH2 domain thereby resulting in phosphatase activation.

Shp1 binds to EGFR and has the capacity to catalyze its dephosphorylation [109]. Shp1 is mainly a negative regulator of signaling pathways in hematopoietic cells that control proliferation, migration, and angiogenesis [107]. It does this by catalyzing the dephosphorylation of EGFR and signaling proteins that are downstream from the receptor. In epithelial cells, however, these enzymes are positive regulators of cell proliferation. Accordingly, Insabato et al. reported that a subset of high-grade breast tumors express an increased amount of Shp1, which has a positive effect in mitogenic signaling in many non-hematopoietic cells [110]. Ras GTPase activating protein (RasGAP) mediates Ras inactivation.

Shp2 catalyzes the dephosphorylation of an EGFR site that attracts RasGAP and thereby negatively regulates RasGAP recruitment to EGFR [111,112]. As a result, Ras remains in its active Ras-GTP state longer and its enhanced signaling promotes cell proliferation and transformation. The precise role of Shp1 and Shp2 in regulating cell proliferation and survival depends on the cellular context.

4.2. ErbB down regulation

Cbl functions as a negative regulator of many signaling pathways that start from receptors at the cell surface, and it mediates the degradation of EGFR. The *c-CBL* proto-oncogene was first discovered as the cellular homolog of *v-Cbl*, a viral transforming gene from a Cas murine retrovirus that causes pre-B cell lymphomas in mice (Cas refers to the Lake Casitas region in California where the virus was isolated) [113]. Cbl family members are components of the ubiquitin ligation machinery involved in the targeting and degradation of phosphorylated proteins. Cbl acts as an E3 ubiquitin-protein ligase, which accepts ubiquitin from specific E2 ubiquitin-conjugating enzymes, and then transfers it to substrates promoting their degradation by the proteasome. The N-terminus of Cbl family proteins contains a conserved tyrosyl kinase binding (TKB) domain composed of a four-helix bundle, a Ca^{2+}-binding EF hand, and a variant SH2 domain. A linker region connects this N-terminal domain with a RING (Really Interesting New Gene) finger domain. The C3HC4 type zinc-finger (RING finger) is a cysteine-rich domain of about 40 residues that coordinates two zinc ions; C3HC4 refers to three cysteines, one histidine, and four cysteines. The RING finger domain recruits a ubiquitin-conjugating enzyme (E2), and the N-terminal tyrosyl kinase-binding domain mediates the conjugation, or covalent attachment, of ubiquitin to target proteins. At the C-terminus of Cbl is a ubiquitin associated (UBA) domain of approximately 40 amino acid residues that is found in diverse proteins involved in the ubiquitin/proteasome pathway and cell signaling via protein kinases.

The nature of the ligand plays a role in the fate of EGFR following endocytosis, ubiquitylation, and degradation [114]. EGF, but not TGFα, efficiently induces the degradation of EGFR. Following endocytosis, Longva et al. reported that TGFα dissociates from the EGFR at the low pH (5.5–6.0) of early endosomes, which leads to a rapid decrease of EGFR ubiquitylation and consequent receptor recycling [114]. EGF, by contrast, has a higher affinity for EGFR and remains persistently bound to the receptor along the endocytic route, thereby favoring continued EGFR ubiquitylation and degradation. These investigators showed that overexpression of dominant negative N-Cbl inhibits (i) ubiquitylation of EGFR and (ii) the degradation of EGF and EGFR. This demonstrates that EGF-induced ubiquitylation of EGFR is important for lysosomal sorting. Both lysosomal and proteasomal inhibitors blocked degradation of EGF and EGFR. Furthermore, lysosomal sorting of EGFR is regulated by proteasomal activity. These investigators found that inhibition of EGFR protein kinase activity resulted in the dissociation of EGFR from Cbl. Following EGF stimulation, Umebayashi reported that Cbl remains associated with EGFR and promotes receptor ubiquitylation along the endocytic route, thereby ensuring that the receptors are directed to multivesicular endosomes and targeted for lysosomal degradation [115]. Taken together, these data support the notion that ubiquitylation of EGFR is a signal for multivesicular endosome sorting and lysosomal degradation [116].

Carpenter and Cohen studied the binding of human ^{131}I-EGF to human foreskin (HF) fibroblasts [117]. They reported that ^{125}I-EGF binding exhibits saturation thereby indicating that there is a finite number of binding sites and that binding is specific. At 37 °C, cell-bound ^{125}I-EGF was recovered initially in a native form by acid extraction; upon subsequent incubation, cell-bound ^{125}I-EGF is degraded rapidly, with the appearance in the medium of ^{125}I-monoiodotyrosine. At 0 °C, cell-bound ^{25}I-EGF is not degraded, but slowly dissociates from the cell. The data are consistent with a mechanism in which ^{125}I-EGF is bound to the cell surface and is subsequently internalized before degradation. After the binding and degradation of ^{125}I-EGF, the fibroblasts are no longer able to rebind added hormone. The binding capacity of these cells is restored by incubation in a serum-containing medium; this restoration is inhibited by the protein synthesis inhibitor cycloheximide and the RNA synthesis inhibitor actinomycin D. These studies indicate that (i) growth factor uptake is temperature dependent, (ii) EGF and EGFR undergo degradation, and (iii) expression of new receptor requires RNA and protein synthesis. Binding of EGF to EGFR at 37 °C rapidly induces the clustering of ligand–receptor complexes into coated pits, internalization of the complexes, and ultimately lysosomal degradation of both EGF and EGFR [118].

Baulida et al. measured the endocytic capacities of all four members of the human EGF receptor family [119]. They used EGF-responsive chimeric receptors containing the extracellular segment of EGFR and the intracellular segments of ErbB2/3/4. They studied the capacity of these growth factor-receptor complexes to mediate ^{125}I-EGF internalization, receptor down regulation, and receptor degradation. They reported that EGF stimulated the phosphorylation of EGFR and each of the receptor chimeras; phosphorylation of EGFR and the EGFR/ErbB3 chimera was low, that of EGFR/ErbB4 was higher, and that of EGFR/ErbB2 was the highest. They found that ^{131}I-EGF is rapidly internalized by EGFR, but the rate of internalization mediated by ErbB2, ErbB3, or ErbB4 cytoplasmic domain-containing chimeras was about one quarter that of EGFR. Baulida et al. measured the half-lives of the receptors after incubating the cells with ^{35}S-labeled amino acids for 14 h. The half-lives for the receptors without or with EGF in the culture medium were as follows: EGFR (6.5 and 1.5 h), EGFR/ErbB2 (8.0 and 7.0 h), EGFR/ErbB3 (3.5 and 3.0 h), and EGFR/ErbB4 (6.0 and 5.5 h). These data indicate that of all of the ErbB family members, only occupied EGFR is rapidly internalized and degraded. Since endocytosis is thought to be an attenuation mechanism for growth factor–receptor complexes, these experiments indicate that substantial differences in this process occur within this family of structurally related receptors.

4.3. Nuclear localization and function of the ErbB family

In addition to the well-studied role of the ErbB receptors functioning from the plasma membrane, there is also evidence that these receptors are translocated to the nucleus where they participate in cell signaling [120]. In experiments with normal and regenerating rat liver published in 1991, Marti et al. reported that (i) isolated nuclei from both normal and regenerating rat liver are capable of binding ^{125}I-EGF, (ii) the nuclear EGF-binding protein is similar in molecular weight to the plasma membrane EGFR, (iii) monoclonal antibodies produced against the plasma membrane EGFR recognize the nuclear EGFR and (iv) the nuclear receptor has an affinity for EGF comparable to that of the plasma membrane receptor, but fewer (approximately 10%) nuclear receptors are found per mg protein when compared with the plasma membrane receptor [121]. These initial studies indicate that full length EGFR resides in the nucleus, but additional studies are required to address the nuclear localization mechanism(s) and the potential signaling function of nuclear receptors, some of which are described next.

Clathrin-dependent and independent endocytosis of EGFR represents the first step in receptor (i) down regulation, (ii) degradation, (iii) recycling back to the plasma membrane, and (iv) nuclear translocation that occurs after endocytic vesicles fuse with early endosomes [122]. The nucleus is separated from the cytoplasm by a double membrane envelope that allows for the selective entrance

of proteins of molecular weight greater than 40 kDa through specialized nuclear pore complexes [123]. Smaller proteins, ions, and metabolites pass through the nuclear pore by diffusion. The nuclear pore complex is made up of approximately 30 different proteins collectively known as nucleoporins [123–125]. Intricate pathways exist for both the nuclear import and export of cellular macromolecules. EGFR and ErbB2 are reported to translocate into the nucleus by importin α/β-dependent mechanisms [126,127].

The classical pathway for the nuclear uptake of proteins involves a nuclear localization signal (NLS) containing either one or two clusters of positively charged amino acids that bind to the importin-α armadillo domain [128]. One nuclear localization signal conforms to the consensus sequence KK/RXK/R (where X is any amino acid). Polar and acidic side chains of importin-α bind to the basic nuclear localization signal side chains. The binary importin-α/cargo complex binds to importin-β, and a ternary complex (importin-β/importin-α/cargo) is translocated into the nucleus. Transport involves the interaction of importin-β with the nucleoporins that constitute the nuclear pore complex. The ternary complex is disassembled on binding Ran-GTP in the nucleus [129]. The cargo is retained in the nucleus and the importins shuttle back into the cytoplasm.

EGFR contains a positively charged sequence that interacts with importin-β. This sequence (residues 645–657 of the mature protein) occurs in the juxtamembrane segment and contains three clusters of basic amino acids: RRRHIVRKRTLRR. The sequence is conserved in the other ErbB family members. Lo et al. reported that EGFR mutated in this basic region is defective in associating with importin-β and in entering the nucleus [126]. This finding suggests that these residues are critical for EGFR/importin-β interaction and EGFR nuclear import. These investigators also found that nuclear export of EGFR may involve exportin-1 (the CRM1 homolog in yeast) as they detected EGFR/exportin-1 complex formation and a marked increase in nuclear EGFR localization following exposure to leptomycin B, an exportin-1 inhibitor.

Hsu and Hung fused the 13-amino-acid basic cluster sequence to the C-terminus of a cytoplasmic protein, chicken pyruvate kinase, which had been tagged with green fluorescent protein [130]. They found that the control tagged pyruvate kinase was predominantly found in the cytoplasm of transfected human HeLa cells, whereas the tagged pyruvate kinase bearing the 13-amino-acid basic sequence was clearly observed in the nucleus. This result suggests that this sequence functions as a nuclear localization signal and can lead to the translocation of a large cytoplasmic protein into the nucleus. They also demonstrated that mutating each of these three basic amino acid clusters to alanine leads to significant impairment of the nuclear localization of EGFR and that of the green fluorescent protein-pyruvate kinase bearing the basic 13-amino-acid residue sequence. They also found that the pyruvate kinase reporter construct bearing the homologous basic amino acid sequences of human ErbB2 and ErbB4 were translocated into the nucleus. They reported that the activity of the ErbB3 sequence in translocating the reporter construct into the nucleus, although significant, was weaker than that of the ErbB1/2/4.

Various functions have been ascribed to the ErbB family localized within the nucleus. These include cell proliferation, DNA replication, DNA damage repair, transcription, development, and cancer growth or spread [131]. The C-terminal regions of ErbB1/2/3/4 display intrinsic gene transactivation activity. Lin et al. reported that nuclear EGFR binds to an A/T-rich sequence in the proximal region of the *CCND1* promoter in the human breast cancer MDA-MB-468 EGFR-overexpressing cell line [132]. This gene encodes cyclin D1 and these results provide a direct link between nuclear EGFR function and cell proliferation. Cyclin D1 activates cyclin-dependent protein kinases, which are important participants in cell cycle regulation.

Brand et al. reported that full-length ErbB3 is expressed in the nucleus of several human cancer cell lines including breast (SKBr3, MCF-7, BT474, HCC1954, and BT549), lung (H226 and SCC6), head and neck (SCC6 and SCC1), and colon (LoVo and CaCO2) [133]. They fused the yeast Gal4 DNA binding domain (Gal4DBD) of the yeast transcription factor Gal4 to the ErbB3 or EGFR (i) intracellular juxtamembrane, (ii) tyrosine kinase, or the (iii) C-terminal tail domains. Following transfection into H226, SKBr3, or human colorectal CHOK1 cells, they found that the ErbB3 and EGFR C-terminal domains, but not the JM segments or kinase domains, increased luciferase reporter activity. Using a series of truncated constructs, they narrowed the transactivation activity in ErbB3 to two regions in the C-terminal tail: B1 (residues 1215–1248) and B2 (residues 1281–1302 of the nascent protein). Using chromatin immunoprecipitation assays (ChIP), they demonstrated that ErbB1, ErbB2, and ErbB3 each interacted with the cyclin D1 promoter in SKBr3 cells. These investigators also found that overexpression of ErbB3 increased cyclin D1 transcript expression in SCC6 cells by 92% and in BT474 cells by 35%. In contrast, siRNA knockdown of ErbB3 decreased cyclin D1 expression in H226 cells by 39% and in MCF-7 cells by 50%. These studies further document the role of the ErbB family in the direct regulation of gene expression.

Other targets of EGFR include the *NOS2* (inducible nitric oxide synthase), *AURKA*, and *BMYB* genes [131]. Nitric oxide synthase catalyzes the formation of nitric oxide (NO) that has diverse signaling functions in inflammation, the cardiovascular system, and neoangiogenesis in cancer [134]. The *AURKA* gene encodes the Aurora A protein-serine/threonine kinase that associates with the centrosome and microtubules during mitosis and B-Myb is a transcription factor that participates in cell differentiation, proliferation, and survival.

The protein kinase activity of the ErbB family also plays a role in its nuclear function [131]. EGFR mediates the phosphorylation of PCNA, the chromatin-associated DNA proliferative cell nuclear antigen. PCNA participates in DNA synthesis and DNA damage repair. Furthermore, nuclear CDK2 is a substrate of ErbB2. Phosphorylation of CDK2 at Tyr15 by ErbB2 inhibits its activity and delays M-phase entry.

The JMa isoform of the ErbB4 receptor possesses a mechanism of nuclear translocation that requires dual-protease cleavage [120]. Binding of Nrg-1 to ErbB4 results in the formation of a 120 kDa membrane-bound fragment following cleavage between His641 and Ser642 as catalyzed by ADAM17 (residues corresponding to the nascent protein). The remaining membrane-anchored portion of ErbB4 (m80) is further cleaved within its transmembrane domain by γ-secretase, which produces a soluble dimeric, active form of the intracellular domain (ICD) of ErbB4 designated E4ICD that is translocated into the nucleus. Sardi et al. discovered that the generation of E4ICD is required for the control of astrogenesis in the developing mouse [135]. These investigators demonstrated that E4ICD forms a complex with TAB2, an adaptor protein, which requires the tyrosyl kinase activity of the ErbB4 fragment. However, TAB2 is not phosphorylated in response to ErbB4 activation by Nrg-1. The dimeric E4ICD/TAB2 complex binds to the nuclear receptor corepressor N-CoR and the ternary E4ICD/TAB2/N-CoR complex translocates into the nucleus.

The nuclear translocation of the E4ICD/TAB2/N-CoR complex represses the transcription of several glial genes that are required for the differentiation of neuronal precursor cells into astrocytes [135]. Nrg-1 stimulation of neuronal precursor cells antagonizes the ability of ciliary neurotrophic factor to promote astrogenesis by repressing genes such as *GFAP* (glial fibrillary acidic protein, an intermediate filament) and *S100B* (a Ca^{2+} and Zn^{2+} binding protein) through the γ-secretase mechanism outlined above, thereby maintaining the neurogenic state. Sardi et al. used RNAi knockdown of TAB2 and ErbB4 to demonstrate that these proteins are critical

for the inhibitory effect of Nrg-1 on astrogenesis [135]. Chromatin immunoprecipitation (ChIP) assays demonstrated that E4ICD associates with the *GFAP* and *S100β* promoters in an Nrg-1-dependent fashion.

Astrogenesis occurs later in development than neurogenesis, and nuclear ErbB4 signaling appears to play a pivotal role in creating this delay by inhibiting the onset of astrogenesis [135]. Mice deficient in ErbB4 show precocious cortical astrogenesis, which can be rescued by expression of the cleavable JMa isoform of ErbB4, but not by the JMb isoform. ErbB4 and other pathways initiate a molecular program in early stages of development that preferentially stimulates neurogenesis more than astrogenesis. Astrogenesis is repressed by the γ-secretase action of the JMa isoform of ErbB4. At a later stage of embryonic development, expression of the JMa ErbB4 isoform in neuronal precursor cells is reduced, and this reduction enables the induction of astrocyte development by other stimulatory signals [136].

Nuclear EGFR has been detected in a variety of cancer types including breast [126], NSCLC [137], and head and neck squamous cell cancers [138]. Wang and Hun discuss the potential role of nuclear ErbB proteins in tumor metastasis (spread from the original site), progression (growth of the tumor), and resistance to radiation therapy [131]. The work of Sardi et al. demonstrated that ErbB4 participates in a biologically significant signaling mechanism mediated by direct nuclear action of an activated ErbB4 fragment that is transported from the cell membrane to the nucleus in a manner that is regulated by Nrg-1, a known ErbB4 ligand [135]. Findings from several studies cited in this section provide evidence for the existence of the full-length ErbB receptors in the nucleus. However, Schlessinger and Lemmon point out several caveats regarding the proposed nuclear translocation mechanisms of these full-length ErbB family receptors [139]. Questions about their precise nuclear functions and translocation mechanisms remain to be determined.

5. *ErbB/HER* family gene amplification, overexpression, mutation, and cancer

5.1. Lung cancer

5.1.1. Classification and general treatment

Lung cancer is the most prevalent malignancy in the world [140]. In 2008, the estimated global incidence of lung cancer was about 1.6 million with about 1.4 million deaths attributed to this malignancy. In 2012, the estimated incidence of lung cancer in the United States was about 228,000 with about 160,000 deaths [141]. These data indicate that lung cancer is a disease of high mortality and that more effective treatments are needed. Lung cancers are classified clinically into two major groups: non-small cell lung cancer (NSCLC), which accounts for about 85% of all lung cancers, and small-cell lung cancer (SCLC), which accounts for the remainder [142]. It is important to distinguish between them because their clinical course and treatments vary.

The most common types of NSCLC include squamous cell carcinoma (≈35% of total lung carcinomas), large cell carcinoma (≈10%), and adenocarcinoma (≈45%) [143]. Squamous cell carcinoma of the lung, which is more common in men than women, is characterized histologically by keratinization in the form of markedly eosinophilic dense cytoplasm and is closely correlated with a history of tobacco smoking (*squamosa* means scale like in Latin). Squamous cell carcinoma most often arises centrally in larger bronchi. While it often metastasizes to hilar lymph nodes early in its course, it generally disseminates outside of the thorax somewhat later than other types of lung cancer. Large-cell lung carcinoma (LCLC) is a heterogeneous group of undifferentiated malignant neoplasms originating from transformed lung epithelial cells. These cells have large nuclei, prominent nucleoli, and a moderate amount of cytoplasm. Adenocarcinoma of the lung, which is the most common type of lung cancer in lifelong non-smokers, is characterized histologically by glandular differentiation and mucin-containing cells (*aden* means gland in Greek). Adenocarcinoma is usually found in the lung periphery, and small cell and squamous cell lung carcinoma are usually found centrally. Small-cell lung cancers are characterized histologically by epithelial cells that are small with scant cytoplasm, ill-defined cell borders, and finely granular nuclear chromatin.

The mainstay of non-metastatic lung cancer treatment is surgical removal [143]. Unfortunately, only 37% of lung cancers are diagnosed before the tumor has spread from its site of origin [141]. Pre-existing medical conditions in patients with stages I or II lung cancer decrease the number of patients that can undergo surgery to 25–33% of the total (down from 37%) (see Ref. [143] for a discussion of the staging classification of lung cancer). Although combined radiotherapy and chemotherapy improves survival of metastatic lung cancer, the overall five-year survival is less that 15% [144]. A common chemotherapeutic regime for non-squamous cell NSCLC includes paclitaxel and carboplatin [145]. Paclitaxel enhances microtubule polymerization and thus interferes with microtubule breakdown during cell division. Carboplatin is a platinum-based antineoplastic agent that interferes with DNA synthesis and function (Table 5). The angiogenesis inhibitor bevacizumab (Avastin®, a monoclonal antibody that binds to vascular endothelial growth factor A, or VEGF-A), in combination with paclitaxel and carboplatin, improves the survival of people with advanced non-squamous cell NSCLC [145,147]. However, bevacizumab increases the risk of pulmonary hemorrhaging, particularly in people with squamous cell carcinoma. A variety of other cytotoxic regimens for all types of NSCLC can be found at the National Comprehensive Cancer Network (www.NCCN.org). This includes first-line treatment of advanced or metastatic NSCLC with Nab-paclitaxel in combination with carboplatin. Nab-paclitaxel is a nanoparticle albumin formulation of paclitaxel (Table 5) [148].

The term advanced cancer has two meanings for clinical scientists and the meaning is usually, but not always, apparent from the context of its usage. In many cases of a therapeutic nature, advanced cancer refers to a tumor that fails to respond or stops responding to a treatment. At other times advanced cancer refers to an incurable cancer. A locally advanced cancer has grown outside of the organ in which it has started, but has not spread to distant parts of the body. A metastatic cancer has spread from the organ in which it started and can include locally advanced cancer and tumors that have spread to distant parts of the body. A lung cancer, for example, may spread to adjacent lymph nodes (locally advanced) and metastasize to the brain (a distant part of the body).

5.1.2. Mutant ERBB1 oncogenic activation

ErbB1/EGFR plays an important role in the pathogenesis of many lung cancers. Herbst et al. reported that *EGFR* mutations in the kinase domain occur in a range of 10–40% of lung cancer samples [142]. The incidence of *EGFR* kinase-domain mutations is about 10% in caucasian populations and 30–40% in Asian patients. They reported that *EGFR* gene amplification occurs in about 15% of adenocarcinomas and 30% of squamous cell carcinomas, while *ERBB2* amplification occurs in 6% of adenocarcinomas and 2% of squamous cell carcinomas [142]. These alterations are rarely, if ever, observed in small-cell lung cancers.

Overexpression of EGFR occurs in about 60% of NSCLCs as measured by immunohistochemistry [142]. An increase in EGFR levels as a result of gene amplification, increased biosynthesis, or decreased degradation in a large percentage of NSCLCs prompted the development of therapies that inhibit EGFR activity [149]. The United States Food and Drug Administration (FDA) approved gefitinib (Table 6) in 2003 as monotherapy after failure of both platinum

Table 5
Mechanism of action of selected cytotoxic and anti-estrogenic compounds used in cancer therapy.[a]

Drug	Mechanism of action[b]	Acute toxicity[b]	Delayed toxicity[b]
Cytotoxic agents			
Actinomycin D	Inhibits DNA-dependent RNA synthesis	Nausea, vomiting, diarrhea	Myelosupression[c]
Bleomycin	Produces oxygen-dependent single and double-stranded DNA breaks that inhibit DNA synthesis	Fever, mild nausea and vomiting	Pulmonary and skin toxicity
Capecitabine[d]	A prodrug that is metabolized to 5-flurorouracil, which inhibits thymidylate synthase, DNA synthesis and function, and RNA function	Nausea and vomiting	Hand-foot syndrome,[e] myelosuppression
Carboplatin	A second-generation platinum-based drug that binds to and cross-links DNA, which inhibits DNA synthesis and function	Nausea and vomiting	Myelosuppression, nephrotoxicity, peripheral neuropathy
Cisplatin	A first-generation platinum-based drug whose mechanism of action is the same as carboplatin, which is noted above	Severe nausea and vomiting	Myelosuppression, nephrotoxicity, peripheral neuropathy, ototoxicity
Cyclophosphamide	An alkylating agent that forms both intrastrand and interstrand DNA cross links that alter DNA structure, base pairing, replication, and transcription	Nausea and vomiting	Myelosupression, alopecia
Dacarbazine	DNA modifying agent	Nausea and vomiting	Myelosuppression, myalgia, and malaise
Docetaxel	An anti-mitotic taxane that binds to and enhances polymerization of microtubules and inhibits their function	Nausea and vomiting, hypersensitivity reaction	Myelosuppression, peripheral neuropathy, alopecia
Doxorubicin	An anthracycline antibiotic that intercalates with DNA, inhibits the progression of topoisomerase II, and produces oxygen-dependent single and double stranded DNA breaks with subsequent inhibition of DNA function	Nausea and vomiting, cardiotoxicity, vesicant[f]	Myelosuppression, cardiotoxicity, alopecia
Etoposide	DNA topoisomerase II inhibitor that causes DNA strand breakage	Nausea and vomiting	Myelosuppression, alopecia
5-Fluorouracil	An anti-metabolite that inhibits thymidylate synthase, DNA synthesis and function, and RNA function	Nausea, diarrhea	Myelosuppression, hand-foot syndrome, neurotoxicity
Folinic acid (leucovorin)	A compound with folic acid vitamin activity that potentiates the activity of 5-fluorouracil, which is metabolized to 5-fluorodeoxyuridylate[g]	None	
Gemcitabine	A nucleoside analog that inhibits (i) DNA synthesis, repair, and function, (ii) ribonucleotide reductase, and (iii) RNA function	Nausea, rash, flu-like symptoms	Myelosuppression, edema
Irinotecan	A DNA topoisomerase I inhibitor that prevents DNA from unwinding and inhibits DNA synthesis	Nausea and vomiting, diarrhea	Myelosuppression, alopecia
Methotrexate	An anti-metabolite that inhibits dihydrofolate reductase leading to decreased synthesis of purines and thymidylate	Nausea and vomiting	Myelosuppression, gastrointestinal mucositis, pneumonitis, neurotoxicity
Nab-paclitaxel	A nanoparticle albumin bound formulation of paclitaxel, whose mechanism is the same as docetaxel, which is noted above	Nausea and vomiting, hypersensitivity reaction (less than paclitaxel)	Myelosuppression, peripheral neuropathy, alopecia
Oxaliplatin	A third-generation platinum-based drug whose mechanism is the same as carboplatin, which is noted above	Nausea and vomiting	Myelosuppression, peripheral neuropathy
Paclitaxel	An anti-mitotic taxane whose mechanism is the same as docetaxel, which is noted above	Nausea and vomiting, hypersensitivity reaction	Myelosuppression, peripheral neuropathy, alopecia
Pemetrexed	An anti-folate that inhibits dihydrofolate reductase, thymidylate synthase, and purine synthesis *de novo*	Fatigue, nausea and vomiting	Myelosuppression
Temozolomide[d]	A DNA alkylating agent whose mechanism is the same as cyclophosphamide, which is noted above	Nausea and vomiting, headache	Myelosuppression
Vinblastine	An anti-mitotic that binds to tubulin to inhibit microtubule function and arrest mitosis	Mild nausea and vomiting	Myelosuppression with thrombocytopenia, alopecia
Vincristine	See vinblastine	Mild nausea and vomiting	Peripheral neurotoxicity, alopecia
Vinorelbine[d]	See vinblastine	Mild nausea and vomiting, vesicant[f]	Myelosuppression, peripheral neuropathy
Anti-estrogens			
Anastrozole[d]	A non-steroidal anti-estrogen aromatase inhibitor	Nausea	Hot flashes, peripheral edema, hypercholesterolemia, headache, osteoporosis
Letrozole[d]	A non-steroidal anti-estrogen aromatase inhibitor	Nausea	See Anastrozole
Tamoxifen[d]	A selective estrogen receptor modulator (SERM)	None	Hot flashes, vaginal discharge, menstrual irregularities

[a] All drugs are given intravenously unless otherwise noted.
[b] See Ref. [146].
[c] Bone-marrow suppression resulting in fewer red blood cells, neutrophils, or platelets.
[d] Orally effective.
[e] Reddening, swelling, numbness, and desquamation (shedding of the outermost layer of skin) of palms and soles.
[f] Causes blistering.
[g] Thymidylate synthase catalyzes a reaction between methylene-tetrahydrofolate and deoxyuridylate to give thymidylate and dihydrofolate. 5-Fluorodeoxyuridylate is a suicide inhibitor that reacts with methylene-tetrahydrofolate to irreversibly inhibit thymidylate synthase. Folinic acid increases the concentration of methylene-tetrahydrofolate and thereby increases thymidylate synthase inhibition.

Table 6
FDA-approved small molecule drugs targeting the kinase domain and antibodies targeting the extracellular domain of the ErbB1 and ErbB2.[a]

Drug	Company	Target (year approved)	Indications
Small molecule inhibitors			
Afatinib/Gilotrif®	Boehringer Ingelheim	ErbB1 (2013)	First-line treatment of NSCLC with exon-19 deletions or the exon-21 L858R mutation.
Erlotinib/Tarceva®	Genentech/OSI	ErbB1 (2004)	(i) First-line treatment of NSCLC with exon-19 deletions or the exon-21 L858R mutation or (ii) second-line treatment following cytotoxic therapy and (iii) first-line treatment of pancreatic cancer in combination with gemcitabine.
Gefitinib/Iressa®	AstraZeneca	ErbB1 (2003)	Second-line treatment of NSCLC after cytotoxic therapies. Approved in dozens of countries worldwide, but approval was withdrawn in the United States.
Lapatinib/Tykerb®	GlaxoSmithKline	ErbB1/2 (2007)	Second-line treatment of patients (i) with capecitabine for ErbB2-positive breast cancer who have previously received cytotoxic chemotherapy or trastuzumab and (ii) with letrozole in post-menopausal hormone receptor-positive breast cancer.
Monoclonal antibodies[b]			
Ado-trastuzumab emtansine/Kadcyla®	Genentech	ErbB2 (2013)	ErbB2-positive metastatic breast cancer previously treated with trastuzumab and/or a taxane.
Cetuximab/Erbitux®	ImClone/Eli Lilly/Bristol-Myers Squibb	ErbB1 (2004)	(i) Wildtype *KRAS* colorectal cancer in combination with cytotoxic therapies and (ii) head and neck cancers in combination with radiation therapy or cytotoxic chemotherapy.
Panitumumab/Vectibix®	Genentech	ErbB1 (2006)	Second-line treatment for metastatic colorectal cancer following cytotoxic therapies. It is not indicated for *KRAS*-positive mutations or mutation status unknown.
Pertuzumab/Omnitarg®	Abgenix	ErbB2 (2012)	ErbB2-positive metastatic breast cancer in combination with trastuzumab and docetaxel in patients who have not received prior anti-ErbB2 therapy or chemotherapy for metastatic disease.
Trastuzumab/Herceptin®	Genentech	ErbB2 (1998)	ErbB2-positive breast, gastric, and gastroesophageal cancer.

[a] www.accessdata.fda.gov/scripts/cder/drugsatfda/index.cfm.
[b] Therapeutic antibody nomenclature conventions: -mab refers to a monoclonal antibody; -mu-mab refers to a human mab (e.g., panitumumab), -xi-mab refers to a chimeric mab (e.g., cetuximab), and zu-mab refers to a humanized mab (e.g., trastuzumab); -tu-xx-mab is directed toward the tumor (pertuzumab), ci-xx-mab is directed toward the cardiovascular system (e.g., bevacizumab).

and taxane-based therapies [150]. An objective response (tumor shrinkage) occurred in about 10% of patients. Responses were more frequent in females and non-smokers, and the median duration of response was 7.0 months. There was no correlation between EGFR expression and response to gefitinib [151]. This is in contrast to breast cancer where increased ErbB2 expression is correlated with the efficacy of monoclonal antibodies directed against ErbB2 as noted later.

The FDA approved erlotinib in 2004 for the treatment of locally advanced or metastatic NSCLC after failure of at least one prior chemotherapeutic regimen [152]. The median survival duration was 6.7 months compared with 4.7 months for placebo-treated patients. Never smokers and those with EGFR-positive tumors survived longer. As with gefitinib, skin rash is one of the most common adverse events with erlotinib [150,152]. Skin contains appreciable levels of EGFR and its inhibition may lead to skin lesions. Skin rashes may represent a biomarker of EGFR inhibition, and although not universally accepted, patients who develop rashes may be more likely to exhibit a therapeutic effect that those who do not [153]. Moreover, the absence of a skin rash may prompt treatment with a higher drug dosage.

About 10% of unselected patients with NSCLC exhibited rapid and often dramatic responses to gefitinib [154]. In 2004, three groups compared the tumors of patients who responded to gefitinib with non-responders [154–156]. Each of the groups reported that most of the responders possessed mutations of the *EGFR* kinase domain while those of non-responders lacked *EGFR* gene mutations. The most common mutations that these groups reported were (i) the deletion of five exon-19 residues (^{746}Glu-Leu-Arg-Glu-Ala^{750}) that occur immediately before the αC-helix and (ii) the exon-21 substitution of an arginine for leucine (Leu858Arg) in the activation segment (residue numbers include the signal peptide). Together, these two mutations correspond to more than 90% of the activating *EGFR* mutations observed in NSCLC. Pao et al. reported patients who responded to erlotinib also possessed these *EGFR* mutations [156]. The ^{719}Gly-Cys-Ala-Arg-Asp-Val-Ser^{725} P-loop mutations account for about 3% of the activating *EGFR* gene mutations. Altogether, more than 200 *EGFR* mutations have been described in NSCLC (www.somaticmutations-egfr.org) [157].

Two phase III clinical trials in 2009 demonstrated that gefitinib was superior to chemotherapy as an initial, or first-line, treatment for *EGFR*-mutant lung cancer [158]. The response rate for gefitinib was 71% when compared with that of the carboplatin–paclitaxel of 47% in the IPASS trial [159]. The gefitinib group had a longer median progression-free survival of 9.2 months when compared with 6.3 months in the cisplatin plus docetaxel group in the WJTOG3405 Japanese trial [160]. Erlotinib was also effective in the treatment of *EGFR*-mutant lung cancer [161]. Although these responses were significant, they were minor when compared with the overall need.

5.1.3. Targeted inhibition of mutant EGFR by gefitinib, erlotinib, and afatinib

The activating mutations of oncokinases generally occur in or near important regulatory domains such as the αC-helix, the activation segment, the ATP-binding site, or the phosphate binding loop. A general mechanism for the oncogenic activation of the ErbB family of receptors involves the destabilization of the dormant resting state that promotes the formation of the active state. Yun et al. have documented this destabilization as the mechanism responsible for the activation of EGFR for the L858R and G791S mutants (residue numbers including the signal peptide) [162]. The L858R mutation lies in the amino-terminal portion of the activation segment; it immediately follows the ^{855}DFG^{857} sequence that marks the beginning of the activation segment. The substitution of the larger positively charged arginine side chain for the hydrophobic leucine side chain prohibits its occurrence in the dormant activation segment while it is readily accommodated in the active conformation of the EGFR protein kinase domain [162]. They

hypothesize that the Leu860Gln activation segment mutant that occurs in gefitinib and erlotinib-responsive NSCLCs is activated by a similar mechanism.

Yun et al. determined the X-ray structure of the activated G719S mutant EGFR kinase domain [162]. This mutation occurs at the beginning of the P-loop (^{719}GSGAFG^{724}). The P-loop is the most mobile portion of protein kinase catalytic domains, and the G719S mutant retains catalytic competence despite substitution of this conserved residue. Substitutions of alanine or cysteine for Gly719 also occur in NSCLC. The crystallographic structures of the various exon-19 deletion mutants have not been determined. These residues (^{746}Glu-Leu-Arg-Glu-Ala^{750}) occur immediately before the regulatory αC-helix, and we infer that deletion of these residues destabilizes the dormant EGFR protein kinase domain.

Yun et al. measured the activity of the L858R and G719S *EGFR*-mutants that occur in some NSCLCs [162]. They found that the former is 50-fold more active and the latter is 10-fold more active that the wild type enzyme based upon the k_{cat} values of the enzymes for an exogenous peptide substrate. These investigators reported that gefitinib binds more tightly to the L858R mutant than to the wild type enzyme (2.6 nM vs. 54 nM). However, it binds less tightly to the G719S mutant (124 vs. 54 nM). Gefitinib is a competitive inhibitor with respect to ATP and the effectiveness of inhibition during enzyme catalysis can be assessed by the ratio of the K_d/K_m of the wild type and mutant enzymes. A lower ratio (higher ATP K_m) correlates with greater effectiveness. The ratio is 6-fold more favorable for the G719S mutant and 97-fold more favorable for the L858R mutant. These data explain the greater inhibitory effectiveness of gefitinib against the mutant enzymes when compared with the wild type enzyme in NSCLC. Note that the K_d is an equilibrium dissociation constant while the K_m is a steady-state (not equilibrium) dissociation constant under conditions in which the enzyme is catalyzing its reaction [163]. The K_m is the ratio of an ensemble of rate constants and any agreement of the K_m and K_d values of an enzyme for one of its substrates is fortuitous.

Red Brewer et al. characterized the interaction of the L834R activated mutant and the L834R/T766M drug-resistant double mutant with wild type EGFR and ErbB2 [164]. They prepared enzymes that could only function as a donor kinase (I682Q) or an acceptor kinase (V924R) to study various donor–acceptor interactions (residue numbers exclude the signal sequence). They reported that the L834R and drug-resistant double mutant enhance the strength of the donor/acceptor receptor interaction using co-immunoprecipitation assays. They demonstrated that both mutant enzymes hyperphosphorylated wild type EGFR or ErbB2 coexpressed in human kidney HEK293 cells. The co-expression of the L834R activated mutant or the L834R/T766M double mutant increased phosphorylation of Akt and STAT-3, which are downstream signaling molecules. They determined the X-ray crystal structure of the L834R/T766M double mutant and observed that the enzyme forms an asymmetric dimer similar to that observed with EGFR. The experiments support the notion that these activated EGFR mutants preferentially serve as acceptors in the asymmetric dimer; these investigators coined the term superacceptor to describe this property. Following activation by the donor, the mutants then catalyze the hyperphosphorylation of donor EGFR or ErbB2 leading to enhanced downstream signaling. The authors note that the L834R mutation or the L834R/T766M double mutation destabilizes the inactive conformation, and the energetic cost of inducing the active conformation of the acceptor kinase is lower in the mutants than in the wild type enzymes. These investigators did not determine whether the proteins with the deletion of the five exon-19 residues or the P-loop mutations [154–156] result in enhanced acceptor protein kinase activation.

Gefitinib, erlotinib, and afatinib are FDA-approved quinazoline derivatives that form a complex with the ATP-binding site of EGFR. Gefitinib and erlotinib are reversible EGFR inhibitors and afatinib is an irreversible inhibitor. Ward et al. initiated the development of quinazoline-based ErbB protein kinase inhibitors by performing steady-state enzyme kinetics on EGFR partially purified from human squamous cell carcinoma A431 cells and from human placenta [165]. A431 cells, which overexpress EGFR and are widely used in EGFR studies, were originally derived from a vulvar carcinoma obtained from an 85-year old female [166]. Ward et al. found that EGFR forms a terniary complex with ATP and protein substrate prior to the release of any products [165]. This mechanism is observed in essentially all protein kinases [51]. The substrate addition order can be random (PKA) or it can be ordered (VEGFR2), with ATP binding first [167,168].

Ward et al. used a pharmacophore discovery algorithm by entering the molecular features that they thought were necessary for the molecular recognition of drugs by the EGFR kinase domain based upon their steady-state enzyme kinetic analysis [165]. This process lead to a study of a 4-(3-chloroanilino) quinazoline (CAQ), which is a potent EGFR inhibitor (K_i = 16 nM) (Fig. 10A). That an anilino quinazoline resulted from the pharmacophore program used was serendipitous because this drug class does not act by the mechanism corresponding to the initial structural data provided by these workers; they included the tyrosyl residue of the protein substrate. Nonetheless, they found that CAQ follows competitive kinetics with respect to ATP and non-competitive kinetics when the peptide substrate is varied, which indicates that CAQ binds to the ATP site. If the drug resembled a portion of the tyrosine residue, competitive inhibition with respect to the protein substrate would be expected.

Wakeling et al. found that CAQ inhibits the growth of the human oral squamous cell carcinoma KB cell line stimulated with EGF with an IC_{50} of 1.2 μM, while it fails to inhibit the growth of these cells stimulated by insulin-like growth factor-1 [169]. CAQ also inhibits the growth of MCF-7 human breast cancer cells stimulated by TGFα. They reported that CAQ completely blocks the proliferation of normal rat kidney NRK49F cells stimulated with EGF, but only inhibits proliferation by 20% when stimulated by PDGF. Such results provide evidence of drug selectivity. These investigators examined 15 compounds with substituents on the aniline ring and found that the electron-withdrawing chlorine atom at the meta-position enhances EGFR protein kinase inhibition. These studies represent the first stage in the development of therapeutic quinazoline-based EGFR inhibitors.

Rewcastle et al. examined about 50 anilino quinazoline derivatives and found that electron donating groups at the 6- or 7-position increased inhibitory activity. They found that the 6,7-dimethoxy quinazoline derivatives were the most potent [170]. Barker et al. characterized the 3-chloro-4-fluoroaniline derivative with the 6,7-dimethoxy side chains [171]. They studied compounds with three carbons between the 6-oxygen of the quinazoline ring and the nitrogen atom of the distal R-group. They found that the morpholinopropoxy side chain was the most potent compound, which completed the development of gefitinib (Fig. 10B).

The steps leading to the development of erlotinib (CP358,774, or OSI-774) (Fig. 10C) have not been published. A procedure for its synthesis and those of related 4-(substituted phenylamino) quinazoline derivatives are described in a World Patent Application (WO 9630347). Moyer et al. found that erlotinib is a reversible EGFR protein kinase inhibitor (IC_{50} = 2 nM) that also inhibits its autophosphorylation in intact human colorectal carcinoma DiFi cells derived from a familial adenomatous polyposis patient (IC_{50} = 20 nM) [172]. Erlotinib induces apoptosis *in vitro* and blocks the cell cycle in G_1 resulting in the significant accumulation of the $p27^{KIP}$ cell cycle inhibitor in the DiFi cells. Pollack et al. reported that erlotinib inhibits EGFR phosphorylation in athymic mice bearing human head and neck (HN5) xenografts for at least 12 h after oral (by gavage) administration [173]. The drug also inhibits the growth of HN5

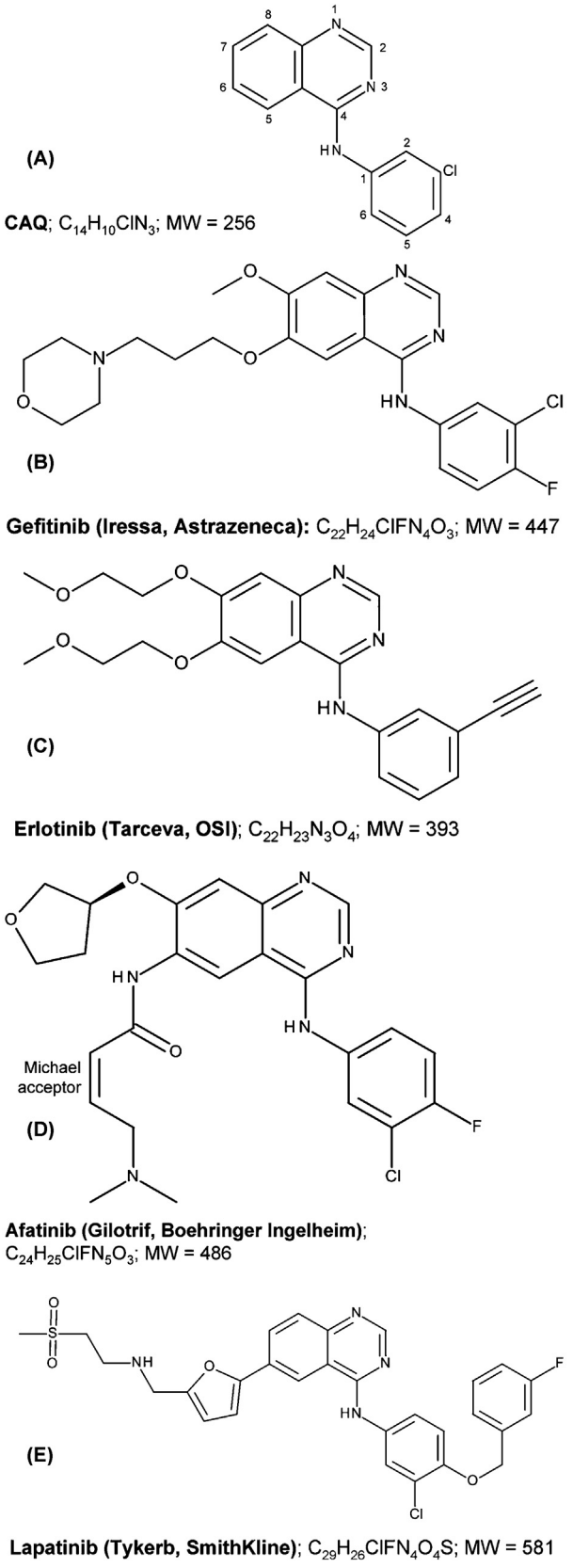

Fig. 10. Structures of quinazoline derivatives that target ErbB1 and ErbB2 protein-tyrosine kinase domains. (A) CAQ, 4-(3-chloroanilino) quinazoline. (B) Gefitinib and (C) erlotinib are reversible ErbB1 inhibitors. (D) Afatinib is an irreversible inhibitor that contains an unsaturated Michael group acceptor that forms a covalent bind with ErbB1 Cys797. (E) Lapatinib is a reversible ErbB1 and ErbB2 inhibitor.

and human A431 tumor xenografts in these mice. These investigators also demonstrated that the co-administration of erlotinib and cisplatin was more effective in inhibiting HN5 xenograft growth than either agent alone. This response was observed when cisplatin was given before, during, or after erlotinib.

The steps leading to the development of afatinib have not been published. A procedure for its synthesis is described in a World Patent Application (WO 2002/50043). This drug was designed to covalently bind to and irreversible block enzymatically active ErbB receptor family members. Li et al. reported that afatinib inhibits wild type EGFR (IC_{50} of 0.5 nM), the Leu858Arg mutant (0.4 nM), the Leu858Arg Thr790Met double mutant (10 nM), and ErbB2 (14 nM) [174]. Solca et al. reported that the drug also inhibits ErbB4 (IC_{50} of 1 nM) [175]. Solca et al. compared afatinib with BI37781, which is the afatinib congener that lacks the acrylamide double bond so that it is unable to form a covalent adduct with the ErbB family members [175]. BI37781 shows similar potency with wild type EGFR, but was 1/5th as potent with the Leu858Arg mutant and 1/500th as potent with the Leu858Arg Thr790Met double mutant when compared with afatinib. These studies show that the irreversible nature of inhibition increases the drug's potency against the clinically important double mutant.

Solca et al. compared the cellular activities of afatinib and BI37781 [175]. They found that both compounds inhibit wild type EGFR phosphorylation in human A431 carcinoma cells with EC_{50} values of 8 and 17 nM, respectively. Whereas afatinib inhibits signaling in cell lines expressing the Leu858Arg Thr790Met double mutant EGFR (NCI-H1975 human NSCLC adenocarcinoma, 49 nM) or wild type ErbB2 (BT474 human breast carcinoma, 75 nM), BI37781 displayed EC_{50} values greater than 500 nM. Afatinib inhibits proliferation of these cells with nanomolar activity (<100 nM), but BI37781 is ineffective even at concentrations as high as 4000 nM. These investigators found that afatinib treatment of human A431 cells inhibits EGF-stimulated EGFR phosphorylation for 24–48 h after removal of the drug from the cells whereas cells treated with a reversible inhibitor (gefitinib) regained about 90% of growth factor-stimulated activity in 8 h.

Li et al. studied the efficacy of afatinib in mice bearing tumor xenografts [174]. They found that the human A431 carcinoma cell line is sensitive to orally administered afatinib. This was accompanied by decreased EGFR and Akt phosphorylation as determined by immunohistochemistry. At the maximum tolerated doses, afatinib was more effective that gefitinib or lapatinib. They reported that xenograft models resistant to first-generation EGFR inhibitors responded to afatinib treatment. These include the NCI-N87 human gastric cancer cell line, which overexpresses ErbB2, and the NCI-H1975 human lung adenocarcinoma NSCLC cell line, which expresses the EGFR double mutant.

Yun et al. compared the X-ray crystal structures of the wild type and *EGFR*-mutant protein kinase domains with bound gefitinib [162]. The mode of gefitinib binding to the wild type and mutant enzymes is very similar so that it is not possible to decipher the reason for the greater affinity of the drug for the Leu858Arg mutant. The quinazoline ring of gefitinib is oriented with its N-1 in the back of the ATP-binding pocket of the Leu858Arg mutant where it accepts a hydrogen bond from the main chain —NH amide of Met793 (residue numbers including the signal peptide) (Fig. 11A). This residue occurs in the hinge that connects the amino and carboxyterminal lobes of protein kinase domains; the ATP substrate characteristically interacts with hinge residues. The anilino ring of gefitinib forms a 45° angle with the plane of the quinazoline and the chloro group points upward. Gefitinib makes hydrophobic contacts with Ala743 and Leu844, which form part of the catalytic spine, and Val726, which forms part of the regulatory spine. The catalytic spine interacts with the adenine portion of ATP.

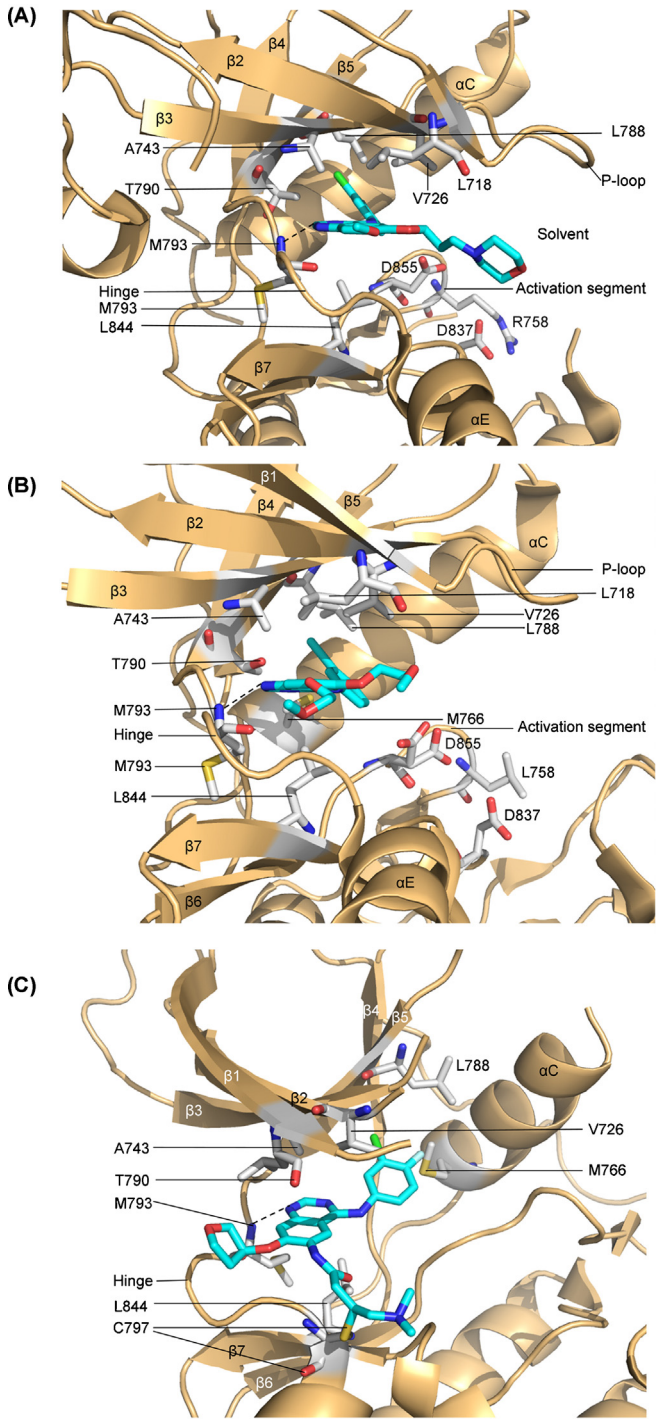

Fig. 11. Binding of FDA-approved quinazoline derivatives to EGFR. (A) Gefitinib bound to the Leu858Arg mutant (PDB ID: 2ITZ). (B) Erlotinib bound to the wild type enzyme (PDB ID: 1M17). (C) Afatinib bound to the wild type enzyme (PDB ID: 4G5J). Hydrogen bonds between the drug and EGFR hinge are depicted as dashes. Nascent EGFR residue numbers. The figure was prepared using the PyMOL Molecular Graphics System.

The structure of erlotinib bound to wild type EGFR is very similar to that described above for gefitinib. The interplaner angle of the aromatic rings of erlotinib is about 42° (Fig. 11B). The quinazoline ring of erlotinib is oriented with its N-1 in the back of the ATP-binding pocket where it accepts a hydrogen bond from the main chain —NH amide of Met793. Leu788 and Thr790 are within 4 Å of the acetylene portion of the anilino ring. The drug makes hydrophobic contacts with several side chains including Ala743 and Leu844 of the catalytic spine. The ether-containing side chains of the quinazoline ring extend into the solvent (toward the right in Fig. 11B).

Afatinib is a quinazoline drug that contains an unsaturated acrylamide side chain that functions as a Michael acceptor (Fig. 10D) that reacts with EGFR Cys797 (nascent protein residue number), a Michael donor, to form a covalent adduct [175]. The covalent attachment, which makes this drug an irreversible inhibitor, is observed in the X-ray crystal structure (Fig. 11C). The drug is bound to the active enzyme form: Lys745 and Glu752 are in contact, the activation loop is in its open form, and the DGF-Asp is in its active state. The N-1 of the afatinib quinazoline hydrogen bonds with the —NH group of the Met793 backbone. The quinazoline ring interacts with the Thr790 gatekeeper and Ala743 and Leu844 of the regulatory spine. The 2-chloro-3-fluoroanilino group of the drug points upward and interacts with Val726 and Met766 of the regulatory spine. These investigators further documented the existence of a covalent bond between the drug and enzyme by mass spectroscopic analysis. These investigators also showed that afatinib reacts with ErbB2 Cys805 and ErbB4 Cys803 and potently inhibits these enzymes. Whether these two inhibitory powers of the drug translate into therapeutic efficacy remains to be established. The comparable residue in ErbB3 is Ser794, which is not expected to react covalently with afatinib.

Nearly all NSCLC patients with EGFR-activating mutations develop resistance to gefitinib or erlotinib after a median duration of 10–13 months [176]. The most common mechanism for resistance is the development of a Thr790Met gatekeeper mutation in exon 20 that occurs in 50–60% of patients with disease progression [177]. This mutation replaces threonine with the larger methionine near the ATP-binding site. Afatinib is a quinazoline derivative that readily fits into the ATP-binding pocket and irreversibly inhibits the Thr790Met mutant suggesting that the substitution of the larger for smaller residue does not sterically block drug binding. Moreover, Yun et al. directly demonstrated that the activating Leu858Arg mutant, the Thr790Met mutant, and the double mutant bind gefitinib more tightly than the wild type enzyme [178]. They found that the K_m for ATP is increased in the Leu858Arg mutant when compared with the wild type enzyme, but the second Thr790Met mutation decreases the K_m for ATP, which increases its ability to compete with gefitinib for binding and decreases the inhibitory effect of the drug. A methionine in the gatekeeper position may also increase the strength of the hydrophobic spine [179], which may lead to greater activity of the EGFR Leu858Arg Thr790Met double mutant. An additional mechanism of resistance to gefitinib or erlotinib is related to the up regulation of c-Met, the hepatocyte growth factor receptor, that may occur in about 22% of patients [180]. These investigators report that *MET* amplification produces ErbB3-dependent activation of the PI3K pathway.

Afatinib is approved by the FDA for the first-line treatment of NSCLC in patients bearing the activating (i) exon-19 deletions or (ii) the Leu858Arg mutation. This drug also inhibits the Leu858Arg Thr790Met double mutant [175] and thus may represent an effective therapy for patients who have developed resistance to erlotinib or gefitinib. Crizotinib is an approved drug for the treatment of ALK-positive NSCLC [181]. Crizotinib was initially developed as an inhibitor of c-Met, and it may prove efficacious in the treatment of patients with c-Met up regulation following erlotinib or gefitinib treatment.

5.1.4. Mutant ERBB2 oncogenic activation and pharmacological inhibition in lung cancer

Arcila et al. found activating *ERBB2* mutations in the protein kinase domain in a subset of lung adenocarcinomas [182]. The incidence of these *ERBB2* mutations in wild type *EGFR/KRAS* and

ALK-negative tumors in their study was about 6%, and they estimate that between 1000 and 2000 of these cases occur annually in the United States. These mutations were more frequent among never-smokers, but there was no association with sex, race, or tumor stage at the time of diagnosis. Of 11 patients studied, none exhibited *ERBB2* gene amplification as determined by fluorescence *in situ* hybridization (FISH) analysis. The overall survival of patients with the *ERBB2* mutations was 19 months, which is similar to those with *EGFR* and *KRAS* mutations. Most of the mutations were small insertions (3, 6, 9, and 12 nucleotides) in exon 20 between codons Met774 and Ala775 corresponding to the nascent protein. Met774 and Ala775 occur in the carboxyterminal end of the regulatory αC-helix.

Cappuzzo et al. reported that trastuzumab was effective in a lung cancer patient with an exon-20 Gly776Leu mutation (not an insertion) after failure of cisplatin, a taxane, and a tyrosine kinase inhibitor [183]. Trastuzumab and lapatinib are potential therapies for patients with the *ERBB2* mutations, and afatinib and dacomitinib are irreversible ErbB2 kinase inhibitors that are in clinical trials for these *ERBB2* mutations [182]. In a study of two lung cancer patients with *ERBB2* insertions after failure of cytotoxic and other EGFR- and ErbB2-targeted therapy, De Grève et al. observed objective responses (tumor shrinkage) following afatinib therapy [184]. Of course larger clinical trials are required to establish the efficacy of afatinib and the other agents for the treatment of *ERBB2*-mutant lung cancers.

5.2. Breast cancer

5.2.1. Classification and general treatment

The estimated global incidence of breast cancer in women in 2008 was about 1.4 million with about 460,000 deaths attributed to this malignancy [140]. Breast cancer is the leading cause of female cancer deaths worldwide. The estimated incidence of new cases of breast cancer in the United States in 2012 was about 230,000 with about 40,000 patients succumbing to the disease, making it the second leading cause of cancer deaths among women in the United States (after lung cancer) [141]. The median age at diagnosis in the United States is 61 years. For purposes of therapy, breast cancers are grouped into three categories, which are not mutually exclusive: (i) hormone receptor positive, (ii) gene amplification or overexpression of *ERBB2*/*HER2*/*NEU*, and (iii) triple negative breast cancer (lacking (i) estrogen and (ii) progesterone receptors and (iii) *ERBB2* amplification or overexpression). These data indicate that the cure rate for breast cancer is significantly better than that for lung cancer, but clearly there is a need for improvement.

Witliff reported that hormone receptors for estrogen, progesterone, or both occur in about 79% of all breast cancers [185]. He stated that 56% of breast cancers contain both the estrogen and progesterone receptors, and 14% contain only the estrogen receptor, while 9% contain only the progesterone receptor, and 21% lack both receptors [185]. ErbB2 overexpression or *ERBB2* gene amplification occurs in 20–30% of breast cancers while 10–20% of breast cancers are triple negative and lack hormone receptors and do not overexpress ErbB2/HER2. ErbB2 overexpression was correlated with a poor prognosis prior to the advent of anti-ErbB2 therapies. Hormone receptor status and ErbB2 overexpression are determined by immunohistochemistry and *ERBB2* gene amplification is determined by FISH analysis.

Surgery is the principal treatment modality for localized breast cancer, followed by chemotherapy (when indicated), radiotherapy, and adjuvant hormonal therapy (with tamoxifen or an aromatase inhibitor) for receptor-positive tumors [141]. Siegel at al. reported that more than 90% of breast cancer patients undergo surgical excision of the tumor [141]. About 30% of patients are treated with surgery and radiation, and 15% are treated with surgery and various drugs, and 21% are treated with surgery, radiation, and drugs. Siegel et al. reported that about 6% of patients in the United States with stage I or stage II breast cancer are treated non-surgically and 1% receive no treatment [186]. They also reported that about 18% of patients with stage III or stage IV breast cancer are treated non-surgically and 7% do not receive any treatment. Chemotherapy may be used before surgery (neoadjuvant therapy), after surgery (adjuvant therapy), or instead of surgery (palliative care) for those cases in which surgery is considered unsuitable.

Many patients that are hormone-receptor positive benefit from treatment with tamoxifen. This drug is effective in pre- and post-menopausal women and binds to the estrogen receptor, but does not activate it. Anastrozole and letrozole are alternative anti-estrogenic compounds that have fewer side effects than tamoxifen, but they can be used only in post-menopausal women. Anastrozole and letrozole are aromatase inhibitors that block the formation of the aromatic A ring of estradiol from androgenic precursors (Table 5). When aromatase inhibitors are used in pre-menopausal women, the decrease in ovarian estrogen production activates the hypothalamus and pituitary to increase gonadotropin secretion. Gonadotropins in turn stimulate the ovary and increase androgen production, which are ordinarily converted to estradiol via the action of aromatase. The heightened gonadotropin levels also upregulate the aromatase promoter, increasing aromatase production in the setting of increased androgenic substrates. This counteracts the effect of the aromatase inhibitor in pre-menopausal women since total estrogen is increased.

Various cytotoxic drugs are used in the treatment of advanced breast cancers, especially those cancers that are hormone receptor negative or triple negative [187]. These include doxorubicin, cyclophosphamide, docetaxel, and paclitaxel. One of the preferred chemotherapeutic regimens recommended by the National Comprehensive Cancer Network includes doxorubicin and cyclophosphamide followed by paclitaxel (www.NCCN.org). Several other cytotoxic drugs are used in the treatment of breast cancer. These include capecitabine, gemcitabine, pemetrexed, and vinorelbine (Table 5).

5.2.2. Targeted breast cancer treatments

5.2.2.1. Lapatinib and ErbB2. Lapatinib is an orally effective FDA-approved drug for the second-line treatment of patients (i) with capecitabine in ErbB2-positive breast cancer who have received cytotoxic drugs or trastuzumab and (ii) with letrozole in post-menopausal hormone receptor-positive breast cancer. Lapatinib is a quinazoline derivative that contains side chains that are quite different from those of gefitinib, erlotinib, and afatinib (Fig. 10). Two other FDA-approved protein kinase targeted quinazoline derivatives include bosutinib, a BCR-Abl inhibitor used in the treatment of chronic myelogenous leukemia, and vandetanib, a RET, EGFR, VEGFR inhibitor used in the treatment of medullary thyroid cancer (www.brimr.org/PKI/PKIs.htm). X-ray crystal structures of lapatinib bound to EGFR and ErbB4 are in the public domain (PDB ID: 1XKK and 3BBT), but not lapatinib bound to ErbB2. Lapatinib most likely binds to ErbB2 in a similar fashion, but it would be informative to examine this directly.

The steps leading to the development of lapatinib (GW572016 or GW2016) (Fig. 10E) have not been published. A procedure for its synthesis and those of related compounds are described in a World Patent Application (WO 9935146). Xia et al. examined the effects of lapatinib, which is a reversible EGFR and ErbB2 inhibitor, on several cell lines in culture and in animal xenografts [188]. They reported that the drug inhibits the phosphorylation of (i) ErbB2 and (ii) downstream Erk1/2 in human S1 cells, which express high levels of ErB2 protein and are derived from normal mammary epithelial cells transformed with SV40 large T antigen (the HB4a cell line). The drug also increased the percentage of apoptotic cells 23-fold

to 46% after 72 h of treatment. These investigators did not report on the effect of lapatinib on the phosphorylation state of Akt in this cell line; inhibition of Akt phosphorylation is expected to be pro-apoptotic.

Xia et al. reported that lapatinib inhibits EGF-stimulated phosphorylation of Akt in the ErbB2-overexpressing BT474 human breast cancer cell line [188]. The compound also inhibits the phosphorylation of basal and EGF-stimulated phosphorylation of EGFR and Akt in HN5 human head and neck cancer cells that overexpress EGFR. These investigators found that the mechanism of lapatinib differs from that of trastuzumab [188]. Lapatinib inhibits Erk1/2 phosphorylation in both BT474 and HN5 cells while trastuzumab does not. Neither agent decreases total Erk1/2 protein levels. These investigators found that lapatinib decreases the phosphorylation of Erk1/2 and Akt in mice bearing HN5 xenografts. Furthermore, they reported that the drug decreases the phosphorylation of ErbB2 and Erk1/2 in BT474 xenografts.

Geyer et al. compared the results of treating 324 women with locally advanced or metastatic ErbB2-positive breast cancer with capecitabine without ($N = 161$) or with ($N = 163$) lapatinib [189]. These women had exhibited disease progression (tumor growth or spread) following treatment with an anthracycline, a taxane, or trastuzumab; when referring to a treatment, progressive disease is often synonymous with drug resistance. The median time to progression was 8.4 months with combination therapy and 4.4 months with monotherapy. The overall response rate was 22% in the combination-therapy group and 14% in the monotherapy group. They reported that skin rash occurred in 27% of patients in the combination group and 15% in the capecitabine group. Non-serious cardiac events occurred in 2.5% of the combination group and 0.6% of the monotherapy group. The addition of lapatinib to capecitabine was associated with a 51% reduction in the risk of disease progression. In a meta-analysis of 18 studies, Riemsma et al. reported that lapatinib with letrozole was superior to letrozole in terms of progression-free survival and the overall response rate [190]. The combination was also better than (i) tamoxifen or (ii) anastrozole monotherapy or (iii) trastuzumab and anastrozole combination therapy.

Metastatic breast cancer patients treated with lapatinib and (i) capecitabine or (ii) letrozole become refractory with tumor growth or spread. The mechanisms of resistance to these dual therapies have not been determined. However, a Thr798Met gatekeeper mutation in ErbB2 confers resistance to lapatinib [191]. Other proposed mechanisms of resistance to lapatinib involve activation of compensatory survival pathways through increased PI3K/Akt or estrogen receptor (ER) signaling (residue includes the signal peptide) [192]. Several strategies to overcome resistance to anti-ErbB2 treatment are in different phases of development and include treatment with pertuzumab, ado-trastuzumab-DM1, and mammalian target of rapamycin (mTOR) inhibitors.

5.2.2.2. Monoclonal antibodies directed against ErbB2.

5.2.2.2.1. Trastuzumab. Trastuzumab is a humanized monoclonal antibody that is directed against domain IV in the extracellular segment of ErbB2 [43]. Trastuzumab is approved for the treatment of breast cancer overexpressing ErbB2 (i) as part of a regimen consisting of doxorubicin, cyclophosphamide, and either paclitaxel or docetaxel, (ii) with carboplatin and docetaxel, or (iii) as a single agent following anthracycline-based therapy. Trastuzumab is also approved for the treatment of metastatic breast cancer (i) in combination with paclitaxel for first-line treatment of ErbB2-overexpressing disease or (ii) as a single agent for the treatment of ErbB2-overexpressing breast cancer in patients who have received one or more prior chemotherapeutic regimens (Table 6).

Hudziak et al. developed a mouse monoclonal antibody (mAb) 4D5 that inhibits the proliferation of human breast carcinoma SK-BR-3 cells that overexpress ErbB2 [193]. They also reported that the antibody prevents human *ERBB2*-transformed mouse NIH 3T3 fibroblasts from forming colonies in soft agar. Carter et al. constructed a humanized form of the 4D5 mouse mAb that contains the mouse antigen binding loops (complementary determining regions, or CDRs) and human variable framework residues and human IgG1 constant domains [194]. They examined the properties of eight variants of the humanized mAb; they found that humAb4D5-8 supports antibody-dependent cellular cytotoxicity (ADCC) against SK-BR-3 tumor cells that overexpress ErbB2 in the presence of human effector cells, but they reported that it is not effective against normal human lung epithelial WI-38 cells. Trastuzumab, a humanized antibody, still contains several mouse-specific residues that are outside of the antigen binding site.

Slamon et al. reported that the combination of trastuzumab with standard cytotoxic chemotherapy produces far better response rates than chemotherapy alone in patients with metastatic breast cancer that overexpress ErbB2 [195]. They reported that combination therapy was associated with a longer median time to disease progression (7.4 vs. 4.6 months), a higher rate of objective response (50% vs. 32%), a longer median duration of response (9.1 vs. 6.1 months), a lower rate of death at one year (22% vs. 33%), and longer median survival (25.1 vs. 20.3 months) [195]. The regimens used in these studies included: (i) doxorubicin (an anthracycline) and cyclophosphamide without or with trastuzumab or (ii) paclitaxel without or with trastuzumab. The most important adverse effect of trastuzumab was cardiac dysfunction, which responded to conventional medical treatment. The cardiotoxicity of trastuzumab is likely the result of ErbB2 expression in cardiomyocytes and is exacerbated when administered with an anthracycline [196].

The mechanism of action of trastuzumab is complex and is incompletely understood. Baselga reported that trastuzumab effectively inhibits the growth of ErbB2-overexpressing human breast cancer cells *in vitro* and *in vivo* [197]. The treatment of cancer cells with trastuzumab results in a modest down regulation of the ErbB2 receptor. Further cellular events resulting from ErbB2 inhibition include the accumulation of the CDK inhibitor p27 and cell cycle arrest. The arrest of cell cycle progression occurs in human breast SK-BR-3 cells, which overexpress ErbB2, but not in human breast MCF-7 cells, which express low levels of ErbB2.

Trastuzumab induces ADCC in human patients and experimental animals. After binding to the cell surface of ErbB2-overexpressing tumor cells, the monoclonal antibody induces the clustering of Fc receptors (FcγRIIIa) on stromal immune natural killer (NK) cells that leads to tumor cell killing mediated by the release of perforin, granzyme, and cytokines [198]. Trastuzumab also inhibits constitutive ErbB2 cleavage/shedding mediated by metalloproteases [197]. The cleavage of the extracellular domain from ErbB2 results in the formation of a 95-kDa membrane-bound carboxyterminal domain and a 110-kDa extracellular domain. Cleavage of the extracellular domain of ErbB2 results in the activation of the membrane-associated ErbB2 protein kinase domain. The ability of trastuzumab to inhibit ErbB2 cleavage may correlate with the clinical anticancer activity of the multifunctional ErbB2-targeting antibody. See Ref. [199] for a general review of antibody therapies in cancer.

Cho et al. determined the structure of the extracellular domain of (i) rat ErbB2 and (ii) human ErbB2 with trastuzumab [43]. In both cases, the ErbB2 structure resembles the extended activated state of EGFR with an exposed and not buried dimerization arm (Fig. 12A) and not the compact tethered state. ErbB2 is poised to interact with other ErbB receptors in the absence of direct ligand binding. Trastuzumab binds to the juxtamembrane region of ErbB2 in domain IV. This interaction is mediated by three loops of ErbB2: loop 1 (557–561, PEADQC) and 3 (593–603, KFPEEGACQP) with

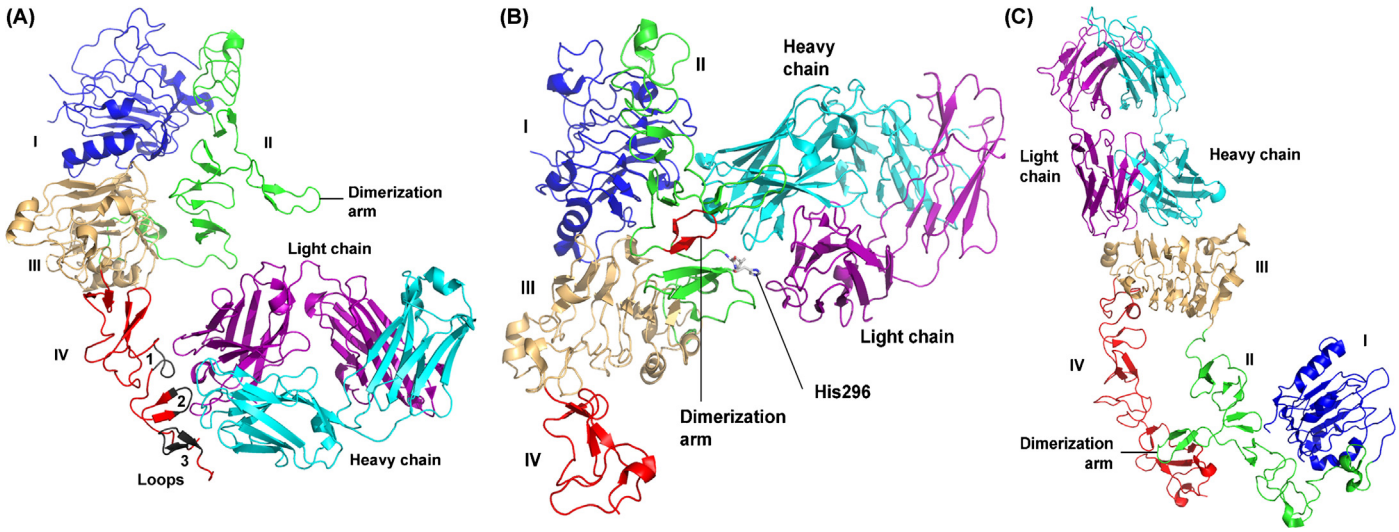

Fig. 12. Binding of monoclonal antibodies to EGFR or ErbB2. (A) Trastuzumab bound to ErbB2 (PDB ID: 1N8Z). (B) Pertuzumab bound to ErbB2 (PDB ID: 1S78). (C) Cetuximab bound to EGFR (PDB ID: 1YY9). Domains I (blue), II (green), III (tan) and IV (red) are indicated, and the monoclonal antibody heavy chain is cyan and the light chain is purple. The figure was prepared using the PyMOL Molecular Graphics System.

primarily electrostatic interactions with the antibody and loop 2 (570–573, DPPF) with hydrophobic interactions (residue numbers exclude the signal peptide) (Fig. 12A).

As with all targeted anticancer therapies, primary and acquired resistances to trastuzumab are important problems. About 50–66% of ErbB2-positive breast cancer patients fail to respond to trastuzumab [200]. The reasons for this primary resistance may be related to the many factors that participate in the pathogenesis of breast cancer besides ErbB2 over activity. After initially responding to trastuzumab patients generally relapse. The mechanisms for such resistance include loss of the PTEN activity [201]. This phosphatase reverses the action of PI3K and downstream Akt/PKB pro-apoptotic action. Activation of alternative signaling pathways may also contribute to the development of trastuzumab resistance including those of the insulin-like growth factor receptor and the hepatic growth factor receptor (c-Met) [202].

5.2.2.2.2. Pertuzumab. Pertuzumab is a humanized monoclonal antibody that is directed against the ErbB2 domain II dimerization arm and the adjacent binding pocket, which interacts with the dimerization arm of a partner ErbB family member, thereby blocking the formation of a heterodimer [203]. Pertuzumab is indicated for use in combination with trastuzumab and docetaxel for the treatment of patients with ErbB2-positive metastatic breast cancer who have not received prior (i) anti-ErbB2 therapy or (ii) chemotherapy for metastatic disease (Table 6).

In the CLEOPATRA clinical trial, Baselga et al. studied 808 patients with ErbB2-positive metastatic breast cancer who were treated with trastuzumab and docetaxel without or with pertuzumab as first-line therapy [204]. The median progression-free survival was 12.4 months in the control group and 18.5 months in the pertuzumab group. An interim analysis of overall survival showed a trend in favor of the pertuzumab group. The safety profile was similar in the two groups. As reported by Blumenthal et al., the combination of pertuzumab in combination with trastuzumab and docetaxel was approved based upon the CLEOPATRA trial [205]. No additional cardiac toxicity was observed with the addition of pertuzumab to trastuzumab (and paclitaxel). Skin rash occurred in 34% of patients receiving three drugs and in 24% of those receiving trastuzumab and docetaxel [204]. Accordingly, we have an example of the successful treatment of patients with two antibodies that target different regions of ErbB2 with correspondingly different mechanisms of action.

Agus et al. examined the mechanism of action of 2C4, which is the mouse monoclonal antibody precursor of humanized pertuzumab, in various cellular and animal contexts [206]. They found that 2C4 inhibits the recruitment of ErbB2 to ErbB3 in a neuregulin-dependent manner in human breast cancer cells that express low levels (MCF-7) and high levels (SK-BR-3) of ErbB2. They reported that 2C4 was much more effective than trastuzumab in disrupting ligand-mediated ErbB2–ErbB3 complex formation. They also demonstrated that 2C4, but not trastuzumab, inhibited the neuregulin-stimulated phosphorylation of ErbB2–ErbB3 in human breast cancer MCF-7 cells. Agus et al. reported that 2C4, but not trastuzumab, inhibited the ligand-stimulated activation of ERK1/2 and PI3K in these cells. These investigators also showed that 2C4 inhibits the growth of both low- and high-ErbB2 expressing human breast cancer xenograft tumors in mice. Adams et al. humanized 2C4 to yield pertuzumab [207], which was then used therapeutically.

Franklin et al. determined the crystal structure of pertuzumab bound to ErbB2 [203] and reported that it is bound to ErbB2 near the junction of domains I, II, and III. The antibody binds to ErbB2 near the center of domain II and sterically blocks a binding pocket necessary for receptor dimerization and signaling. Contact is primarily made with the heavy chain of the antibody binding fragment (Fab) with a small contribution from the light chain. Most of the ErbB2–pertuzumab contacts involve the complementary determining regions (CDRs) of the Fab, while the dimerization hairpin of domain II lies along side of the heavy chain variable domain (Fig. 12B). Despite the contact with the Fab, the conformation of the dimerization hairpin is essentially the same as that seen in the free and trastuzumab-bound ErbB2 structures as well as that in the EGFR receptor dimer. Both structural and mutational studies indicate that the carboxyterminal portion of domain II is involved in heterodimerization. Moreover, Leu295 and His 296 (Fig. 12B) are important for both heterodimerization and pertuzumab binding (residue numbers including the signal peptide). These investigators found that mutation of either of these ErbB2 residues to alanine severely decreased pertuzumab binding. Pertuzumab is specific for human ErbB2 and does not bind to rat ErbB2 despite the close sequence homology; only five of 144 residues of the rat domain II differ from those of human domain II.

5.2.2.2.3. Ado-trastuzumab emtansine. Ado-trastuzumab-DM1 is an ErbB2-targeted antibody–drug conjugate (ADC), composed of

trastuzumab, a stable thioether linker, and a derivative of maytansine, which is a potent antimitotic agent that inhibits the assembly of microtubules. This antibody–drug conjugate is approved for the treatment of ErbB2-positive metastatic breast cancer in patients who have previously received trastuzumab and a taxane, separately or in combination. Patients should have either (i) received prior therapy for metastatic disease or (ii) developed disease recurrence during or within six months of completing cytotoxic chemotherapy.

The covalent attachment of cytotoxic drugs to monoclonal antibodies represents an alternative approach to naked antibody-targeted therapy. Because ErbB2 is differentially expressed in 20–30% of breast cancers when compared with normal epithelial cells, ErbB2 represents an attractive target for antibody–drug conjugate therapy. Emtansine is a potent antimitotic agent that is too toxic to administer alone. Lewis Phillips et al. developed several covalent linkers to attach emtansine (DM1) to trastuzumab [208]. These included various reducible disulfide derivatives ($-CH_2-S-S-CH_2-$) and a non-reducible thioether ($-CH_2-S-CH_2-$) derivative.

Lewis Phillips et al. found that the thioether derivative was less toxic when administered to rats [208]. They reported that several ErbB2-overexpressing trastuzumab-resistant human cell lines responded to ado-trastuzumab-DM1 including HCC1954, KPL-4, and BT-474 EEI. These three breast cancer lines showed the same degree of sensitivity to ado-trastuzumab-DM1 as SK-BR-3 and BT-474, which are ErbB2-overexpressing breast cancer cell lines. Normal human cells (HMEC and NHEK) and breast cancer cells expressing low levels of ErbB2 (MCF-7 and MDA-MB-468) were resistant to growth inhibition by the thioether antibody–drug conjugate. These investigators found that ado-trastuzumab-DM1 inhibits growth and causes tumor regression in mice with implanted breast tumor cells. Lewis Phillips et al. suggested that the thioether drug conjugate is internalized upon binding the ErbB2-overexpressing tumor cells and undergoes intracellular proteolytic degradation to release the active maytansinoid [208]. They reported that BT-474 cells metabolize ado-trastuzumab-DM1 to lysine-N^{ε} covalently linked to emtansine via the thioether; this proteolytic metabolite is presumably the active antimitotic agent within the cell.

Verma et al. compared the efficacy of (i) ado-trastuzumab-DM1 with (ii) lapatinib plus capecitabine for the treatment of ErbB2-positive advanced breast cancer in patients who had previously been treated with trastuzumab and a taxane [209]. In their phase III clinical trial, ado-trastuzumab-DM1 improved progression-free survival (9.6 vs. 6.4 months) and overall survival (30.9 vs. 25.1 months) in these patients. The objective response rate was also better in the ado-trastuzumab-DM1 group (44% vs. 31%). Moreover, the ado-trastuzumab-DM1 group experienced less toxicity than the lapatinib plus capecitabine group. The dose and half-life of ado-trastuzumab-DM1 (3.6 mg/kg every three weeks, 4 days) or trastuzumab (6 mg/kg every three weeks, 3–4 weeks) given to patients differ [210]. In addition to delivering the cytotoxic drug to ErbB2-positive cells, the antibody maintains known mechanisms of actions of trastuzumab. However, the lower dose and half-life suggest that the antibody-only action of ado-trastuzumab-DM1 is considerably less than that of trastuzumab in the clinical setting.

Hurvitz et al. summarized the results of a clinical trial that compared ado-trastuzumab-DM1 vs. trastuzumab plus docetaxel in patients with ErbB2-positive metastatic breast cancer [211]. Many of the patients in both groups had received prior treatment with trastuzumab, a taxane, or an anthracycline. The ado-trastuzumab-DM1 group had a longer progression-free survival (14.2 months vs. 9.2 months), a greater overall response rate (64% vs. 58%), and fewer grade 3 adverse events (7% vs. 41%). An ongoing three-arm phase III clinical trial (NCT01120184) is evaluating the efficacy and safety of (i) ado-trastuzumab-DM1 with pertuzumab, (ii) ado-trastuzumab-DM1 with pertuzumab-placebo (blinded for pertuzumab), and (iii) the combination of trastuzumab plus taxane (docetaxel or paclitaxel) in patients with ErbB2-positive progressive or recurrent locally advanced or previously untreated metastatic breast cancer. The data from this trial will be available in 2016.

5.2.3. Activating ERBB2 mutations and breast cancer

Although wild type *ERBB2* overexpression occurs in 20–30% of breast cancers, Bose et al. estimate that about 1.6% of breast cancer patients possess an *ERBB2* mutation [212]. They estimated that the incidence of new cases of *ERBB2*-mutant breast cancer in the United States is about 4000 per year. They reviewed the results from 25 patients with *ERBB2* mutations that occurred in a total of 1499 patients that lacked *ERBB2*/*HER2* gene amplification. These investigators used reverse transcription of RNA, DNA amplification, and DNA sequence analysis in their characterization of two new mutations. In their overall summary, they reported that two of the mutations occur in the extracellular domain at codon 309 and three occurred at codon 310 (nascent protein residue numbers are used in this section). They reported that one mutation occurred at codon 1220 in the carboxyterminal tail, and 12 different mutations occurred within the protein kinase domain. The most common mutation, which was observed in six patients, was a Leu755Ser mutation.

Bose et al. found that seven *ERBB2* mutations activated the protein as determined by enzyme activity, the ability to increase cell growth in matrigel and soft agar, the ability to activate downstream ErbB2 signaling, or the ability of the mutant to increase tumor formation in mouse xenografts [212]. The activated mutants include a Gly309Ala extracellular mutation. This residue participates in the heterodimerization of ErbB2 with ErbB1 and the mutation may facilitate heterodimer formation. The Asp769His/Tyr mutations occur in the αC-helix and the mutations may destabilize the dormant enzyme state. Alternatively, these hydrophobic mutations may increase the ability of these enzymes to function as a receiver kinase during the formation an activated asymmetric dimer. The Val777Leu mutant and the Pro780 insertion, which occurs immediately after the αC-helix, are also activated. The Pro780 insertion was described in NSCLC, but the other mutations are unique to breast cancer. The Val777Leu is homologous to the ALK activating Phe1174Leu mutation found in childhood neuroblastomas [181]. The Val842Ile and the Arg896Cys mutation occur in the carboxyterminal lobe and are not near any of the classical regulatory sites nor important residues in the activator kinase in the asymmetric dimer so that the mechanism for this activation is unclear.

The most common *ERBB2* mutant, Leu755Ser, which occurs at the end of the β-3 strand in the amino-terminal lobe, does not cause oncogenic transformation [212]. The non-activated Arg678Gln mutant occurs intracellularly proximal to the kinase domain. The Ile767Met mutant, which occurs in the αC-helix in the amino-terminal lobe, and the Tyr835Phe mutant, which occurs in the αE-helix in the carboxyterminal lobe, have no effect on ErbB2 protein kinase activity. These investigators did not examine the activities of the Leu755Trp mutant, which occurs at the end of the amino-terminal β-3 strand, or the Gly1201Val mutant, which occurs in the carboxyterminal tail.

Bose et al. found that the Leu755Ser mutant is resistant to lapatinib, a reversible ErbB2 inhibitor, but all of their other mutants are sensitive to neratinib, an irreversible ErbB2 inhibitor [212]. MCF10A cells are a non-transformed estradiol receptor-positive breast epithelial cell line that express EGFR and require supplementary EGF in their culture media for growth. NCF10A cultures expressing wild type ErbB2 form spherical cells. MCF10A cells expressing the activated Val777Leu, Asp769His, Val842Ile, or Gly309Ala mutants form irregular non-spherical cells, a morphology that is corrected

by the addition of trastuzumab. The effect of pertuzumab or ado-trastuzumab-DM1 was not examined in these studies.

The identification of these *ERBB2* mutants provides additional targets for drug discovery. That these mutations occur in several locations will hinder the development of a comprehensive diagnostic test for these *ERBB2* mutations. Bose et al. point out that the incidence of *ERBB2* mutations in breast cancer is similar to the incidence of chronic myelogenous leukemia, a disease for which extensive drug development and clinical trials have been performed [212]. However, these patients have Philadelphia chromosome positive disease [213] so that identifying them is considerably easier than will be the case for various *ERBB2*-mutant breast cancers. However, in the next few years when it may be possible to sequence an entire human genome for $1000, it may become feasible to identify these various *ERBB2* mutations.

5.2.4. *BRCA1 and BRCA2 genes and breast cancer*

The greatest risk factor for breast and ovarian cancer is the inheritance of a mutation in one of the breast cancer susceptibility genes, *BRCA1*, which was discovered in 1994 [214] or *BRCA2*, which was discovered in 1995 [215]. Mutations in these two genes are present in fewer than 3% of all breast cancers, but they account for about 20% of familial breast cancers [216]. The number of different mutations identified in each of these genes is in the hundreds. The probability that a breast cancer is associated with a mutation in these genes increases (i) if there are multiple affected first-degree relatives, (ii) if individuals develop breast cancer before menopause, or (iii) if family members also develop ovarian cancer. Most breast cancers in women with a *BRCA1* mutation are diagnosed at a young age (typically between ages 30 and 50 years) and those with *BRCA2* mutations are diagnosed near 50 years of age. The median age at the time of diagnosis of breast cancer in the United States is 61 years [141].

The coding regions *BRCA1* and *BRCA2* show no homology to previously described proteins or to each other [217]. Both BRCA1 and BRCA2 function in homologous recombination, a vital DNA repair process that uses the undamaged sister chromatid to carry out high-fidelity repair of predominantly replication-associated DNA double-strand breaks. These two genes are traditionally known as tumor suppressor genes [217], but Weinberg suggests that they should be considered as caretakers (DNA repair proteins) rather than gatekeepers (tumor suppressor genes) [218]. It is unclear why mutations of these genes are associated most generally with breast as opposed to other cancers. One hypothesis is that the intermittent proliferation of breast epithelium (as opposed to the constitutive proliferation of other epithelia such as colon or skin) makes this organ more susceptible to the accumulation of genetic damage.

If one copy of either breast cancer susceptibility gene is mutated in the germ line, the result is hereditary breast and ovarian cancer syndrome, which is inherited in an autosomal-dominant manner [217]. Not only is this syndrome associated with early-onset breast cancer, but it also carries an increased risk of ovarian, pancreatic, stomach, laryngeal, and fallopian tube cancer. Women bearing these mutations have a lifetime risk of 50–80% developing breast cancer and 30–50% chance of developing ovarian cancer. Genetic testing is difficult and often inconclusive unless the individual belongs to an ethnic group with a known high incidence of specific mutations. For example, women of Ashkenazi Jewish descent have a 2–3% risk of three specific mutations: *BRCA1* (185delAG, 5382insC) and *BRCA2* (6174delT). Two other groups with a high incidence of specific founder mutations include French-Canadians and Icelanders.

Identification of *BRCA1* or *BRCA2* carriers is important because prophylactic mastectomy and bilateral salpingo-oophorectomy or both can reduce the risk of cancer mortality [219–222]. Mastectomy or removal of both fallopian tubes and ovaries (bilateral salpingo-oophorectomy) or both procedures decrease the possibility of developing cancer in these organs. After the diagnosis of a cancer in one breast, a woman with a *BRCA1* or *BRCA2* mutation experiences a high risk of contralateral (in the opposite) breast cancer [223]. Work by Phillips et al. suggests that tamoxifen is effective in reducing the risk of contralateral breast cancer for carriers of these mutations [224]. Tamoxifen is approved by the FDA for the prevention of breast cancer in women at high risk of developing the disease and for the reduction of contralateral breast cancer. Women with *BRCA1* or *BRCA2* mutations, when they develop breast cancer, usually lack an estrogen receptor in their tumors [225]. Because there is no clear association of ErbB and the pathogenesis of breast cancer in carriers of *BRCA1* or *BRACA2* mutations, these hereditary disorders are not discussed any further in this review.

5.3. *Gastric cancer*

Gastric cancer is the second leading cause of total (male plus female) cancer deaths globally (after lung cancer) [140]. In 2008, the estimated global incidence of stomach cancer was about 1.0 million with about 730,000 deaths attributed to this malignancy. In 2012, the estimated incidence of stomach cancer in the United States was about 22,000 with 11,000 deaths [141]. The highest incidence rates for stomach cancer are in Eastern Asia, Eastern Europe, and South America, and the lowest incidence rates are in North America and most parts of South Africa [140]. Stomach cancer rates have decreased during the past 70 years in most parts of the world owing to the increased availability and use of refrigeration and the decreased use of salted, smoked, and preserved foods.

Histologically, gastric carcinomas fall into two subtypes: intestinal and diffuse [226]. The intestinal subtype (70–80%) consists of bulky tumors composed of glandular structures, and the diffuse subtype (20–30%) consists of infiltrative tumors with a signet-ring morphology. The intestinal subtype is more common in men than women (2:1) and primarily affects older people (mean age of 63 years). The diffuse subtype occurs equally in men and women and occurs in younger people. The incidence of the intestinal subtype is falling worldwide while that for the diffuse subtypes has remained constant. Chronic infection with *Helicobacter pylori* increases the risk for gastric carcinoma by about 6-fold. However, the vast majority of people infected with *H. pylori* do not develop stomach cancer.

Surgical resection is the basis of curative gastric cancer treatment [227]. About 2/3rds of patients with gastric cancer undergo surgery and one quarter of these patients will have tumors that are unresectable owing to metastasis or spread. Chemotherapy is considered in patients with metastatic disease who have good functional status and are expected to survive for several months. Preferred regimens include (i) paclitaxel and carboplatin, (ii) cisplatin and fluorouracil, (iii) oxaliplatin and fluorouracil, (iv) cisplatin and capecitabine, and (v) oxaliplatin and capecitabine (www.NCCN.org).

In the ≈22% of gastric cancer patients who have tumors overexpressing ErbB2 as determined by immunohistochemistry or FISH analysis (to establish *ERBB2* gene amplification), trastuzumab is given with the cytotoxic therapies [226]. The incidence of ErbB2 positivity is about the same in Europe and in Asia, and the incidence of ErbB2 overexpression is higher in the intestinal subtype than in the diffuse cancer subtype (32% vs. 21%). The addition of trastuzumab to chemotherapy increased objective response rate from 35% to 47% and it improved progression-free survival from 5.5 months to 6.7 months [228]. Furthermore, overall survival improved from 11.1 months to 13.8 months.

Although these results demonstrate efficacy, there is considerable room for improvement in the treatment of gastric cancer. Clinical trials are underway to examine the efficacy of lapatinib in combination with paclitaxel compared with paclitaxel alone

in the treatment of ErbB2-positive gastric carcinoma (ClinicalTrials.gov ID: NCT01705340). Other clinical trials are examining the effect of adding pertuzumab to chemotherapy (ClinicalTrials.gov ID: NCT01461057) and comparing trastuzumab to paclitaxel or docetaxel as second-line treatment of ErbB2-overexpressing gastric cancer patients (ClinicalTrials.gov ID: NCT01641939).

5.4. Colorectal cancer

5.4.1. Classification and general treatment

Colorectal cancer was the fourth leading cause of cancer deaths worldwide in 2008 [140]. The worldwide incidence was about 1,230,000 and the number of deaths was about 610,000. In 2012, the incidence in the United States was about 41,000 and the number of deaths was about 7900 [141]. On the order of 98% of all cancers in the large intestine are adenocarcinomas, which usually arise in polyps. The peak incidence occurs in people between ages 60–79 years of age. The single most important prognostic indicator of colorectal cancer is the extent of the tumor at the time of diagnosis: the more the tumor invades the colon and the greater the spread to regional lymph nodes or more distantly, the worse is the prognosis.

With localized colorectal carcinoma, surgery alone can be curative. For non-localized cancers or when metastasis has occurred, various chemotherapeutic regimens are used. These include (i) FOLinic acid/leucovorin, Fluorouracil, and OXaliplatin (which is abbreviated as FOLFOX) without or with bevacizumab or panitumumab, (ii) oxaliplatin plus capecitabine without or with bevacizumab, (iii) FOLinate/leucovorin, Fluorouracil, and IRInotecan (which is abbreviated FOLFIRI) without or with bevacizumab, cetuximab, or panitumumab, and (iv) regorafenib monotherapy for second-line treatment (www.NCCN.org).

5.4.2. Targeted treatments for colorectal cancer

5.4.2.1. Cetuximab. Cetuximab is a human–mouse chimeric IgG1 monoclonal antibody that binds to domain III of the extracellular segment of the tethered inactive state of EGFR and directly blocks activating ligand binding [229]. In therapeutic chimeric antibodies, the mouse constant region is replaced by the human constant region. If parts of the variable domains are also replaced by portions of human variable domains, humanized antibodies are obtained as in the case of trastuzumab and pertuzumab. Cetuximab is approved for the treatment of wild type *KRAS* EGFR-expressing metastatic colorectal cancer (i) for first-line treatment in combination with fluorouracil, leucovorin, irinotecan, (ii) in combination with irinotecan in patients who are refractory to irinotecan-based chemotherapy, and (iii) as a single agent in patients who have failed oxaliplatin and irinotecan-based chemotherapy or who are intolerant to irinotecan.

Gill et al. developed a panel of monoclonal antibodies by immunizing mice with human A431 carcinoma cells that express high levels of EGFR [230]. They screened for antibodies that inhibited binding of EGF to EGFR and prevented EGF-stimulated EGFR phosphorylation. These antibodies inhibited cellular proliferation *in vitro* and *in vivo*. Goldstein et al. generated a human–murine chimeric version from mAb 225 to produce cetuximab (IMC-C225) [231]. They reported that the human monoclonal antibody had a greater affinity for EGFR with K_d about 1/5th that the mouse antibody. They suggested that the increased capacity of humanized C225 to compete with ligand for binding to EGFR was responsible for its enhanced antitumor effect in mice bearing human A431 cancer cells when compared with mouse mAb 225. Cetuximab limits the activation of several signal transduction pathways downstream from EGFR including Ras/Raf/MEK/ERK1/2, PI3K/Akt, and protein kinase C. The antibody also down regulates VEGF expression, a process that inhibits angiogenesis.

Binding of EGF to EGFR results in receptor dimerization and activation of receptor tyrosine kinase, followed by internalization of the ligand and receptor complex as noted in Section 4.2 [1,117]. Internalization and proteolytic EGFR degradation plays an important role in attenuating ligand-induced receptor signaling. Experiments with *EGFR* mutants have shown that the tyrosine kinase activity of the receptor is not required for ligand-induced internalization. Fan et al. examined the effects of mouse mAb 225 (the mouse monoclonal antibody that is the precursor to chimeric cetuximab) on the proliferation of human A431 carcinoma cells in culture [232]. They found that the bivalent antibody inhibits cell proliferation while the monovalent antibody (prepared by pepsin digestion) fails to inhibit proliferation. Moreover, they reported that bivalent mAb 225 down-regulates EGFR while the monovalent antibody does not. They found that bivalent mAb 225 induced EGFR dimerization without activating receptor tyrosine kinase in A431 cells, and this was followed by receptor down regulation. These observations indicate that ligand-induced EGFR dimerization (biological dimer) and antibody-induced EGFR dimerization (immunological dimer) differ in their capacity to activate receptor tyrosine phosphorylation. While both receptor dimerizations resulted in ligand and receptor internalization, the kinetics and the degree of down regulation differed. These studies suggest that EGFR down regulation following receptor internalization and degradation is an important mechanism of action of mAb 225; by inference, cetuximab-mediated EGFR down regulation contributes to its therapeutic effect in humans.

In a phase II clinical trial with 57 patients, Saltz et al. reported that five patients with chemotherapy-refractive EGFR-positive colorectal carcinoma achieved a partial response (50% decrease in a tumor's bidimensional area) to cetuximab and 21 additional patients had stable disease or exhibited minor responses [233]. Cunningham et al. reported that cetuximab with irinotecan was more effective than cetuximab alone in the treatment of irinotecan-refractory metastatic colorectal carcinoma [234]. The overall response rate for 218 patients who received the combination of irinotecan plus cetuximab was 23% while 111 patients who received the antibody alone demonstrated an 11% response rate. The median time to progression (tumor growth or spread) was 4.1 months for the combination group and 1.5 months for the cetuximab monotherapy group. An acneiform maculopapular rash of the upper torso and scalp developed in about 80% of the patients and the rash was positively correlated with higher survival and radiographic response rates.

Cunningham et al. found that the predictability of cetuximab response failed to correlate with the degree of EGFR expression in colorectal cancer [234]. More surprisingly, Chung et al. reported that cetuximab can be effective in colorectal cancer in patients with tumors that fail to express EGFR protein as measured by immunohistochemistry [235]. Such results may be related to the insensitivity of the test or to the ability of a small number of receptors per cell (10–1000), which are below the detection limit, to provide a therapeutic target. Another possibility is that EGFR exhibits intratumoral heterogeneity so that the particular fields examined were EGFR negative. The studies indicate that immunohistochemistry-based assays of EGFR expression fail to predict the efficacy of cetuximab therapy in colorectal cancer. In contrast, Moroni et al. reported that increased *EGFR* copy number in eight of nine patients as assessed by FISH exhibited an objective tumor response to cetuximab or panitumumab therapy [236].

Van Cutsem et al. investigated the efficacy of irinotecan, fluorouracil, and leucovorin without and with cetuximab as first-line treatment for metastatic colorectal cancer and they tested the mutational status of the *KRAS* gene in tumors and clinical response to the cetuximab regimen [237]. In patients with wild type *KRAS* genes, median progression-free survival in the cetuximab-chemotherapy group was 9.9 months compared with 8.7 months

in the chemotherapy group. The median overall survival in patients with wild type *KRAS* genes the cetuximab-chemotherapy group was 24.9 months compared with 21.0 months in the chemotherapy group while the data for the mutant-*KRAS* population was 17.5 and 17.7 months, respectively. The administration of cetuximab plus chemotherapy as compared with chemotherapy alone was associated with more skin reactions (20% vs. 0.2%). Median progression-free survival in the cetuximab-chemotherapy group increased with increasing grade of rash. The incidence of treatment-related serious adverse reactions was 26% for the combination group and 19% for the chemotherapy group. These results indicated that cetuximab is effective in patients with *KRAS* wild type, but not mutant tumors. Moreover, anecdotal data support the idea that treatment with cetuximab is detrimental in the *KRAS*-mutant group.

Li et al. determined the X-ray crystallographic structure of the antigen binding fragment (Fab) of cetuximab bound to the extracellular domain of EGFR [229]. The structure of EGFR bound to the antibody occurs in the closed, tethered conformation that is characterized by the intramolecular interaction between domains II and IV observed in ligand-free EGFR and is distinct from that observed in the ligand-mediated dimer (compare Figs. 2A and 12C). Neither the structure of the antibody nor the structure of domain III changes upon the formation of the complex. The majority of the specific interactions between FabC225 and EGFR come from the complementary determining regions (CDRs) of the heavy chain. Importantly, the structure indicates that the binding site for cetuximab partially overlaps that determined for EGF. The EGFR amino acids that bind to both cetuximab and EGF include Ser468, Ser440, Val417, Lys465, Ala415, Phe412, Gln384, Gln408, and His 409 residues of the mature protein. The structure indicates that cetuximab prevents ligand binding to EGFR, which secondarily inhibits receptor dimerization, and thus blocks EGFR activation and autophosphorylation. Although the EGFR ligands bind to portions of domains I and III, the antibody binds to domain III only. The structure also indicates that cetuximab prevents the formation of the active, extended, open conformation of EGFR.

5.4.2.2. Panitumumab. Panitumumab is a fully human monoclonal antibody that binds to the extracellular domain of EGFR. It is approved as a single agent for the second-line treatment of EGFR-expressing *KRAS* wild type metastatic cancer with disease progression (tumor growth or spread) on or following fluorouracil, oxaliplatin, and irinotecan therapy. Yang et al. developed panitumumab by immunization of transgenic mice (XenoMouse®), which are able to produce human immunoglobulin light and heavy chains, with human A431 carcinoma cells [238]. After immunization of these animals, a specific clone of B cells that produced an antibody against EGFR was selected and immortalized in CHO cells. These cells were then used for the full scale manufacture of the 100% human antibody. Although panitumumab (IgG2) and cetuximab (IgG1) both target EGFR, they differ in their isotype and they might differ in their mechanism of action. Monoclonal antibodies of the IgG1 isotype may mediate ADCC, whereas the panitumumab IgG2 isotype is unable to do this.

Panitumumab binds EGFR with high affinity (K_i = 50 pM), blocks the binding of both EGF and TGFα to various EGFR-expressing human carcinoma cell lines, and inhibits EGF-dependent tumor cell activation, EGFR tyrosine phosphorylation, and cell proliferation [238]. *In vivo*, panitumumab prevents the formation of human A431 carcinoma tumors in athymic mouse xenografts. Furthermore, administration of the human monoclonal antibody without concomitant chemotherapy results in complete eradication of established tumors in these animals. These investigators reported that tumors expressing more than 17,000 EGFR molecules per cell showed significant growth inhibition when treated with panitumumab. It had no effect on EGFR-negative tumors. They reported that normal skin keratinocytes express about 9200 EGFR molecules per cell so that panitumumab is expected to have no impact on their growth, but it does produce an acneiform rash. The potency of panitumumab in eradicating well-established tumors without concomitant chemotherapy indicates its potential as a monotherapeutic agent for treatment of multiple EGFR-expressing human solid tumors, including those where no effective chemotherapy is available.

Giusti et al. compared the responses of patients with EGFR expressing metastatic colorectal carcinoma after cytotoxic chemotherapy receiving (i) best supportive care or (ii) panitumumab [239]. Most patients had a high level of EGFR expression with 70% having immunohistochemical staining of 2+ or 3+. The criterion for inclusion was only 1+ staining in 1% or more of the cells. The mean progression-free survival was 56 days receiving best supportive care vs. 96 days for those receiving panitumumab. While 8% of patients in the panitumumab group achieved a partial response (50% decrease in a tumor's bidimensional area), none in the control group had an objective response (tumor shrinkage). The median duration of response was 17 weeks. About 90% of the panitumumab group exhibited skin toxicity (57% of the total with acneiform rash), but severe skin toxicity was observed in only 16% of patients. The results of this clinical trial were sufficient to lead to the approval of panitumumab as second-line treatment for metastatic colorectal cancer in patients with wild type *KRAS*. Panitumumab is not as effective in patients with *KRAS* mutations; accordingly the human antibody is not approved for patients with a *KRAS* mutation or for those with unknown *KRAS* mutation status. Studies on the addition of panitumumab to first-line cytotoxic therapies in the treatment of metastatic colorectal cancer have demonstrated promising results [240].

Douillard et el. compared the treatment of oxaliplatin, fluorouracil, and folinic acid (leucovorin) without and with panitumumab [241]. In 512 patients without *KRAS* mutations, median progression-free survival in the panitumumab group was 10.1 months compared with 7.9 months for the control group. Median overall survival was 26.0 months in the panitumumab group and 20.2 months in the control group. They studied a group of 108 metastatic colorectal cancer patients with a non-mutated *KRAS* exon 2 that possessed other *KRAS* mutations. The latter patients had an inferior progression-free and overall survival with panitumumab and the other three agents. Thus patients with *KRAS* exon-2 or other *KRAS* mutations failed to benefit with the addition of the antibody. The addition of panitumumab to cytotoxic chemotherapy appears to be efficacious in the treatment of patients with wild type *RAS*. Currently, there is no X-ray structure in the public domain of panitumumab bound to EGFR.

5.4.2.3. Regorafenib. Regorafenib is a multi-protein kinase inhibitor that is approved for the treatment of metastatic colorectal cancer that had been treated previously with all standard therapies [242]. This drug inhibits several protein kinases including VEGFR1/2/3, Tie2, Kit, Ret, RAF, BRAF, and $BRAF^{V600E}$ [243,244]. Inhibition of VEGFR1/2/3 is antiangiogenic and has wide applicability in cancer therapy [245]. Kit is the stem cell factor receptor that is important in the pathogenesis of gastrointestinal stromal tumors [246], which represents another potential regorafenib target. $BRAF^{V600E}$ is activated in 30–60% of melanomas, 30–50% of thyroid cancers, and 5–20% of colorectal cancers [86]. Inhibition of $BRAF^{V600E}$ may be one of the regorafenib targets in colorectal cancer. Regorafenib apparently does not inhibit EGFR, and there is no available X-ray crystal structure in the public domain of regorafenib bound to any protein kinase.

5.4.3. Oncogenic ERBB3 mutations in human cancers

Jaiswal et al. performed whole exome sequencing of *ERBB3* in 100 primary colorectal tumors along with their matched normal samples [247]. They found protein-altering *ERBB3* mutations in 11% of these tumors. They also examined 92 gastric cancers (12% positive for mutations), 71 NSCLC adenocarcinomas (1%), and 67 squamous cell NSCLCs (1%). Moreover, they tested 37 melanomas and 45 renal, 32 ovarian, 16 large-cell lung, 15 esophageal, 12 small-cell lung, 11 hepatocellular, and small numbers of nine other cancers, but found no *ERBB3* mutations.

The majority of the *ERBB3* mutations occurred in the extracellular domain and several of them occurred multiple times at Val104, Ala232, Pro262, Gly284, Asp297, Gly325, and Thr355 mutational hot spots (nascent protein residue numbers) [247]. Val104, Ala232, and Gly284 cluster at the interface between domain I and II. Pro262 is at the base of domain II, close to Gln271, which is involved in the domain II/IV interaction and is required for the formation of the tethered inactive conformation. Asp297 is adjacent to the long arm of domain II and plays a role in heterodimerization. Asp297, Gly325, and Thr355 occur in positions where large conformational transitions occur during the switch from the inactive to active state. Furthermore, they identified two recurring mutations in the kinase domain: Ser846Ile and Glu928Gly. Residue 846 may be involved in receptor endocytosis and Glu928 occurs near the protein–protein interface observed in the asymmetric kinase dimer.

Jaiswal et al. examined the ability of several of the mutants to promote anchorage-independent growth and tumorigenesis *In vivo* when expressed alone or with ErbB2 [247]. They found that wild type or mutant *ERBB3* when expressed alone did not promote anchorage-independent growth. The majority of their mutants promoted such growth when expressed with ErbB2. These investigators expressed wild type and two extracellular domain *ERBB3* mutants (Pro262His or Gly284Arg) or the Gln809Arg kinase domain mutant in mouse bone-marrow derived BaF3 cells and implanted them in mice where they can promote a leukemia-like disease. All of the mutants when expressed with wild type *ERBB2* promoted the disorder with a median survival of 22–27 days. Mice receiving cells expressing wild type *ERBB3* and *ERBB2* developed the leukemia-like disease with a longer median latency of 39 days. Mice implanted with wild type *ERBB3* but not *ERBB2* were alive at the end of the 60-day test period.

Jaiswal et al. examined the ability of several ErbB inhibitors to inhibit interleukin-3 independent proliferation of mouse bone-marrow derived BaF3 cells expressing human wild type or the Pro262His, Gly284Arg, or Gln809Arg *ERBB3* mutant [247]. They found that lapatinib, an ErbB1/ErbB2 inhibitor, blocked proliferation of all three *ERBB3* mutants, which confirms the notion that ErbB2 is necessary for the ErbB3 response. They found that trastuzumab, which is directed against ErbB2, also blocked proliferation of all three mutants. However, pertuzumab blocked the proliferation of the two extracellular domain mutants, but was only modestly effective against the Gln809Arg kinase domain mutant. The authors suggest that the extracellular domain mutants shift the equilibrium from the tethered to open conformation of ErbB3 that facilitates dimerization with ErbB2. They found that the Gln809Arg mutant does not increase protein kinase activity of ErbB3 and suggest that the mutation alters its conformation to facilitate the formation of ErbB2/ErbB3 heterodimers in a ligand-independent fashion. The authors cite other studies on the occurrence of *ERBB3* mutations in ovarian (1%), head and neck (1%), and hormone receptor positive breast (4%) cancers where functional studies were not performed. The occurrence of *ERBB3* mutations in ≈10% of colorectal and gastric cancers and in ≈4% of certain breast cancers provides another target in the treatment of these disorders.

5.5. Head and neck cancer

Head and neck cancers include cancers of the oral cavity (mouth) including the lip and tongue, nasopharynx (nose and throat), larynx (voice box), salivary glands, and the paranasal sinuses. The estimated incidence of head and neck cancer worldwide in 2008 was about 350,000 and the number of deaths was about 190,000 [140]. In 2012, the estimated incidence of head and neck cancer in the United States was about 41,000 with about 7900 deaths. The success rate in the treatment of head and neck cancers is considerably better than that in the treatment of lung cancer.

More than 95% of head and neck cancers exhibit squamous cell histology. Many patients can be cured by surgery when the tumor is localized (www.NCCN.org). Non-localized cancers are treated by a combination of surgery, radiation therapy, cytotoxic chemotherapy, and targeted therapy. Typical cytotoxic chemotherapy includes a combination of carboplatin and paclitaxel. Cetuximab is an EGFR-targeted therapy that is approved for the treatment of (i) locally or regionally advanced squamous cell carcinoma of the head and neck in combination with radiation therapy, (ii) metastatic disease in combination with platinum-based therapy, and (iii) recurrent or metastatic squamous cell carcinoma progressing after platinum-based therapy.

Cetuximab was approved for the treatment of locally or regionally advanced squamous cell carcinoma of the head and neck in 2006 [248]. An international clinical trial compared cetuximab plus radiation to radiation alone. The median duration of disease control increased from 14.9 months to 24.4 months with the addition of cetuximab, and the median survival increased from 29.3 months to 49.0 months with cetuximab. Cetuximab was also approved as a single agent for the treatment of recurrent or metastatic head and neck cancers in patients who failed platinum-based therapy.

Cohen et al. reported that the FDA approved cetuximab in combination with cisplatin or carboplatin and 5-fluorouracil for the first-line treatment of patients with recurrent local, regional, or metastatic squamous cell head and neck cancer in 2011 [249]. Overall survival, the primary efficacy endpoint, was significantly improved in cetuximab-treated patients (10.1 months) when compared with the control group (7.4 months). Progression-free survival was also significantly improved in patients receiving cetuximab (5.5 months) when compared with the control group (3.3 months). Response rates were 35.6% for the cetuximab treated group and 19.5% for the control group.

Numerous clinical trials are underway testing the efficacy of other EGFR-targeted drugs for head and neck cancers (www.Clinicaltrials.gov). These include the ErbB1 protein-tyrosine kinase inhibitors afatinib, dacomitinib, erlotinib, gefitinib, and lapatinib. The efficacy of other monoclonal antibodies including panitumumab and zalutumumab is also being tested.

5.6. Pancreatic cancer

Pancreatic cancer was the fourth leading cause of cancer deaths in developed countries in 2008, which corresponds to about 162,000 fatalities [140]. In 2012, the incidence of new cases of pancreatic cancer in the United States was about 45,000 and the number of deaths was about 38,000 [141]. The poor prognosis for patients with pancreatic cancer is attributed to early metastasis, its aggressive nature, and the limited efficacy of available systemic treatments [250]. Almost all pancreatic cancers are infiltrating ductal adenocarcinomas that form glands and secrete mucin. About 60% of cancers of the pancreas arise in the head of the gland, 15% in the body, 5%, in the tail, and 20% diffusely involve the entire gland. Patients with pancreatic cancer generally seek medical attention after their disease has progressed. Computerized tomography (CT)

scans are helpful in determining the extent of the disease preoperatively.

Only 15–20% of pancreatic cancer patients will have resectable tumors and only one in five of those undergoing surgery have long-term survival [251]. The operation of choice is a pancreatoduodenectomy, or Whipple operation. This procedure is associated with significant operative morbidity and mortality, even in the hands of experienced surgeons. For those patients with localized disease and small cancers (<2 cm) with no lymph node metastases and no extension beyond the capsule of the pancreas, the five-year survival is still only 20%. On average, when all patients are considered, deaths usually occur within 5–8 months after diagnosis.

Pancreatic cancer has a very poor response to systemic treatments [252]. Gemcitabine has been considered to be the reference treatment in advanced pancreatic cancer since 1997 [253]. Gemcitabine was more effective than 5-fluorouracil in the treatment of advanced and metastatic pancreatic cancer [254]. Conroy et al. reported that FOLFIRINOX (5-fluorouracil, folinic acid, irinotecan, and oxaliplatin) had a longer median overall survival (11.1 months) when compared with gemcitabine (6.8 months) [255]. The four-drug regimen also had a better objective response rate and progression-free survival when compared with gemcitabine. However, such improved efficacy comes at the price of significantly higher toxicity (both hematological and non-hematological), which restricts the use of such regimen to young and fit patients. Páez et al. reviewed the effectiveness of chemotherapeutic and radiation therapies in the treatment of pancreatic cancer [256].

Pancreatic adenocarcinomas often overexpress ErbB1 and this is associated with a worse prognosis [257]. Ng et al. demonstrated that erlotinib inhibited EGFR and potentiated gemcitabine-induced apoptosis in primary pancreatic cancer xenografts in severe combined immunodeficient mice [258]. Moore et al. found that the overall survival in patients with advanced pancreatic cancer was significantly improved with erlotinib and gemcitabine (5.91 months) compared with placebo plus gemcitabine (6.24 months) [259]. Although the results were statistically significant, the data indicate that the ErbB1-targeted inhibitor increases patient life by only 10 days. Nevertheless, this study led to the FDA approval of combination therapy. The effectiveness of treatment was the same in EGFR-positive and negative tumors. Van Cutsem et al. reported that the addition of bevacizumab to gemcitabine and erlotinib failed to improve overall survival in patients with metastatic pancreatic cancer; bevacizumab binds to VEGF-A and inhibits angiogenesis [260].

The high incidence of *KRAS* mutations in pancreatic cancer [261,262] may be one of the factors that limits the benefit of erlotinib and cytotoxic therapies. Ng et al. determined that the hazard ratio was 0.82 in their study, and this represents an 18% reduction in the risk of death (from 1.0 to 0.82), or alternately, an overall 22% improvement in survival (from 0.82 to 1.0) in the group that received gemcitabine and erlotinib [258]. The hazard ratio is the chance of an event occurring in one treatment group divided by the chance of an event occurring in the other treatment group. They indicated that the hazard ratio is the more appropriate measure of overall and progression-free survival in rapidly progressive diseases such as pancreatic cancer because it encompasses the whole observation period and not that of just a single period, such as the median.

5.7. Glioblastoma

The incidence of glioblastoma, a central nervous system (CNS) tumor, is about 3 per 100,000 people in the United States [263]. Thus, the calculated incidence of new cases of glioblastoma in the United States is about 10,000 per year. The approximate incidence of all primary tumors arising within the CNS is about 60,000 per year [263] and that arising within the CNS from metastasis from primary tumors from outside of the CNS including breast, colorectal, and lung cancers is about 160,000 per year [264]. Glioblastomas originate from non-neuronal astrocytic glial cells. Glioblastomas have the histologic appearance similar to undifferentiated astrocytes with cellular polymorphism, atypical nuclei, necrosis (cell death), and microvascular proliferation. The most common presenting signs and symptoms include seizures, headaches, and neurological deficits related to the anatomic site of involvement. Lesions of the left cerebral hemisphere can result in aphasia (inability to speak, read, or write) and lesions in the left/right side of the brain can result in right/left hemiparesis (weakness of the right/left side of the body). The disease has rapid progression with median survival of 1.5 years after diagnosis. This disorder is associated with a 100% mortality rate.

Front-line treatment of glioblastoma includes temozolomide and radiation therapy followed by maintenance temozolomide, an orally effective alkylating agent (Table 5). Surgical resection followed by radiation therapy or combined radiation therapy and chemotherapy is an alternative. Glioblastoma has a propensity to invade surrounding tissue so that complete surgical resection is usually impossible. Surgery also represents one form of palliative treatment for patients with progressive disease. Owing to the increased vascularity of these tumors, studies indicate that bevacizumab has some therapeutic efficacy that lead to its approval for the treatment of glioblastoma [265,266].

About 40% of glioblastomas exhibit *ERBB1* amplification and overexpression [267]. Moreover, an *ERBB1* mutant (*EGFRvIII* (version III)) that possesses a deletion of exons 2–7 occurs in about one-half of tumors with *ERBB1* gene amplification [267–269]. This deletes residues 6–273 in domains I and II and results in a receptor that cannot bind any ligand owing to the deletion of domain I. This deletion allows for the oncogenic activation of ErbB1, which is similar to the activation of the receptor that lacks the extracellular domain.

Both overexpression of ErbB1 and the existence of an activating mutation prompted efforts at drugs targeting the receptor. Numerous clinical trials are underway testing the efficacy of various ErbB1-targeted drugs. These include the ErbB1 protein-tyrosine kinase inhibitors afatinib, dacomitinib, erlotinib, gefitinib, and lapatinib. The efficacy of cetuximab monoclonal antibody is also being tested. These include studies of (i) intraarterial infusion of cetuximab, (ii) combination therapy of cetuximab with bevacizumab and irinotecan, and (iii) combination therapy of cetuximab, radiation therapy, and temozolomide (www.Clinicaltrials.gov).

6. Orally active ErbB protein kinase domain inhibitors, Lipinski's rule of five, lipophilic efficiency, and ligand efficiency

Pharmacologists and medicinal chemists have searched for drug-like chemical properties that result in compounds with oral therapeutic efficacy in a predictable fashion. Lipinski's "rule of five" represents an initial experimental and computational approach to estimate solubility, permeability, and efficacy in the drug discovery and development setting [270]. This rule predicts that poor absorption or permeation is more likely when there are more than 5 hydrogen-bond donors, 10 (5×2) hydrogen-bond acceptors, a molecular weight greater than 500 (5×100) and a calculated Log P (cLog P) greater than 5, where P is the partition coefficient that reflects the ratio of the solubility of a drug in octanol/water. The number of hydrogen-bond donors is expressed as the sum of OH and NH groups, and the number of hydrogen-bond acceptors is expressed as the sum of nitrogen (N) and oxygen (O) atoms. Afatinib, erlotinib, gefitinib, and lapatinib fulfill all of these criteria

(Table 7) with the exception of lapatinib which has a molecular weight of 581.

Since Lipinski's publication in 2001 [270], a deeper understanding of the physicochemical contributions to drug-likeness has led to the refinement of the rule of 5 [272–274]. The concept of lipophilic efficiency (LipE) is a useful check on the tendency to use lipophilicity-driven binding to increase potency. During drug development, the progress of optimization can be assessed by using LipE as an index of binding effectiveness, which is given by the following equations:

$$\text{LipE} = \text{p}K_\text{i} - \text{cLog } D \quad (1)$$

$$\text{LipE} = \text{pIC}_{50} - \text{cLog } D \quad (2)$$

The first term is minus the log of the K_d, K_i, or IC_{50}; larger values indicate greater potency. Although these terms are used interchangeably, they differ in value. When comparing a series of drugs during development, it is best to use the same assay to make valid comparisons. The K_d, or dissociation constant, is measured biochemically and represents an equilibrium constant. The K_i is also measured biochemically and is often reported as an "apparent" constant ($^{\text{app}}K_\text{i}$) because the value depends upon the concentrations of substrates during an assay. For example, if the drug is a competitive inhibitor with respect to one of the substrates, increasing the concentration of that substrate will decrease inhibition and increase the apparent K_i. The IC_{50} is the concentration of compound that inhibits a process by 50%. It can be determined biochemically for an enzyme *in vitro* or in a cell. Its value *in vitro* can change as a function of substrate concentrations. However, substrate concentrations in the cell, in general, cannot be controlled or readily varied.

The second term (−cLog *D*, or minus cLog *D*) represents the lipophilicity of a compound or drug where c indicates that the value is calculated, or computed, using an algorithm based upon the behavior of thousands of organic compounds, and *D* is the distribution coefficient determined at a particular pH. This term is the log of the ratio of the solubility of the compound in octanol/water. The more soluble the compound is in octanol, the greater is its lipophilicity, and the greater is the value of −cLog *D*. Leeson and Springthorpe suggest that compound lipophilicity, as estimated by −cLog *P*, is the most important chemical property to consider during drug development [275]. Lipophilicity plays a dominant role in promoting binding to unwanted drug targets. The goal for drug optimization in the developmental stage is to increase potency without increasing lipophilicity at the same time.

cLog *D* can be determined for several compounds *in silico* in a matter of minutes; the experimental determination of Log *D* is time-consuming and is performed only in select cases. Optimal values of LipE range from 5 to 10 [273]. Increasing potency and decreasing the lipophilicity during drug development, in general, leads to better pharmacological properties. The lipophilic efficiency values for the four FDA-approved EGFR kinase-domain inhibitors are listed in Table 7. Based upon enzyme biochemical data, those for afatinib and erlotinib are in the optimal range of 5–10, but those for gefitinib and lapatinib are not. Based upon cellular inhibition data, only afatinib falls within the optimal range.

The ligand efficiency (LE), which is another key molecular property, is a measurement that relates the potency per heavy atom (non-hydrogen atom) in a drug [276]. The ligand efficiency is given by the following equation:

$$\text{LE} = \frac{\Delta G^{\circ\prime}}{N} = -\text{RT ln } \frac{K_\text{eq}}{N} = -2.303\,\text{RT Log}_{10}\frac{K_\text{eq}}{N} \quad (3)$$

$\Delta G^{\circ\prime}$ represents the standard free energy change at pH 7 during the binding of a drug to its target, *N* is the number of non-hydrogen atoms ("heavy atoms") in the drug, *R* is the universal temperature-energy coefficient, or gas constant (0.00198 kcal/degree mol), *T* is

Table 7
Properties of FDA-approved EGFR kinase-domain inhibitors.

Drug	MW/non-H atoms	*D*/*A*[a]	cLog *P*[b]	cLog *D*[b]	Enzyme pIC_{50}	Enzyme LipE	Enzyme LE	Cell $-\text{Log IC}_{50}$	Cell LipE	Cell LE	Refs.[c]
Afatinib	486/34	2/8	3.97	3.02	9.30	6.28	0.39	8.10	5.08	0.34	[174,175]
Erlotinib	393/29	1/7	3.14	3.12	8.70	5.58	0.42	7.70	4.58	0.37	[172]
Gefitinib	447/31	1/7	4.50	4.33	7.64	3.31	0.35	7.10	2.77	0.32	[171]
Lapatinib	581/39	2/8	4.97	4.48	8.00	3.52	0.29	6.80	2.32	0.25	[271]

[a] *D*, number of hydrogen bond donors; *A*, number of hydrogen-bond acceptors.
[b] Calculations performed with MedChem Designer™, version 2.0, Simulationsplus, Inc., Lancaster, CA 93534.
[c] Sources of primary data on which the calculations are based.

the absolute temperature in Kelvin, and K_{eq} is the equilibrium constant. Ideal values of LE are greater than 0.3 (in kcal/mol). Since it is rarely possible or practical to measure the equilibrium constant, the K_i or IC_{50} is used instead. At 37 °C, or 310 K, Eq. (3) becomes $-(2.303 \times (0.00198 \text{ kcal/mol K}) \times 310 \text{ K Log}_{10} K_{eq})/N$ or $-1.41 \text{ Log}_{10} K_{eq}/N$.

The value of N serves as a surrogate for the molecular weight. The larger the value of N, the greater the molecular weight, and the smaller is the ligand efficiency. The greater the potency or binding affinity, the greater is $-\text{Log}_{10} K_{eq}$, and the greater is the ligand affinity. The ligand efficiency represents the relative binding affinity per non-hydrogen atom in the drug or compound of interest. The ligand efficiency values for the four FDA-approved EGFR kinase-domain inhibitors are listed in Table 7. Except for lapatinib, the values for the other drugs have favorable enzyme-based and cell-based ligand efficiencies (>0.3).

7. Epilog

7.1. Adverse effects and toxicity of non-targeted and targeted anticancer agents

Although nearly all drugs have associated adverse side-effects and toxicities, these are considerably more serious for cytotoxic drugs than for targeted agents [146]. Cytotoxic agents indiscriminately cause macromolecular lesions whereas targeted therapies regulate the activity of specific signaling pathways. The cytotoxic agents are poisons that wreak havoc on the recipient; moreover, many of them are administered at the maximum tolerated dose. The term pharmaceutical is derived from *pharmacon*, which is Greek for poison. During World War II, several nations possessed nitrogen mustard gases as chemical warfare agents or poisons, but they were never used in combat. Gilman provided a historical account on the development of nitrogen mustards in the treatment of lymphomas, based initially on classified work with these agents at Yale University and the University of Chicago during wartime [277]. Referring to the idea of anti-cancer therapies in the 1940s, Gilman wrote "in the minds of most physicians the administration of drugs, other than an analgesic, in the treatment of malignant disease was the act of a charlatan." Great strides in the strategic use of anti-cancer agents have transpired over the past 70 years. Although cytotoxic agents prolong useful life despite debilitating side effects during and after treatment, one of the main goals of targeted cancer therapy is to prolong life with minimal ill effects as a result of treatment.

Nearly all of the cytotoxic drugs listed in Table 5 cause myelosuppression that can produce (i) neutropenia (abnormally low levels of neutrophils, or polymorphonuclear leukocytes), (ii) thrombocytopenia (abnormally low levels of blood platelets), or (iii) anemia (abnormally low levels of erythrocytes, or red blood cells). The sensitivity to suppression occurs in the following rank order: neutrophils > platelets > erythrocytes. This order is inversely correlated with the half-life of the entity: the shorter the half-life, the greater the suppression. Mortality from an uncontrolled infection can result from a decreased neutrophil level, especially if the value is <500/μL. Fortunately, dangerous degrees of thrombocytopenia are uncommon during the management of patients with solid tumors receiving cytotoxic chemotherapy. Severe bleeding can occur with increased frequency at platelet values <20,000/μL. Anemia can be treated with blood transfusions or by erythropoietin injection. Granulocyte colony-stimulating factor (neupogen) and granulocyte macrophage colony-simulating factor (sargramostim) are currently FDA approved for the treatment of neutropenia, and erythropoietin (darbepoetin) and interleukin-11 (oprelvekin) are currently approved for the treatment of anemia and thrombocytopenia, respectively. The development and use of these biological agents has markedly improved the treatment of complications arising from cytotoxic therapies over the last 20 years.

The most common side effect of chemotherapy is nausea, with or without vomiting. High-dose cyclophosphamide and cisplatin are highly emetogenic (causing emesis or vomiting); moderately emetogenic drugs include carboplatin, conventional-dose cyclophosphamide, and anthracyclines such as doxorubicin [146]. Low-risk emetogenic agents include fluorouracil, docetaxel, and paclitaxel. A serotonin 5HT3 antagonist (dolasetron) and a neurokine (KN1) inhibitor (aprepitant) are anti-emetics acting in the medulla oblongata of the CNS that are given prior to the administration of chemotherapy regimens with a high risk of inducing vomiting. The development and use of these agents has made cytotoxic anti-cancer treatments more tolerable. Chemotherapeutic agents vary widely in their propensity to produce alopecia. However, anthracyclines, alkylating agents, and topoisomerase inhibitors reliably cause near-total alopecia. No bona fide treatment of chemotherapeutic-induced alopecia exists, but psychological support and the use of cosmetic resources are standard. As much clinical acumen, knowledge, and judgment is required to treat or prevent adverse events resulting from the use of cytotoxic agents as is required to treat the malignancies themselves.

All four of the small molecule protein kinase inhibitors listed in Table 6 can cause skin rash and diarrhea [146]. Afatinib can cause interstitial lung disease in 1–2% of patients and severe skin blistering or fulminating liver disease in less than 0.2% of patients. Erlotinib can produce hepatotoxicity, interstitial lung disease, or renal failure on rare occasions; it uncommonly produces gastrointestinal perforation and severe skin blistering in which case the drug must be permanently discontinued. Lapatinib can cause nausea, vomiting, and diarrhea, cardiac dysfunction, impaired liver function, and hand-foot syndrome (described in Table 5), but life-threatening events are rare. Gefitinib or erlotinib occasionally produce corneal inflammation. Regorafenib sporadically produces gastrointestinal perforation, after which drug must be permanently discontinued. It can also produce hemorrhage (bleeding), hypertension (high blood pressure), and cardiac ischemia (restricted blood flow to the heart), but these are uncommon events. When severe adverse effects occur, the drugs are discontinued. After standard medical treatment of these adverse events, it is generally possible to re-start the drug.

Toxicity for protein-kinase-domain inhibitors can be exacerbated by eating grapefruit or drinking grapefruit juice. Grapefruit contains several furanocoumarins of which bergamottin is the major component [278]. These phytochemicals (derived from plants) consist of a furan ring fused to aromatic coumarin of the benzopyrone chemical class. Of the 57 human cytochrome P450s, cytochrome P450 3A4 (CYP3A4), which is located in the small intestine and liver, is one of the most abundant and important human drug-metabolizing enzymes acting on the majority of pharmaceuticals taken by people [279,280] including anastrozole, antidepressants, antipsychotics, benzodiazepines, cyclophosphamide, doxorubicin, irinotecan, statins, tamoxifen, and taxanes. Furanocoumarins inhibits intestinal CYP3A4, which leads to elevated levels felodipine (a calcium ion channel blocker used in the treatment of hypertension) and other CYP3A4 substrates [281], which include orally-effective protein-kinase-domain inhibitors.

Studying healthy human subjects, Lilja et al. measured blood levels of simvastatin, a CYP3A4 substrate used in the treatment of hypercholesterolemia, before and several times after its oral administration for a period up to 12 h in subjects taking grapefruit juice three times daily for three days [282]. They found that the maximum blood concentration during the 12 h after taking simvastatin was significantly elevated 2-fold 24 h after the last ingestion of grapefruit juice ($P < 0.01$); the levels measured after three and seven days after ingesting grapefruit juice were not significantly

elevated. However when grapefruit juice and simvastatin were taken together on the fourth day (after three days of grapefruit juice priming), the maximal blood levels were elevated about 12-fold, which was significant ($P < 0.001$). Accordingly, CYP3A4 inhibition occurs rapidly in response to grapefruit juice and the blockade subsides within three days. Whether inhibition of CYP3A4 by grapefruit juice causes similar elevations of any of the kinase-domain targeted inhibitors remains to be established. The FDA labels for erlotinib, lapatinib, and regorafenib recommend avoiding grapefruit when taking these drugs, but those for afatinib and gefitinib do not. However, most health-care providers recommend that patients taking any of the kinase-domain targeted inhibitors avoid dietary grapefruit.

Each of the monoclonal antibodies listed in Table 6 can cause infusion-reactions including panitumumab, a fully human antibody [146]. Each of the four agents can produce pulmonary toxicity, although rarely, and all except ado-trastuzumab-DM1 can cause diarrhea. Cetuximab and panitumumab can cause an acneiform skin rash, and pertuzumab and trastuzumab can produce cardiotoxicity. Trastuzumab occasionally causes neutropenia, and ado-trastuzumab-DM1 rarely produces thrombocytopenia. Although the so-called targeted drugs are associated with overall lower toxicity when compared with cytotoxic agents, patients must still be closely monitored.

7.2. The enigmatic biology of cancers

Of the ErbB/HER-associated cancers considered in this review, pancreatic cancer and glioblastoma have an extremely poor prognosis; they usually result in death within several months after diagnosis. Unfortunately, only 10% of patients with gastric cancers and 15% of patients with lung cancers survive for five years after the time of diagnosis. In the United States, head and neck squamous cell cancers have a favorable prognosis with a curative outcome of 70–90% if treated early (stage I/II); survival is considerably less in patients with more advanced disease at the time of diagnosis. The five-year survival for unselected head and neck cancer patients is 35–50%. If the diagnosis is made prior to metastasis, colorectal cancer can be cured by surgery. However, the overall five-year survival rate is about 60%. The five-year survival rate for breast cancer is about 80% in developed countries. However, this malady is the most common cause of female cancer deaths in the world [140], and this poor outcome is due in part to the unavailability of medical treatment in many regions.

In contrast to the grim prognoses of patients with metastatic pancreatic, stomach, or lung carcinomas, some patients with disseminated tumors can be cured with cytotoxic drugs as discussed next. Germ cell tumors of the testis account for more than 95% of all testicular tumors, and they are the most common solid malignancies to affect young men with an estimated incidence of 7900 new cases in the United States in 2013 [141,283]. Stage III disseminated testicular cancer is treated with three cycles of bleomycin, etoposide, and cisplatin (Table 5) [284], and cure rates are 90% or more [146]. Hodgkin's disease or Hodgkin lymphoma is a disease of B-cell lineage [285] with an estimated incidence of 9200 new cases in the United States in 2013 [141]. Hodgkin lymphoma is treated with dacarbazine, doxorubicin, bleomycin, and vinblastine [286] with cure rates for the stage III or stage IV disease of 70% or higher [146].

Gestational choriocarcinoma is a trophoblastic tumor that results from the abnormal union of a sperm and ovum [287]. Choriocarcinoma is a malignancy that arises from the placental villous and extravillous trophoblast [288]. The estimated incidence of this disorder is 1/40,000 pregnancies. The tumor can perforate the uterine wall, metastasize, and lead to death if left untreated. Choriocarcinoma produces easily detectable amounts of chorionic gonadotropin and is highly responsive to chemotherapy with an overall cure rate exceeding 90%, making it usually possible to achieve cure while preserving reproductive function. Low risk patients are treated with methotrexate and actinomycin D [288,289]. High risk patients are treated very successfully with methotrexate, actinomycin D, cyclophosphamide, and vincristine with cures in 90% of patients [146]. This success is attributable to several factors, the most important of which are the unique sensitivity of choriocarcinoma to chemotherapeutic agents and the use of chorionic gonadotropin as a tumor marker for diagnosis, monitoring treatment, and follow-up.

As noted by Winer and colleagues "Biologically, the cancer cell is notoriously wily; each time we throw an obstacle in its path, it finds an alternate route that must then be blocked" [290]. Resistance occurs in essentially all of the targeted and cytotoxic drugs that are mentioned in Tables 5 and 6. Primary or intrinsic resistance indicates that a cancer does not respond to a drug or combination of drugs, and secondary or acquired resistance indicates that a cancer responds and then becomes resistant. Development of resistance to biological agents (antibodies) and protein-kinase-domain inhibitors within one or two years is the rule. The only exception appears to be the first FDA-approved protein kinase inhibitor (imatinib) that is used for the treatment of chronic myelogenous leukemia. Khorashad and Deininger estimated that 60–80% of people with chronic myelogenous leukemia will receive a long-term clinical benefit that can last for a decade or more [291], and Kantarjian and O'Brien reported that imatinib has improved the 10-year survival rate from 20% to 85% [292]. For targeted protein-kinase-domain inhibitors, acquired resistance results from mutations in the target protein kinase, to activation of by-pass pathways, and to unknown mechanisms.

A few cancers have a major oncogenic driver that contributes to the disease state such as the BCR-Abl oncogene of chronic myelogenous leukemia [291]. However, most cancers exhibit dysregulation of many signaling pathways that promote proliferation, evade growth suppressors, sustain invasion and metastasis, enable replicative immortality, induce angiogenesis, and inhibit apoptosis [293]. Targeting an oncogenic driver often results in short-term benefits, but more must be done to increase long-term benefits. One strategy to prevent or delay resistance to the ErbB-targeted agents is to administer agents that inhibit (i) angiogenesis, (ii) Akt-mediated cell survival, or (iii) Ras/Raf/MEK/ERK1/2-mediated cell proliferation before resistance occurs. One commonly observed mechanism of resistance involves activation of by-pass pathways. Akt and Ras signaling are downstream from many protein-tyrosine kinase receptors and inhibition of these pathways may abrogate the cell proliferative and survival signaling that is mediated through by-pass pathway activation.

Different strategies are used to combine targeted therapies most effectively. One idea is to use two inhibitors directed at the same target, e.g., inhibition of ErbB2 with both trastuzumab and pertuzumab. This combination has been successfully exploited in the treatment of ErbB2-positive breast cancers along with docetaxel, a cytotoxic agent. Another strategy is to target different parts of an oncogenic signal transduction pathway, e.g., a receptor and one or more of its downstream pathways. A clinical trial is underway for the study of the combination of afatinib (an EGFR antagonist) and sirolimus (an inhibitor of the anti-apoptotic enzyme mTOR) in the treatment of NSCLC (Clinicaltrials.gov). Another trial is examining the combination of lapatinib (an ErbB1/2 antagonist) and MK 2206 (a MEK inhibitor) in the treatment of metastatic breast cancer. Flaherty et al. reported that the combination of dabrafenib (a B-RAF inhibitor) and trametinib (a MEK1/2 inhibitor) was more effective in treating patients with metastatic melanoma than dabrafenib monotherapy [294]; both drugs, which are products of GlaxoSmithKline, were given at their full monotherapeutic

doses. Although the incidence of pyrexia (fever) was greater in the combination group, Flaherty observed no other increases in toxicity in the combination group than in the dabrafenib monotherapy group.

Thus far the combination of monoclonal antibodies and small molecule protein kinase inhibitors in the treatment of malignancies has been unsuccessful [199]. However, clinical trials using a combination of afatinib with (i) trastuzumab in the treatment of breast or stomach cancer and (ii) cetuximab in the treatment of colorectal cancer are underway (Clinicaltrials.gov). Studies using lapatinib and (i) cetuximab for the treatment of lung or head and neck squamous cell carcinomas and (ii) trastuzumab for the treatment of ErbB2-positive breast cancer are on-going. The preparation of antibody drug conjugates of trastuzumab and platinum-based drugs represents another approach in the treatment of ErB2-positive breast cancers [295]. Moreover, numerous clinical trials are in progress to compare the combination of afatinib, gefitinib, erlotinib, or lapatinib with one or more cytotoxic agents for the treatment of various solid tumors.

Preclinical (laboratory-based) and clinical experiments will be required to determine whether co-administration, alternating administration, or intercalated administration of two inhibitors is more effective in preventing the acquisition of drug resistance. Unfortunately, clinical trials that compare combinations of inhibitors are time consuming and expensive. Furthermore, deciding which combinations to use is problematic. As Knight et al. have pointed out, there is a need "for companies to collaborate to test new combinations of investigational drugs in oncology, where there is arguably the greatest need and opportunity" [296]. Unless the cost of protein-kinase-domain inhibitors decreases, the combined use of two or more of these inhibitors promises to be rather expensive.

Kuczynski et al. noted that one of the dogmas of anti-cancer treatment is to initiate a different therapy following the emergence of resistant disease using non-cross-resistant drugs [297]. However, they report that there are many examples of cases where patients respond to the reintroduction of the same therapy (drug rechallenge) following a drug holiday or a second course of treatment. A small number of patients with NSCLC have been studied who had become resistant to gefitinib, who were treated with cytotoxic therapy or no therapy, and then received second course of gefitinib to which they responded [298,299]. In a case report, Wong et al. described a lung cancer patient who responded and then acquired resistance to gefitinib, who subsequently responded and then came resistant to erlotinib, and who then responded to a second course of gefitinib treatment [300]. This patient's tumor displayed a lack of cross-resistance to the same class of drug. In a review of VEGFR kinase domain-targeted therapy of renal cell carcinoma, Escudier et al. reported that there is a lack of total cross resistance of sorafenib and sunitinib and that the sequential use of these agents may prolong cumulative progression-free survival [301]. The case described by Wong et al. and the more extensive review by Escudier et al. describe the potential emergence of non-inheritable resistance mechanisms [300,301].

Chaft et al. reported that discontinuing erlotinib or gefitinib after the development of acquired resistance to these agents during the treatment of *EGFR*-mutant drug cancer resulted in accelerated disease progression, or flare up of the disease, in 14 of 61 patients [302]. Accordingly, following the general practice of anti-cancer therapeutics to initiate a different therapy following the emergence of resistant disease can have untoward consequences. Gainor and Shaw further reviewed various mechanisms for the development of resistance to tyrosyl kinase inhibitors in *EGFR*-mutant and ALK-positive lung cancers [303]. They remark that knowledge of the mechanisms underlying resistance to these targeted kinase inhibitors will be helpful in the development of new treatment strategies.

Santini et al. carried out a phase II multicenter trial in patients with *KRAS* wild type colorectal cancer to examine the potential benefit of cetuximab rechallenge after progression on cetuximab-based therapy [304]. Of the 39 patients rechallenged following disease progression on intervening therapy, 54% achieved an objective response, 36% had stable disease, and 51% achieved the same or better response as was observed during the initial cetuximab-based treatment. The authors suggested that intervening therapy caused an increase in the proportion of sensitive tumor cells prior to cetuximab re-exposure. However, Kuczynski et al. report that progression-free survival is generally shorter and objective responses are usually weaker at rechallenge in a variety of cancers [297]. Nonetheless, the mechanisms responsible for the beneficial effect of rechallenge treatments are unclear.

Kuczynski et al. argue that the main implication of transient or reversible drug resistance is that an agent should not be uniformly excluded from further use in a patient for whom it was previously found to be effective and well-tolerated [297]. If a patient on long-term therapy desires a drug holiday, early interruption of therapy might be considered without the concern of accelerating drug resistance or potentially compromising overall survival. If all other treatment options have been exhausted, continuing the same therapy indefinitely or a drug rechallenge is a viable alternative. This preference could also be desirable even if other agents are available.

Moreover, if a previously used drug is inexpensive and the other agent is expensive, a cost-benefit assessment might favor retreatment with the less-expensive agent. Continuing a high-cost drug ($5000–$12,000 per month) such as a protein-kinase-domain inhibitor or a biologic such as trastuzumab beyond progression can be troubling given the modest improvement in survival that these agents provide. See Ref. [305] for the monthly cost of 20 targeted anticancer drugs in the United States; the authors discuss the unfortunate lack of effectiveness of many of these drugs in extending the life of the patient despite their high cost. Overall, the question should not be what can we be improving, but rather what can we not be improving.

Conflict of interest

The author is unaware of any affiliations, memberships, or financial holdings that might be perceived as affecting the objectivity of this review.

Acknowledgements

The author thanks Prof. John Kuriyan for providing the protein data bank file for the EGFR asymmetric dimer. He also thanks the library staff of the University of North Carolina at Chapel Hill Health Sciences library for providing bibliographic assistance and Laura M. Roskoski for providing editorial support.

References

[1] Lemmon MA, Schlessinger J. Cell signaling by receptor tyrosine kinases. Cell 2010;141:1117–34.
[2] Cohen S. The epidermal growth factor (EGF). Cancer 1983;51:1787–91.
[3] Carpenter G, Cohen S. Epidermal growth factor. J Biol Chem 1990;265:7709–12.
[4] Cohen S, Ushiro H, Stoscheck C, Chinkers M. A native 170,000 epidermal growth factor receptor-kinase complex from shed plasma membrane vesicles. J Biol Chem 1982;257:1523–31.
[5] Thompson DM, Gill GN. The EGF receptor: structure, regulation, and potential role in malignancy. Cancer Surv 1985;4:767–88.
[6] Manning G, Whyte DB, Martinez R, Hunter T, Sudarsanam S. The protein kinase complement of the human genome. Science 2002;298:1912–34.
[7] Alonso A, Sasin J, Bottini N, Friedberg I, Friedberg I, Osterman A, et al. Protein tyrosine phosphatases in the human genome. Cell 2004;117:699–711.

[8] Wain HM, Bruford EA, Lovering RC, Lush MJ, Wright MW, Povey S. Guidelines for human gene nomenclature. Genomics 2002;79:464–70.
[9] Maltais LJ, Blake JA, Chu T, Lutz CM, Eppig JT, Jackson I. Rules and guidelines for mouse gene, allele, and mutation nomenclature: a condensed version. Genomics 2002;79:471–4.
[10] Levan G, Hedrich HJ, Remmers EF, Serikawa T, Yoshida MC. Standardized rat genetic nomenclature. Mamm Genome 1995;6:447–8.
[11] Schechter AL, Stern DF, Vaidyanathan L, Decker SJ, Drebin JA, Greene MI, et al. The neu oncogene: an erb-B-related gene encoding a 185,000-Mr tumour antigen. Nature 1984;312:513–6.
[12] Citri A, Yarden Y. EGF-ERBB signalling: towards the systems level. Nat Rev Mol Cell Biol 2006;7:505–16.
[13] Britsch S. The neuregulin-I/ErbB signaling system in development and disease. Adv Anat Embryol Cell Biol 2007;190:1–6.
[14] Rajagopalan V, Zucker IH, Jones JA, Carlson M, Ma YJ. Cardiac ErbB-1/ErbB-2 mutant expression in young adult mice leads to cardiac dysfunction. Am J Physiol Heart Circ Physiol 2008;295:H543–54.
[15] Miettinen PJ, Berger JE, Meneses J, Phung Y, Pedersen RA, Werb Z, et al. Epithelial immaturity and multiorgan failure in mice lacking epidermal growth factor receptor. Nature 1995;376:337–41.
[16] Threadgill DW, Dlugosz AA, Hansen LA, Tennenbaum T, Lichti U, Yee D, et al. Targeted disruption of mouse EGF receptor: effect of genetic background on mutant phenotype. Science 1995;269:230–4.
[17] Gassmann M, Casagranda F, Orioli D, Simon H, Lai C, Klein R, et al. Aberrant neural and cardiac development in mice lacking the ErbB4 neuregulin receptor. Nature 1995;378:390–4.
[18] Lee KF, Simon H, Chen H, Bates B, Hung MC, Hauser C. Requirement for neuregulin receptor erbB2 in neural and cardiac development. Nature 1995;378:394–8.
[19] Riethmacher D, Sonnenberg-Riethmacher E, Brinkmann V, Yamaai T, Lewin GR, Birchmeier C. Severe neuropathies in mice with targeted mutations in the ErbB3 receptor. Nature 1997;389:725–30.
[20] Ullrich A, Coussens L, Hayflick JS, Dull TJ, Gray A, Tam AW, et al. Human epidermal growth factor receptor cDNA sequence and aberrant expression of the amplified gene in A431 epidermoid carcinoma cells. Nature 1984;309:418–25.
[21] Elenius K, Corfas G, Paul S, Choi CJ, Rio C, Plowman GD, et al. A novel juxtamembrane domain isoform of HER4/ErbB4. Isoform-specific tissue distribution and differential processing in response to phorbol ester. J Biol Chem 1997;272:26761–8.
[22] Ghosh R, Narasanna A, Wang SE, Liu S, Chakrabarty A, Balko JM, et al. Trastuzumab has preferential activity against breast cancers driven by ERBB2 homodimers. Cancer Res 2011;71:1871–82.
[23] Shi F, Telesco SE, Liu Y, Radhakrishnan R, Lemmon MA. ErbB3/HER3 intracellular domain is competent to bind ATP and catalyze autophosphorylation. Proc Natl Acad Sci USA 2010;107:7692–7.
[24] Tzahar E, Waterman H, Chen X, Levkowitz G, Karunagaran D, Lavi S, et al. A hierarchical network of interreceptor interactions determines signal transduction by Neu differentiation factor/neuregulin and epidermal growth factor. Mol Cell Biol 1996;16:5276–87.
[25] Graus-Porta D, Beerli RR, Daly JM, Hynes NE. ErbB-2, the preferred heterodimerization partner of all ErbB receptors, is a mediator of lateral signaling. EMBO J 1997;16:1647–55.
[26] Pinkas-Kramarski R, Soussan L, Waterman H, Levkowitz G, Alroy I, Klapper L, et al. Diversification of Neu differentiation factor and epidermal growth factor signaling by combinatorial receptor interactions. EMBO J 1996;15:2452–67.
[27] Gullick WJ. The Type 1 growth factor receptors and their ligands considered as a complex system. Endocr Relat Cancer 2001;8:75–82.
[28] Blobel CP. ADAMs: key components in EGFR signalling and development. Nat Rev Mol Cell Biol 2005;6:32–43.
[29] Rocks N, Paulissen G, El Hour M, Quesada F, Crahay C, Gueders M, et al. Emerging roles of ADAM and ADAMTS metalloproteinases in cancer. Biochimie 2008;90:369–79.
[30] Scheller J, Chalaris A, Garbers C, Rose-John S. ADAM17: a molecular switch to control inflammation and tissue regeneration. Trends Immunol 2011;32:380–7.
[31] Rose-John S. ADAM17, shedding, TACE as therapeutic targets. Pharmacol Res 2013;71:19–22.
[32] Schlessinger J. Ligand-induced, receptor-mediated dimerization and activation of EGF receptor. Cell 2002;110:669–72.
[33] Aritomi M, Kunishima N, Okamoto T, Kuroki R, Ota Y, Morikawa K. Atomic structure of the GCSF-receptor complex showing a new cytokine-receptor recognition scheme. Nature 1999;401:713–7.
[34] Ogiso H, Ishitani R, Nureki O, Fukai S, Yamanaka M, Kim JH, et al. Crystal structure of the complex of human epidermal growth factor and receptor extracellular domains. Cell 2002;110:775–87.
[35] Garrett TP, McKern NM, Lou M, Elleman TC, Adams TE, Lovrecz GO, et al. Crystal structure of a truncated epidermal growth factor receptor extracellular domain bound to transforming growth factor α. Cell 2002;110:763–73.
[36] Garrett TP, McKern NM, Lou M, Elleman TC, Adams TE, Lovrecz GO, et al. The crystal structure of a truncated ErbB2 ectodomain reveals an active conformation, poised to interact with other ErbB receptors. Mol Cell 2003;11:495–505.
[37] Ferguson KM, Berger MB, Mendrola JM, Cho HS, Leahy DJ, Lemmon MA. EGF activates its receptor by removing interactions that autoinhibit ectodomain dimerization. Mol Cell 2003;11:507–17.
[38] Burgess AW, Cho HS, Eigenbrot C, Ferguson KM, Garrett TP, Leahy DJ, et al. An open-and-shut case? Recent insights into the activation of EGF/ErbB receptors. Mol Cell 2003;12:541–52.
[39] Lu HS, Chai JJ, Li M, Huang BR, He CH, Bi RC. Crystal structure of human epidermal growth factor and its dimerization. J Biol Chem 2001;276:34913–7.
[40] Domagala T, Konstantopoulos N, Smyth F, Jorissen RN, Fabri L, Geleick D, et al. Stoichiometry, kinetic and binding analysis of the interaction between epidermal growth factor (EGF) and the extracellular domain of the EGF receptor. Growth Factors 2000;18:11–29.
[41] Cho HS, Leahy DJ. Structure of the extracellular region of HER3 reveals an interdomain tether. Science 2002;297:1330–3.
[42] Bouyain S, Longo PA, Li S, Ferguson KM, Leahy DJ. The extracellular region of ErbB4 adopts a tethered conformation in the absence of ligand. Proc Natl Acad Sci USA 2005;102:15024–9.
[43] Cho HS, Mason K, Ramyar KX, Stanley AM, Gabelli SB, Denney Jr DW, et al. Structure of the extracellular region of HER2 alone and in complex with the Herceptin Fab. Nature 2003;421:756–60.
[44] Liu P, Cleveland 4th TE, Bouyain S, Byrne PO, Longo PA, Leahy DJ. A single ligand is sufficient to activate EGFR dimers. Proc Natl Acad Sci USA 2012;109:1086–96.
[45] Alvarado D, Klein DE, Lemmon MA. Structural basis for negative cooperativity in growth factor binding to an EGF receptor. Cell 2010;142:568–79.
[46] Macdonald-Obermann JL, Adak S, Landgraf R, Piwnica-Worms D, Pike LJ. Dynamic analysis of the epidermal growth factor (EGF) receptor-ErbB2-ErbB3 protein network by luciferase fragment complementation imaging. J Biol Chem 2013;288:30773–84.
[47] Huse M, Kuriyan J. The conformational plasticity of protein kinases. Cell 2002;109:275–82.
[48] Taylor SS, Keshwani MM, Steichen JM, Kornev AP. Evolution of the eukaryotic protein kinases as dynamic molecular switches. Philos Trans R Soc Lond Biol Sci 2012;367:2517–28.
[49] Knighton DR, Zheng JH, Ten Eyck LF, Ashford VA, Xuong NH, Taylor SS, et al. Crystal structure of the catalytic subunit of cyclic adenosine monophosphate-dependent protein kinase. Science 1991;253:407–14.
[50] Hanks SK, Quinn AM, Hunter T. The protein kinase family: conserved features and deduced phylogeny of the catalytic domains. Science 1988;241:42–52.
[51] Schwartz PA, Murray BW. Protein kinase biochemistry and drug discovery. Bioorg Chem 2011;39:192–210.
[52] Kornev AP, Haste NM, Taylor SS, Eyck LF. Surface comparison of active and inactive protein kinases identifies a conserved activation mechanism. Proc Natl Acad Sci USA 2006;103:17783–8.
[53] Meharena HS, Chang P, Keshwani MM, Oruganty K, Nene AK, Kannan N, et al. Deciphering the structural basis of eukaryotic protein kinase regulation. PLoS Biol 2013;11:e1001680.
[54] Nolen B, Taylor S, Ghosh G. Regulation of protein kinases: controlling activity through activation segment conformation. Mol Cell 2004;15:661–75.
[55] Gotoh N, Tojo A, Hino M, Yazaki Y, Shibuya M. A highly conserved tyrosine residue at codon 845 within the kinase domain is not required for the transforming activity of human epidermal growth factor receptor. Biochem Biophys Res Commun 1992;186:768–74.
[56] Tice DA, Biscardi JS, Nickles AL, Parsons SJ. Mechanism of biological synergy between cellular Src and epidermal growth factor receptor. Proc Natl Acad Sci USA 1999;96:1415–20.
[57] Guy PM, Platko JV, Cantley LC, Cerione RA, Carraway 3rd KL. Insect cell-expressed p180erbB3 possesses an impaired tyrosine kinase activity. Proc Natl Acad Sci USA 1994;91:8132–6.
[58] Citri A, Skaria KB, Yarden Y. The deaf and the dumb: the biology of ErbB-2 and ErbB-3. Exp Cell Res 2003;284:54–65.
[59] Boudeau J, Miranda-Saavedra D, Barton GJ, Alessi DR. Emerging roles of pseudokinases. Trends Cell Biol 2006;16:443–52.
[60] Zhang Q, Park E, Kani K, Landgraf R. Functional isolation of activated and unilaterally phosphorylated heterodimers of ERBB2 and ERBB3 as scaffolds in ligand-dependent signaling. Proc Natl Acad Sci USA 2012;109:13237–42.
[61] Taylor SS, Kornev AP. Protein kinases: evolution of dynamic regulatory proteins. Trends Biochem Sci 2011;36:65–77.
[62] Zhang J, Yang PL, Gray NS. Targeting cancer with small molecule kinase inhibitors. Nat Rev Cancer 2009;9:28–39.
[63] Biscardi JS, Maa MC, Tice DA, Cox ME, Leu TH, Parsons SJ. c-Src-mediated phosphorylation of the epidermal growth factor receptor on Tyr845 and Tyr1101 is associated with modulation of receptor function. J Biol Chem 1999;274:8335–43.
[64] Zhang X, Gureasko J, Shen K, Cole PA, Kuriyan J. An allosteric mechanism for activation of the kinase domain of epidermal growth factor receptor. Cell 2006;125:1137–49.
[65] Macdonald-Obermann JL, Piwnica-Worms D, Pike LJ. Mechanics of EGF receptor/ErbB2 kinase activation revealed by luciferase fragment complementation imaging. Proc Natl Acad Sci USA 2012;109:137–42.
[66] Red Brewer M, Choi SH, Alvarado D, Moravcevic K, Pozzi A, Lemmon MA, et al. The juxtamembrane region of the EGF receptor functions as an activation domain. Mol Cell 2009;34:641–51.
[67] Arkhipov A, Shan Y, Das R, Endres NF, Eastwood MP, Wemmer DE, et al. Architecture and membrane interactions of the EGF receptor. Cell 2013;152:557–69.
[68] Jura N, Endres NF, Engel K, Deindl S, Das R, Lamers MH, et al. Mechanism for activation of the EGF receptor catalytic domain by the juxtamembrane segment. Cell 2009;137:1293–307.

[69] Wood ER, Shewchuk LM, Ellis B, Brignola P, Brashear RL, Caferro TR, et al. 6-Ethynylthieno[3,2-d]- and 6-ethynylthieno[2,3-d]pyrimidin-4-anilines as tunable covalent modifiers of ErbB kinases. Proc Natl Acad Sci USA 2008;105:2773–8. Erratum in: Proc Natl Acad Sci USA 2008;105:6208.
[70] Bocharov EV, Mineev KS, Volynsky PE, Ermolyuk YS, Tkach EN, Sobol AG, et al. Spatial structure of the dimeric transmembrane domain of the growth factor receptor ErbB2 presumably corresponding to the receptor active state. J Biol Chem 2008;283:6950–6.
[71] Mineev KS, Bocharov EV, Pustovalova YE, Bocharova OV, Chupin VV, Arseniev AS. Spatial structure of the transmembrane domain heterodimer of ErbB1 and ErbB2 receptor tyrosine kinases. J Mol Biol 2010;400:231–43.
[72] Brosig B, Langosch D. The dimerization motif of the glycophorin A transmembrane segment in membranes: importance of glycine residues. Protein Sci 1998;7:1052–6.
[73] Escher C, Cymer F, Schneider D. Two GxxxG-like motifs facilitate promiscuous interactions of the human ErbB transmembrane domains. J Mol Biol 2009;389:10–6.
[74] Lu C, Mi LZ, Grey MJ, Zhu J, Graef E, Yokoyama S, et al. Structural evidence for loose linkage between ligand binding and kinase activation in the epidermal growth factor receptor. Mol Cell Biol 2010;30:5432–43.
[75] Endres NF, Das R, Smith AW, Arkhipov A, Kovacs E, Huang Y, et al. Conformational coupling across the plasma membrane in activation of the EGF receptor. Cell 2013;152:543–56.
[76] Bessman NJ, Lemmon MA. Finding the missing links in EGFR. Nat Struct Mol Biol 2012;19:1–3.
[77] Chung I, Akita R, Vandlen R, Toomre D, Schlessinger J, Mellman I. Spatial control of EGF receptor activation by reversible dimerization on living cells. Nature 2010;464:783–7.
[78] Mi LZ, Lu C, Li Z, Nishida N, Walz T, Springer TA. Simultaneous visualization of the extracellular and cytoplasmic domains of the epidermal growth factor receptor. Nat Struct Mol Biol 2011;18:984–9.
[79] Kästner J, Loeffler HH, Roberts SK, Martin-Fernandez ML, Winn MD. Ectodomain orientation, conformational plasticity and oligomerization of ErbB1 receptors investigated by molecular dynamics. J Struct Biol 2009;167:117–28.
[80] Yarden Y, Sliwkowski MX. Nat Rev Mol Cell Biol 2001;2:127–37.
[81] Yarden Y, Pines G. The ERBB network: at last, cancer therapy meets systems biology. Nat Rev Cancer 2012;12:553–63.
[82] Seshacharyulu P, Ponnusamy MP, Haridas D, Jain M, Ganti AK, Batra SK. Targeting the EGFR signaling pathway in cancer therapy. Expert Opin Ther Targets 2012;16:15–31.
[83] Wilson KJ, Gilmore JL, Foley J, Lemmon MA, Riese 2nd DJ. Functional selectivity of EGF family peptide growth factors: implications for cancer. Pharmacol Ther 2009;122:1–8.
[84] Engelman JA. Targeting PI3K signalling in cancer: opportunities, challenges and limitations. Nat Rev Cancer 2009;9:550–62.
[85] Vanhaesebroeck B, Stephens L, Hawkins P. PI3K signalling: the path to discovery and understanding. Nat Rev Mol Cell Biol 2012;13:195–203.
[86] Roskoski Jr R. RAF protein-serine/threonine kinases: structure and regulation. Biochem Biophys Res Commun 2010;399:313–7.
[87] Roskoski Jr R. MEK1/2 dual-specificity protein kinases: structure and regulation. Biochem Biophys Res Commun 2012;417:5–10.
[88] Roskoski Jr R. ERK1/2 MAP kinases: structure, function, and regulation. Pharmacol Res 2012;66:105–43.
[89] Lowenstein EJ, Daly RJ, Batzer AG, Li W, Margolis B, Lammers R, et al. The SH2 and SH3 domain-containing protein GRB2 links receptor tyrosine kinases to ras signaling. Cell 1992;70:431–42.
[90] Li W, She H. The SH2 and SH3 adapter Nck: a two-gene family and a linker between tyrosine kinases and multiple signaling networks. Histol Histopathol 2000;15:947–55.
[91] Kobashigawa Y, Sakai M, Naito M, Yokochi M, Kumeta H, Makino Y, et al. Structural basis for the transforming activity of human cancer-related signaling adaptor protein CRK. Nat Struct Mol Biol 2007;14:503–10.
[92] Tamás P, Solti Z, Bauer P, Illés A, Sipeki S, Bauer A, et al. Mechanism of epidermal growth factor regulation of Vav2, a guanine nucleotide exchange factor for Rac. J Biol Chem 2003;278:5163–71.
[93] Xia L, Wang L, Chung AS, Ivanov SS, Ling MY, Dragoi AM, et al. Identification of both positive and negative domains within the epidermal growth factor receptor COOH-terminal region for signal transducer and activator of transcription (STAT) activation. J Biol Chem 2002;277:30716–3023.
[94] Mazzocco M, Maffei M, Egeo A, Vergano A, Arrigo P, Di Lisi R, et al. The identification of a novel human homologue of the SH3 binding glutamic acid-rich (SH3BGR) gene establishes a new family of highly conserved small proteins related to thioredoxin superfamily. Gene 2002;291:233–9.
[95] Khalil AA, James P. Biomarker discovery: a proteomic approach for brain cancer profiling. Cancer Sci 2007;98:201–13.
[96] Downward J. Targeting RAS signalling pathways in cancer therapy. Nat Rev Cancer 2003;3:11–22.
[97] Tocque B, Delumeau I, Parker F, Maurier F, Multon MC, Schweighoffer F. Ras-GTPase activating protein (GAP): a putative effector for Ras. Cell Signal 1997;9:153–8.
[98] Roskoski Jr R. Src protein-tyrosine kinase structure and regulation. Biochem Biophys Res Commun 2004;324:1155–64.
[99] Panjarian S, Iacob RE, Chen S, Engen JR, Smithgall TE. Structure and dynamic regulation of Abl kinases. J Biol Chem 2013;288:5443–50.
[100] Stewart ZA, Pietenpol JA. Syk: a new player in the field of breast cancer. Breast Cancer Res 2001;3:5–7.
[101] Kadamur G, Ross EM. Mammalian phospholipase C. Annu Rev Physiol 2013;75:127–54.
[102] Martiny-Baron G, Fabbro D. Classical PKC isoforms in cancer. Pharmacol Res 2007;55:477–86.
[103] Totoń E, Ignatowicz E, Skrzeczkowska K, Rybczyńska M. Protein kinase Cε as a cancer marker and target for anticancer therapy. Pharmacol Rep 2011;63:19–29.
[104] Mochly-Rosen D, Das K, Grimes KV. Protein kinase C, an elusive therapeutic target? Nat Rev Drug Discov 2012;11:937–57.
[105] Basu A, Sivaprasad U. Protein kinase Cε makes the life and death decision. Cell Signal 2007;19:1633–42.
[106] Krasnitsky E, Baumfeld Y, Freedman J, Sion-Vardy N, Ariad S, Novack V, et al. PKCη is a novel prognostic marker in non-small cell lung cancer. Anticancer Res 2012;32:1507–13.
[107] López-Ruiz P, Rodriguez-Ubreva J, Cariaga AE, Cortes MA, Colás B. SHP-1 in cell-cycle regulation. Anticancer Agents Med Chem 2011;11:89–98.
[108] Yang J, Liu L, He D, Song X, Liang X, Zhao ZJ, et al. Crystal structure of human protein-tyrosine phosphatase SHP-1. J Biol Chem 2003;278:6516–20.
[109] Tenev T, Böhmer SA, Kaufmann R, Frese S, Bittorf T, Beckers T, et al. Perinuclear localization of the protein-tyrosine phosphatase SHP-1 and inhibition of epidermal growth factor-stimulated STAT1/3 activation in A431 cells. Eur J Cell Biol 2000;79:261–71.
[110] Insabato L, Amelio I, Quarto M, Zannetti A, Tolino F, de Mauro G, et al. Elevated expression of the tyrosine phosphatase SHP-1 defines a subset of high-grade breast tumors. Oncology 2009;77:378–84.
[111] Agazie YM, Hayman MJ. Development of an efficient substrate-trapping mutant of Src homology phosphotyrosine phosphatase 2 and identification of the epidermal growth factor receptor, Gab1, and three other proteins as target substrates. J Biol Chem 2003;278:13952–8.
[112] Zhou X, Agazie YM. Molecular mechanism for SHP2 in promoting HER2-induced signaling and transformation. J Biol Chem 2009;284:12226–34.
[113] Langdon WY, Hartley JW, Klinken SP, Ruscetti SK, Morse HC. v-cbl, an oncogene from a dual-recombinant murine retrovirus that induces early B-lineage lymphomas. Proc Natl Acad Sci USA 1989;86:1168–72.
[114] Longva KE, Blystad FD, Stang E, Larsen AM, Johannessen LE, Madshus IH. Ubiquitination and proteasomal activity is required for transport of the EGF receptor to inner membranes of multivesicular bodies. J Cell Biol 2002;156:843–54.
[115] Umebayashi K, Stenmark H, Yoshimori T. Ubc4/5 and c-Cbl continue to ubiquitinate EGF receptor after internalization to facilitate polyubiquitination and degradation. Mol Biol Cell 2008;19:3454–62.
[116] Haglund K, Dikic I. The role of ubiquitylation in receptor endocytosis and endosomal sorting. J Cell Sci 2012;125:265–75.
[117] Carpenter G, Cohen S. ^{125}I-labeled human epidermal growth factor. Binding, internalization, and degradation in human fibroblasts. J Cell Biol 1976;71:159–71.
[118] Sorkin A, Waters CM. Endocytosis of growth factor receptors. Bioessays 1993;15:375–82.
[119] Baulida J, Kraus MH, Alimandi M, Di Fiore PP, Carpenter G. All ErbB receptors other than the epidermal growth factor receptor are endocytosis impaired. J Biol Chem 1996;271:5251–7.
[120] Carpenter G, Liao HJ. Trafficking of receptor tyrosine kinases to the nucleus. Exp Cell Res 2009;315:1556–66.
[121] Marti U, Burwen SJ, Wells A, Barker ME, Huling S, Feren AM, et al. Localization of epidermal growth factor receptor in hepatocyte nuclei. Hepatology 1991;13:15–20.
[122] Wang YN, Yamaguchi H, Hsu JM, Hung MC. Nuclear trafficking of the epidermal growth factor receptor family membrane proteins. Oncogene 2010;29:3997–4006.
[123] Xu L, Massagué J. Nucleocytoplasmic shuttling of signal transducers. Nat Rev Mol Cell Biol 2004;5:209–19.
[124] Hoelz A, Debler EW, Blobel G. The structure of the nuclear pore complex. Annu Rev Biochem 2011;80:613–43.
[125] Chow KH, Factor RE, Ullman KS. The nuclear envelope environment and its cancer connections. Nat Rev Cancer 2012;12:196–209.
[126] Lo HW, Ali-Seyed M, Wu Y, Bartholomeusz G, Hsu SC, Hung MC. Nuclear-cytoplasmic transport of EGFR involves receptor endocytosis, importin β1 and CRM1. J Cell Biochem 2006;98:1570–83.
[127] Giri DK, Ali-Seyed M, Li LY, Lee DF, Ling P, Bartholomeusz G, et al. Endosomal transport of ErbB-2: mechanism for nuclear entry of the cell surface receptor. Mol Cell Biol 2005;25:11005–18.
[128] Xu D, Farmer A, Chook YM. Recognition of nuclear targeting signals by Karyopherin-β proteins. Curr Opin Struct Biol 2010;20:782–90.
[129] Kuersten S, Ohno M, Mattaj IW. Nucleocytoplasmic transport: Ran, beta and beyond. Trends Cell Biol 2001;11:497–503.
[130] Hsu SC, Hung MC. Characterization of a novel tripartite nuclear localization sequence in the EGFR family. J Biol Chem 2007;282:10432–40.
[131] Wang SC, Hung MC. Nuclear translocation of the epidermal growth factor receptor family membrane tyrosine kinase receptors. Clin Cancer Res 2009;15:6484–9.
[132] Lin SY, Makino K, Xia W, Matin A, Wen Y, Kwong KY, et al. Nuclear localization of EGF receptor and its potential new role as a transcription factor. Nat Cell Biol 2001;3:802–8.

[133] Brand TM, Iida M, Luthar N, Wleklinski MJ, Starr MM, Wheeler DL. Mapping C-terminal transactivation domains of the nuclear HER family receptor tyrosine kinase HER3. PLoS One 2013;8:e71518.
[134] Napoli C, Giordano A, Casamassimi A, Pentimalli F, Ignarro LJ, De Nigris F. Directed in vivo angiogenesis assay and the study of systemic neoangiogenesis in cancer. Int J Cancer 2011;128:1505–8.
[135] Sardi SP, Murtie J, Koirala S, Patten BA, Corfas G. Presenilin-dependent ErbB4 nuclear signaling regulates the timing of astrogenesis in the developing brain. Cell 2006;127:185–97.
[136] Fox IJ, Kornblum HI. Developmental profile of ErbB receptors in murine central nervous system: implications for functional interactions. J Neurosci Res 2005;79:584–97.
[137] Li C, Iida M, Dunn EF, Ghia AJ, Wheeler DL. Nuclear EGFR contributes to acquired resistance to cetuximab. Oncogene 2009;28:3801–13.
[138] Brand TM, Dunn EF, Iida M, Myers RA, Kostopoulos KT, Li C, et al. Erlotinib is a viable treatment for tumors with acquired resistance to cetuximab. Cancer Biol Ther 2011;12:436–46.
[139] Schlessinger J, Lemmon MA. Nuclear signaling by receptor tyrosine kinases: the first robin of spring. Cell 2006;127:45–8.
[140] Jemal A, Bray F, Center MM, Ferlay J, Ward E, Forman D. Global cancer statistics. CA Cancer J Clin 2011;61:69–90.
[141] Siegel R, Naishadham D, Jemal A. Cancer statistics, 2013. CA Cancer J Clin 2013;63:11–30.
[142] Herbst RS, Heymach JV, Lippman SM. Lung cancer. N Engl J Med 2008;359:1367–80.
[143] Collins LG, Haines C, Perkel R, Enck RE. Lung cancer: diagnosis and management. Am Fam Physician 2007;75:56–63.
[144] Goldstraw P, Crowley J, Chansky K, Giroux DJ, Groome PA, Rami-Porta R, et al. The IASLC Lung Cancer Staging Project: proposals for the revision of the TNM stage groupings in the forthcoming (seventh) edition of the TNM classification of malignant tumours. J Thorac Oncol 2007;2:706–14. Erratum in: J Thorac Oncol 2007;2:985.
[145] Sandler A, Gray R, Perry MC, Brahmer J, Schiller JH, Dowlati A, et al. Paclitaxel–carboplatin alone or with bevacizumab for non-small-cell lung cancer. N Engl J Med 2006;355:2542–50.
[146] Chabner BA, Longo DL, editors. Cancer chemotherapy and biotherapy: principles and practice. 5th ed. Philadelphia: Lippincott Williams & Wilkins; 2011.
[147] Soria JC, Mauguen A, Reck M, Sandler AB, Saijo N, Johnson DH, et al. Systematic review and meta-analysis of randomised, phase II/III trials adding bevacizumab to platinum-based chemotherapy as first-line treatment in patients with advanced non-small-cell lung cancer. Ann Oncol 2013;24:20–30. Erratum in: Ann Oncol 2013;24:1133.
[148] Wang M, Thanou M. Targeting nanoparticles to cancer. Pharmacol Res 2010;62:90–9.
[149] Cataldo VD, Gibbons DL, Pérez-Soler R, Quintás-Cardama A. Treatment of non-small-cell lung cancer with erlotinib or gefitinib. N Engl J Med 2011;364:947–55.
[150] Cohen MH, Williams GA, Sridhara R, Chen G, McGuinn Jr WD, Morse D, et al. United States Food and Drug Administration drug approval summary: Gefitinib (ZD1839; Iressa) tablets. Clin Cancer Res 2004;10:1212–8.
[151] Bailey R, Kris M, Wolf M, et al. Gefitinib (Iressa, ZD 1839) monotherapy for pretreated advanced non-small cell lung cancer in IDEAL 1 and 2: tumor response is not clinically relevantly predictable from tumor EGFR membrane staining alone. Lung Cancer 2003;41:S71 [abstract O-242].
[152] Cohen MH, Johnson JR, Chen YF, Sridhara R, Pazdur R. FDA drug approval summary: erlotinib (Tarceva) tablets. Oncologist 2005;10:461–6.
[153] Liu HB, Wu Y, Lv TF, Yao YW, Xiao YY, Yuan DM, et al. Skin rash could predict the response to EGFR tyrosine kinase inhibitor and the prognosis for patients with non-small cell lung cancer: a systematic review and meta-analysis. PLoS One 2013;8:e55128.
[154] Lynch TJ, Bell DW, Sordella R, Gurubhagavatula S, Okimoto RA, Brannigan BW, et al. Activating mutations in the epidermal growth factor receptor underlying responsiveness of non-small-cell lung cancer to gefitinib. N Engl J Med 2004;350:2129–39.
[155] Paez JG, Jänne PA, Lee JC, Tracy S, Greulich H, Gabriel S, et al. EGFR mutations in lung cancer: correlation with clinical response to gefitinib therapy. Science 2004;304:1497–500.
[156] Pao W, Miller V, Zakowski M, Doherty J, Politi K, Sarkaria I, et al. EGF receptor gene mutations are common in lung cancers from never smokers and are associated with sensitivity of tumors to gefitinib and erlotinib. Proc Natl Acad Sci USA 2004;101:13306–11.
[157] Massarelli E, Johnson FM, Erickson HS, Wistuba II, Papadimitrakopoulou V. Uncommon epidermal growth factor receptor mutations in non-small cell lung cancer and their mechanisms of EGFR tyrosine kinase inhibitors sensitivity and resistance. Lung Cancer 2013;80:235–41.
[158] Pao W, Chmielecki J. Rational, biologically based treatment of EGFR-mutant non-small-cell lung cancer. Nat Rev Cancer 2010;10:760–74.
[159] Mok TS, Wu YL, Thongprasert S, Yang CH, Chu DT, Saijo N, et al. Gefitinib or carboplatin–paclitaxel in pulmonary adenocarcinoma. N Engl J Med 2009;361:947–57.
[160] Mitsudomi T, Morita S, Yatabe Y, Negoro S, Okamoto I, Tsurutani J, et al. Gefitinib versus cisplatin plus docetaxel in patients with non-small-cell lung cancer harbouring mutations of the epidermal growth factor receptor (WJTOG3405): an open label, randomised phase 3 trial. Lancet Oncol 2010;11:121–8.
[161] Rosell R, Moran T, Queralt C, Porta R, Cardenal F, Camps C, et al. Screening for epidermal growth factor receptor mutations in lung cancer. N Engl J Med 2009;361:958–67.
[162] Yun CH, Boggon TJ, Li Y, Woo MS, Greulich H, Meyerson M, et al. Structures of lung cancer-derived EGFR mutants and inhibitor complexes: mechanism of activation and insights into differential inhibitor sensitivity. Cancer Cell 2007;11:217–27.
[163] Cook PF, Cleland WW. Enzyme kinetics and mechanism. New York: Garland Science; 2007. p. 8.
[164] Red Brewer M, Yun CH, Lai D, Lemmon MA, Eck MJ, Pao W. Mechanism for activation of mutated epidermal growth factor receptors in lung cancer. Proc Natl Acad Sci USA 2013;110:E3595–604.
[165] Ward WH, Cook PN, Slater AM, Davies DH, Holdgate GA, Green LR. Epidermal growth factor receptor tyrosine kinase. Investigation of catalytic mechanism, structure-based searching and discovery of a potent inhibitor. Biochem Pharmacol 1994;48:659–66.
[166] Giard DJ, Aaronson SA, Todaro GJ, Arnstein P, Kersey JH, Dosik H, et al. In vitro cultivation of human tumors: establishment of cell lines derived from a series of solid tumors. J Natl Cancer Inst 1973;51:1417–23.
[167] Cook PF, Neville Jr ME, Vrana KE, Hartl FT, Roskoski Jr R. Adenosine cyclic 3′,5′-monophosphate dependent protein kinase: kinetic mechanism for the bovine skeletal muscle catalytic subunit. Biochemistry 1982;21:5794–9.
[168] Parast CV, Mroczkowski B, Pinko C, Misialek S, Khambatta G, Appelt K. Characterization and kinetic mechanism of catalytic domain of human vascular endothelial growth factor receptor-2 tyrosine kinase (VEGFR2 TK), a key enzyme in angiogenesis. Biochemistry 1998;37:16788–801.
[169] Wakeling AE, Barker AJ, Davies DH, Brown DS, Green LR, Cartlidge SA, et al. Specific inhibition of epidermal growth factor receptor tyrosine kinase by 4-anilinoquinazolines. Breast Cancer Res Treat 1996;38:67–73.
[170] Rewcastle GW, Denny WA, Bridges AJ, Zhou H, Cody DR, McMichael A, et al. Tyrosine kinase inhibitors. 5. Synthesis and structure–activity relationships for 4-[(phenylmethyl) amino]- and 4-(phenylamino)quinazolines as potent adenosine 5′-triphosphate binding site inhibitors of the tyrosine kinase domain of the epidermal growth factor receptor. J Med Chem 1995;38:3482–7.
[171] Barker AJ, Gibson KH, Grundy W, Godfrey AA, Barlow JJ, Healy MP, et al. Studies leading to the identification of ZD1839 (IRESSA): an orally active, selective epidermal growth factor receptor tyrosine kinase inhibitor targeted to the treatment of cancer. Bioorg Med Chem Lett 2001;11:1911–4.
[172] Moyer JD, Barbacci EG, Iwata KK, Arnold L, Boman B, Cunningham A, et al. Induction of apoptosis and cell cycle arrest by CP-358,774, an inhibitor of epidermal growth factor receptor tyrosine kinase. Cancer Res 1997;57:4838–48.
[173] Pollack VA, Savage DM, Baker DA, Tsaparikos KE, Sloan DE, Moyer JD, et al. Inhibition of epidermal growth factor receptor-associated tyrosine phosphorylation in human carcinomas with CP-358,774: dynamics of receptor inhibition in situ and antitumor effects in athymic mice. J Pharmacol Exp Ther 1999;291:739–48.
[174] Li D, Ambrogio L, Shimamura T, Kubo S, Takahashi M, Chirieac LR, et al. BIBW2992, an irreversible EGFR/HER2 inhibitor highly effective in preclinical lung cancer models. Oncogene 2008;27:4702–11.
[175] Solca F, Dahl G, Zoephel A, Bader G, Sanderson M, Klein C, et al. Target binding properties and cellular activity of afatinib (BIBW 2992), an irreversible ErbB family blocker. J Pharmacol Exp Ther 2012;343:342–50.
[176] Paz-Ares L, Soulières D, Melezínek I, Moecks J, Keil L, Mok T, et al. Clinical outcomes in non-small-cell lung cancer patients with EGFR mutations: pooled analysis. J Cell Mol Med 2010;14:51–69.
[177] Sequist LV, Waltman BA, Dias-Santagata D, Digumarthy S, Turke AB, Fidias P, et al. Genotypic and histological evolution of lung cancers acquiring resistance to EGFR inhibitors. Sci Trans Med 2011;3:75ra26.
[178] Yun CH, Mengwasser KE, Toms AV, Woo MS, Greulich H, Wong KK, et al. The T790M mutation in EGFR kinase causes drug resistance by increasing the affinity for ATP. Proc Natl Acad Sci USA 2008;105:2070–5.
[179] Roskoski Jr R. Anaplastic lymphoma kinase (ALK): structure, oncogenic activation, and pharmacological inhibition. Pharmacol Res 2013;68:68–94.
[180] Engelman JA, Zejnullahu K, Mitsudomi T, Song Y, Hyland C, Park JO, et al. MET amplification leads to gefitinib resistance in lung cancer by activating ERBB3 signaling. Science 2007;316:1039–43.
[181] Roskoski Jr R. The preclinical profile of crizotinib for the treatment of non-small-cell lung cancer and other neoplastic disorders. Expert Opin Drug Discov 2013;8:1165–79.
[182] Arcila ME, Chaft JE, Nafa K, Roy-Chowdhuri S, Lau C, Zaidinski M, et al. Prevalence, clinicopathologic associations, and molecular spectrum of ERBB2 (HER2) tyrosine kinase mutations in lung adenocarcinomas. Clin Cancer Res 2012;18:4910–8.
[183] Cappuzzo F, Bemis L, Varella-Garcia M. HER2 mutation and response to trastuzumab therapy in non-small-cell lung cancer. N Engl J Med 2006;354:2619–21.
[184] De Grève J, Teugels E, Geers C, Decoster L, Galdermans D, De Mey J, et al. Clinical activity of afatinib (BIBW 2992) in patients with lung adenocarcinoma with mutations in the kinase domain of HER2/neu. Lung Cancer 2012;76:123–7.
[185] Wittliff JL. Steroid-hormone receptors in breast cancer. Cancer 1984;53:630–43.
[186] Siegel R, DeSantis C, Virgo K, Stein K, Mariotto A, Smith T, et al. Cancer treatment and survivorship statistics, 2012. CA Cancer J Clin 2012;62:220–41. Erratum in: CA Cancer J Clin 2012;62:348.

[187] von Minckwitz G. Docetaxel/anthracycline combinations for breast cancer treatment. Expert Opin Pharmacother 2007;8:485–95.
[188] Xia W, Mullin RJ, Keith BR, Liu LH, Ma H, Rusnak DW, et al. Anti-tumor activity of GW572016: a dual tyrosine kinase inhibitor blocks EGF activation of EGFR/erbB2 and downstream Erk1/2 and AKT pathways. Oncogene 2002;21:6255–63.
[189] Geyer CE, Forster J, Lindquist D, Chan S, Romieu CG, Pienkowski T, et al. Lapatinib plus capecitabine for HER2-positive advanced breast cancer. N Engl J Med 2006;355:2733–43. Erratum in: N Engl J Med 2007;356:1487.
[190] Riemsma R, Forbes CA, Amonkar MM, Lykopoulos K, Diaz JR, Kleijnen J, et al. Systematic review of lapatinib in combination with letrozole compared with other first-line treatments for hormone receptor positive (HR+) and HER2+ advanced or metastatic breast cancer (MBC). Curr Med Res Opin 2012;28:1263–79.
[191] Rexer BN, Ghosh R, Narasanna A, Estrada MV, Chakrabarty A, Song Y, et al. Human breast cancer cells harboring a gatekeeper T798M mutation in HER2 overexpress EGFR ligands and are sensitive to dual inhibition of EGFR and HER2. Clin Cancer Res 2013;19:5390–401.
[192] Puglisi F, Minisini AM, De Angelis C, Arpino G. Overcoming treatment resistance in HER2-positive breast cancer: potential strategies. Drugs 2012;72:1175–93.
[193] Hudziak RM, Lewis GD, Winget M, Fendly BM, Shepard HM, Ullrich A. p185HER2 monoclonal antibody has antiproliferative effects *in vitro* and sensitizes human breast tumor cells to tumor necrosis factor. Mol Cell Biol 1989;9:1165–72.
[194] Carter P, Presta L, Gorman CM, Ridgway JB, Henner D, Wong WL, et al. Humanization of an anti-p185HER2 antibody for human cancer therapy. Proc Natl Acad Sci USA 1992;89:4285–9.
[195] Slamon DJ, Leyland-Jones B, Shak S, Fuchs H, Paton V, Bajamonde A, et al. Use of chemotherapy plus a monoclonal antibody against HER2 for metastatic breast cancer that overexpresses HER2. N Engl J Med 2001;344:783–92.
[196] Verma S, Ewer MS. Is cardiotoxicity being adequately assessed in current trials of cytotoxic and targeted agents in breast cancer? Ann Oncol 2011;22:1011–8.
[197] Baselga J, Albanell J, Molina MA, Arribas J. Mechanism of action of trastuzumab and scientific update. Semin Oncol 2001;28:4–11.
[198] Varchetta S, Gibelli N, Oliviero B, Nardini E, Gennari R, Gatti G, et al. Elements related to heterogeneity of antibody-dependent cell cytotoxicity in patients under trastuzumab therapy for primary operable breast cancer overexpressing Her2. Cancer Res 2007;67:11991–9.
[199] Sliwkowski MX, Mellman I. Antibody therapeutics in cancer. Science 2013;341:1192–8.
[200] Hudis CA. Trastuzumab – mechanism of action and use in clinical practice. N Engl J Med 2007;357:39–51.
[201] Shepard HM, Brdlik CM, Schreiber H. Signal integration: a framework for understanding the efficacy of therapeutics targeting the human EGFR family. J Clin Invest 2008;118:3574–81.
[202] Rexer BN, Arteaga CL. Intrinsic and acquired resistance to HER2-targeted therapies in HER2 gene-amplified breast cancer: mechanisms and clinical implications. Crit Rev Oncog 2012;17:1–16.
[203] Franklin MC, Carey KD, Vajdos FF, Leahy DJ, de Vos AM, Sliwkowski MX. Insights into ErbB signaling from the structure of the ErbB2-pertuzumab complex. Cancer Cell 2004;5:317–28.
[204] Baselga J, Cortés J, Kim SB, Im SA, Hegg R, Im YH, et al. Pertuzumab plus trastuzumab plus docetaxel for metastatic breast cancer. N Engl J Med 2012;366:109–19.
[205] Blumenthal GM, Scher NS, Cortazar P, Chattopadhyay S, Tang S, Song P, et al. First FDA approval of dual anti-HER2 regimen: pertuzumab in combination with trastuzumab and docetaxel for HER2-positive metastatic breast cancer. Clin Cancer Res 2013;19:4911–6.
[206] Agus DB, Akita RW, Fox WD, Lewis GD, Higgins B, Pisacane PI, et al. Targeting ligand-activated ErbB2 signaling inhibits breast and prostate tumor growth. Cancer Cell 2002;2:127–37.
[207] Adams CW, Allison DE, Flagella K, Presta L, Clarke J, Dybdal N, et al. Humanization of a recombinant monoclonal antibody to produce a therapeutic HER dimerization inhibitor, pertuzumab. Cancer Immunol Immunother 2006;55:717–27.
[208] Lewis Phillips GD, Li G, Dugger DL, Crocker LM, Parsons KL, Mai E, et al. Targeting HER2-positive breast cancer with trastuzumab-DM1, an antibody–cytotoxic drug conjugate. Cancer Res 2008;68:9280–90.
[209] Verma S, Miles D, Gianni L, Krop IE, Welslau M, Baselga J, et al. Trastuzumab emtansine for HER2-positive advanced breast cancer. N Engl J Med 2012;367:1783–91. Erratum in: N Engl J Med 2013;368:2442.
[210] LoRusso PM, Weiss D, Guardino E, Girish S, Sliwkowski MX. Trastuzumab emtansine: a unique antibody–drug conjugate in development for human epidermal growth factor receptor 2-positive cancer. Clin Cancer Res 2011;17:6437–47.
[211] Hurvitz SA, Dirix L, Kocsis J, Bianchi GV, Lu J, Vinholes J, et al. Phase II randomized study of trastuzumab emtansine versus trastuzumab plus docetaxel in patients with human epidermal growth factor receptor 2-positive metastatic breast cancer. J Clin Oncol 2013;31:1157–63.
[212] Bose R, Kavuri SM, Searleman AC, Shen W, Shen D, Koboldt DC, et al. Activating HER2 mutations in HER2 gene amplification negative breast cancer. Cancer Discov 2013;3:224–37.
[213] Roskoski Jr R. STI-571: an anticancer protein-tyrosine kinase inhibitor. Biochem Biophys Res Commun 2003;309:709–17.
[214] Miki Y, Swensen J, Shattuck-Eidens D, Futreal PA, Harshman K, Tavtigian S, et al. A strong candidate for the breast and ovarian cancer susceptibility gene *BRCA1*. Science 1994;266:66–71.
[215] Wooster R, Bignell G, Lancaster J, Swift S, Seal S, Mangion J, et al. Identification of the breast cancer susceptibility gene BRCA2. Nature 1995;378:789–92. Erratum in: Nature 1996;379:749.
[216] Wooster R, Weber BL. Breast and ovarian cancer. N Engl J Med 2003;348:2339–47.
[217] Roy R, Chun J, Powell SN. BRCA1 and BRCA2: different roles in a common pathway of genome protection. Nat Rev Cancer 2011;12:68–78.
[218] Weinberg RA. The biology of cancer. 2nd ed. New York: Garland Science; 2014. p. 550.
[219] Kauff ND, Satagopan JM, Robson ME, Scheuer L, Hensley M, Hudis CA, et al. Risk-reducing salpingo-oophorectomy in women with a *BRCA1* or *BRCA2* mutation. N Engl J Med 2002;346:1609–15.
[220] Rebbeck TR, Lynch HT, Neuhausen SL, Narod SA, Van't Veer L, Garber JE, et al. Prophylactic oophorectomy in carriers of *BRCA1* or *BRCA2* mutations. N Engl J Med 2002;346:1616–22.
[221] Rebbeck TR, Kauff ND, Domchek SM. Meta-analysis of risk reduction estimates associated with risk-reducing salpingo-oophorectomy in *BRCA1* or *BRCA2* mutation carriers. J Natl Cancer Inst 2009;101:80–7.
[222] Domchek SM, Friebel TM, Singer CF, Evans DG, Lynch HT, Isaacs C, et al. Association of risk-reducing surgery in *BRCA1* or *BRCA2* mutation carriers with cancer risk and mortality. J Am Med Assoc 2010;304:967–75.
[223] Narod SA. BRCA mutations in the management of breast cancer: the state of the art. Nat Rev Clin Oncol 2010;7:702–7.
[224] Phillips KA, Milne RL, Rookus MA, Daly MB, Antoniou AC, Peock S, et al. Tamoxifen and risk of contralateral breast cancer for *BRCA1* and *BRCA2* mutation carriers. J Clin Oncol 2013;31:3091–9.
[225] Foulkes WD, Metcalfe K, Sun P, Hanna WM, Lynch HT, Ghadirian P, et al. Estrogen receptor status in BRCA1- and BRCA2-related breast cancer: the influence of age, grade, and histological type. Clin Cancer Res 2004;10:2029–34.
[226] Lee J, Ou SH. Towards the goal of personalized medicine in gastric cancer – time to move beyond HER2 inhibition. Part I: Targeting receptor tyrosine kinase gene amplification. Discov Med 2013;15:333–41.
[227] Wöll E, Devries A, Eisterer W, Hejna M, Keil F, Stein H, et al. Chemotherapy in gastric cancer. Anticancer Res 2008;28(2B):1213–9.
[228] Bang YJ, Van Cutsem E, Feyereislova A, Chung HC, Shen L, Sawaki A, et al. Trastuzumab in combination with chemotherapy versus chemotherapy alone for treatment of HER2-positive advanced gastric or gastro-oesophageal junction cancer (ToGA): a phase 3, open-label, randomised controlled trial. Lancet 2010;376:687–97.
[229] Li S, Schmitz KR, Jeffrey PD, Wiltzius JJ, Kussie P, Ferguson KM. Structural basis for inhibition of the epidermal growth factor receptor by cetuximab. Cancer Cell 2005;7:301–11.
[230] Gill GN, Kawamoto T, Cochet C, Le A, Sato JD, Masui H, et al. Monoclonal anti-epidermal growth factor receptor antibodies which are inhibitors of epidermal growth factor binding and antagonists of epidermal growth factor binding and antagonists of epidermal growth factor-stimulated tyrosine protein kinase activity. J Biol Chem 1984;259:7755–60.
[231] Goldstein NI, Prewett M, Zuklys K, Rockwell P, Mendelsohn J. Biological efficacy of a chimeric antibody to the epidermal growth factor receptor in a human tumor xenograft model. Clin Cancer Res 1995;1:1311–8.
[232] Fan Z, Lu Y, Wu X, Mendelsohn J. Antibody-induced epidermal growth factor receptor dimerization mediates inhibition of autocrine proliferation of A431 squamous carcinoma cells. J Biol Chem 1994;269:27595–602.
[233] Saltz LB, Meropol NJ, Loehrer Sr PJ, Needle MN, Kopit J, Mayer RJ. Phase II trial of cetuximab in patients with refractory colorectal cancer that expresses the epidermal growth factor receptor. J Clin Oncol 2004;22:1201–8.
[234] Cunningham D, Humblet Y, Siena S, Khayat D, Bleiberg H, Santoro A, et al. Cetuximab monotherapy and cetuximab plus irinotecan in irinotecan-refractory metastatic colorectal cancer. N Engl J Med 2004;351:337–45.
[235] Chung KY, Shia J, Kemeny NE, Shah M, Schwartz GK, Tse A, et al. Cetuximab shows activity in colorectal cancer patients with tumors that do not express the epidermal growth factor receptor by immunohistochemistry. J Clin Oncol 2005;23:1803–10.
[236] Moroni M, Veronese S, Benvenuti S, Marrapese G, Sartore-Bianchi A, Di Nicolantonio F, et al. Gene copy number for epidermal growth factor receptor (EGFR) and clinical response to antiEGFR treatment in colorectal cancer: a cohort study. Lancet Oncol 2005;6:279–86.
[237] Van Cutsem E, Köhne CH, Hitre E, Zaluski J, Chang Chien CR, Makhson A, et al. Cetuximab and chemotherapy as initial treatment for metastatic colorectal cancer. N Engl J Med 2009;360:1408–17.
[238] Yang XD, Jia XC, Corvalan JR, Wang P, Davis CG. Development of ABX-EGF, a fully human anti-EGF receptor monoclonal antibody, for cancer therapy. Crit Rev Oncol Hematol 2001;38:17–23.
[239] Giusti RM, Shastri KA, Cohen MH, Keegan P, Pazdur R. FDA drug approval summary: panitumumab (Vectibix). Oncologist 2007;12:577–83.
[240] Köhne CH, Hofheinz R, Mineur L, Letocha H, Greil R, Thaler J, et al. First-line panitumumab plus irinotecan/5-fluorouracil/leucovorin treatment in patients with metastatic colorectal cancer. J Cancer Res Clin Oncol 2012;138:65–72.
[241] Douillard JY, Oliner KS, Siena S, Tabernero J, Burkes R, Barugel M, et al. Panitumumab-FOLFOX4 treatment and RAS mutations in colorectal cancer. N Engl J Med 2013;369:1023–34.

[242] Grothey A, Van Cutsem E, Sobrero A, Siena S, Falcone A, Ychou M, et al. Regorafenib monotherapy for previously treated metastatic colorectal cancer (CORRECT): an international, multicentre, randomised, placebo-controlled, phase 3 trial. Lancet 2013;381:303–12.
[243] Wilhelm SM, Dumas J, Adnane L, Lynch M, Carter CA, Schütz G, et al. Regorafenib (BAY 73-4506): a new oral multikinase inhibitor of angiogenic, stromal and oncogenic receptor tyrosine kinases with potent preclinical antitumor activity. Int J Cancer 2011;129:245–55.
[244] Festino L, Fabozzi A, Manzo A, Gambardella V, Martinelli E, Troiani T, et al. Critical appraisal of the use of regorafenib in the management of colorectal cancer. Cancer Manage Res 2013;5:49–55.
[245] Roskoski Jr R. Vascular endothelial growth factor (VEGF) signaling in tumor progression. Crit Rev Oncol Hematol 2007;62:179–213.
[246] Roskoski Jr R. Structure and regulation of Kit protein-tyrosine kinase – the stem cell factor receptor. Biochem Biophys Res Commun 2005;338:1307–15.
[247] Jaiswal BS, Kljavin NM, Stawiski EW, Chan E, Parikh C, Durinck S, et al. Oncogenic ERBB3 mutations in human cancers. Cancer Cell 2013;23:603–17.
[248] No authors listed. Cancer Biol Ther 2006;5:340–2.
[249] Cohen MH, Chen H, Shord S, Fuchs C, He K, Zhao H, et al. Approval summary: cetuximab in combination with cisplatin or carboplatin and 5-fluorouracil for the first-line treatment of patients with recurrent locoregional or metastatic squamous cell head and neck cancer. Oncologist 2013;18:460–6.
[250] Vaccaro V, Melisi D, Bria E, Cuppone F, Ciuffreda L, Pino MS, et al. Emerging pathways and future targets for the molecular therapy of pancreatic cancer. Expert Opin Ther Targets 2011;15:1183–96.
[251] Gillen S, Schuster T, Meyer Zum Büschenfelde C, Friess H, Kleeff J. Preoperative/neoadjuvant therapy in pancreatic cancer: a systematic review and meta-analysis of response and resection percentages. PLoS Med 2010;7:e1000267.
[252] Tamburrino A, Piro G, Carbone C, Tortora G, Melisi D. Mechanisms of resistance to chemotherapeutic and anti-angiogenic drugs as novel targets for pancreatic cancer therapy. Front Pharmacol 2013;4:56.
[253] Giuliani F, Di Maio M, Colucci G, Perrone F. Conventional chemotherapy of advanced pancreatic cancer. Curr Drug Targets 2012;13:795–801.
[254] Burris 3rd HA, Moore MJ, Andersen J, Green MR, Rothenberg ML, Modiano MR, et al. Improvements in survival and clinical benefit with gemcitabine as first-line therapy for patients with advanced pancreas cancer: a randomized trial. J Clin Oncol 1997;15:2403–13.
[255] Conroy T, Desseigne F, Ychou M, Bouché O, Guimbaud R, Bécouarn Y, et al. FOLFIRINOX versus gemcitabine for metastatic pancreatic cancer. N Engl J Med 2011;364:1817–25.
[256] Páez D, Labonte MJ, Lenz HJ. Pancreatic cancer: medical management (novel chemotherapeutics). Gastroenterol Clin North Am 2012;41:189–209.
[257] Ueda S, Ogata S, Tsuda H, Kawarabayashi N, Kimura M, Sugiura Y, et al. The correlation between cytoplasmic overexpression of epidermal growth factor receptor and tumor aggressiveness: poor prognosis in patients with pancreatic ductal adenocarcinoma. Pancreas 2004;29:e1–8.
[258] Ng SS, Tsao MS, Nicklee T, Hedley DW. Effects of the epidermal growth factor receptor inhibitor OSI-774, Tarceva, on downstream signaling pathways and apoptosis in human pancreatic adenocarcinoma. Mol Cancer Ther 2002;1:777–83.
[259] Moore MJ, Goldstein D, Hamm J, Figer A, Hecht JR, Gallinger S, et al. Erlotinib plus gemcitabine compared with gemcitabine alone in patients with advanced pancreatic cancer: a phase III trial of the National Cancer Institute of Canada Clinical Trials Group. J Clin Oncol 2007;25:1960–6.
[260] Van Cutsem E, Vervenne WL, Bennouna J, Humblet Y, Gill S, Van Laethem JL, et al. Phase III trial of bevacizumab in combination with gemcitabine and erlotinib in patients with metastatic pancreatic cancer. J Clin Oncol 2009;27:2231–7.
[261] Almoguera C, Shibata D, Forrester K, Martin J, Arnheim N, Perucho M. Most human carcinomas of the exocrine pancreas contain mutant c-K-*ras* genes. Cell 1988;53:549–54.
[262] Smit VT, Boot AJ, Smits AM, Fleuren GJ, Cornelisse CJ, Bos JL. KRAS codon 12 mutations occur very frequently in pancreatic adenocarcinomas. Nucleic Acids Res 1988;16:7773–82.
[263] Dolecek TA, Propp JM, Stroup NE, Kruchko C. CBTRUS statistical report: primary brain and central nervous system tumors diagnosed in the United States in 2005–2009. Neuro-oncol 2012;14:1–49. Erratum in: Neuro-Oncol 2013;15:646–7.
[264] Kamar FG, Posner JB. Brain metastases. Semin Neurol 2010;30:217–35.
[265] Vredenburgh JJ, Desjardins A, Herndon 2nd JE, Marcello J, Reardon DA, Quinn JA, et al. Bevacizumab plus irinotecan in recurrent glioblastoma multiforme. J Clin Oncol 2007;25:4722–9.
[266] Spasic M, Chow F, Tu C, Nagasawa DT, Yang I. Molecular characteristics and pathways of Avastin for the treatment of glioblastoma multiforme. Neurosurg Clin N Am 2012;23:417–27.
[267] Hatanpaa KJ, Burma S, Zhao D, Habib AA. Epidermal growth factor receptor in glioma: signal transduction, neuropathology, imaging, and radioresistance. Neoplasia 2010;12:675–84.
[268] Ekstrand AJ, James CD, Cavenee WK, Seliger B, Pettersson RF, Collins VP. Genes for epidermal growth factor receptor, transforming growth factor α, and epidermal growth factor and their expression in human gliomas *in vivo*. Cancer Res 1991;51:2164–72.
[269] Wong AJ, Ruppert JM, Bigner SH, Grzeschik CH, Humphrey PA, Bigner DS, et al. Structural alterations of the epidermal growth factor receptor gene in human gliomas. Proc Natl Acad Sci USA 1992;89:2965–9.
[270] Lipinski CA, Lombardo F, Dominy BW, Feeney PJ. Experimental and computational approaches to estimate solubility and permeability in drug discovery and development settings. Adv Drug Deliv Rev 2001;46:3–26.
[271] Rusnak DW, Lackey K, Affleck K, Wood ER, Alligood KJ, Rhodes N, et al. The effects of the novel, reversible epidermal growth factor receptor/ErbB-2 tyrosine kinase inhibitor, GW2016, on the growth of human normal and tumor-derived cell lines in vitro and in vivo. Mol Cancer Ther 2001;1:85–94.
[272] Arnott JA, Planey SL. The influence of lipophilicity in drug discovery and design. Expert Opin Drug Discov 2012;86(10):3–75.
[273] Smith GF. Medicinal chemistry by the numbers: the physicochemistry, thermodynamics and kinetics of modern drug design. Prog Med Chem 2009;48:1–29.
[274] Meanwell NA. Improving drug candidates by design: a focus on physicochemical properties as a means of improving compound disposition and safety. Chem Res Toxicol 2011;24:1420–56.
[275] Leeson PD, Springthorpe B. The influence of drug-like concepts on decision-making in medicinal chemistry. Nat Rev Drug Discov 2007;6:881–90.
[276] Bembenek SD, Tounge BA, Reynolds CH. Ligand efficiency and fragment-based drug discovery. Drug Discovery Today 2009;14:278–83.
[277] Gilman A. The initial clinical trial of nitrogen mustard. Am J Surg 1963;105:574–8.
[278] He K, Iyer KR, Hayes RN, Sinz MW, Woolf TF, Hollenberg PF. Inactivation of cytochrome P450 3A4 by bergamottin, a component of grapefruit juice. Chem Res Toxicol 1998;11:252–9.
[279] Sevrioukova IF, Poulos TL. Understanding the mechanism of cytochrome P450 3A4: recent advances and remaining problems. Dalton Trans 2013;42:3116–26.
[280] Kato M. Intestinal first-pass metabolism of CYP3A4 substrates. Drug Metab Pharmacokinet 2008;23:87–94.
[281] Paine MF, Widmer WW, Hart HL, Pusek SN, Beavers KL, Criss AB, et al. A furanocoumarin-free grapefruit juice establishes furanocoumarins as the mediators of the grapefruit juice–felodipine interaction. Am J Clin Nutr 2006;83:1097–105. Erratum in: Am J Clin Nutr 2006;84:264.
[282] Lilja JJ, Neuvonen M, Neuvonen PJ. Effects of regular consumption of grapefruit juice on the pharmacokinetics of simvastatin. Br J Clin Pharmacol 2004;58:56–60.
[283] Ma YT, Cullen MH, Hussain SA. Biology of germ cell tumors. Hematol Oncol Clin North Am 2011;25:457–71.
[284] Saxman SB, Finch D, Gonin R, Einhorn LH. Long-term follow-up of a phase III study of three versus four cycles of bleomycin, etoposide, and cisplatin in favorable-prognosis germ-cell tumors: the Indiana University experience. J Clin Oncol 1998;16:702–6.
[285] Küppers R, Engert A, Hansmann ML. Hodgkin lymphoma. J Clin Invest 2012;122:3439–47.
[286] Advani R. Optimal therapy of advanced Hodgkin lymphoma. Hematology (Am Soc Hematol Educ Program) 2011;2011:310–6.
[287] Horowitz NS, Goldstein DP, Berkowitz RS. Management of gestational trophoblastic neoplasia. Semin Oncol 2009;36:181–9.
[288] Goldstein DP, Berkowitz RS. Current management of gestational trophoblastic neoplasia. Hematol Oncol Clin North Am 2012;26:111–31.
[289] Deng L, Zhang J, Wu T, Lawrie TA. Combination chemotherapy for primary treatment of high-risk gestational trophoblastic tumour. Cochrane Database Syst Rev 2013;1:CD005196.
[290] Winer E, Gralow J, Diller L, Karlan B, Loehrer P, Pierce L, et al. Clinical cancer advances 2008: major research advances in cancer treatment, prevention, and screening – a report from the American Society of Clinical Oncology. J Clin Oncol 2009;27:812–26. Erratum in: J Clin Oncol 2009;27:3070–1.
[291] Khorashad JS, Deininger MW. Selection of therapy: rational decisions based on molecular events. Hematol Oncol Clin North Am 2011;25:1009–23.
[292] Kantarjian H, O'Brien S. The chronic leukemias. In: Goldman L, Schafer A, Arend W, editors. Cecil medicine. 24th ed. Philadelphia: Elsevier Saunders; 2012. p. 1209–18.
[293] Hanahan D, Weinberg RA. Hallmarks of cancer: the next generation. Cell 2011;144:646–74.
[294] Flaherty KT, Infante JR, Daud A, Gonzalez R, Kefford RF, Sosman J, et al. Combined BRAF and MEK inhibition in melanoma with BRAF V600 mutations. N Engl J Med 2012;367:1694–703.
[295] Colombo M, Corsi F, Foschi D, Mazzantini E, Mazzucchelli S, Morasso C, et al. HER2 targeting as a two-sided strategy for breast cancer diagnosis and treatment: outlook and recent implications in nanomedical approaches. Pharmacol Res 2010;62:150–65.
[296] Knight ZA, Lin H, Shokat KM. Targeting the cancer kinome through polypharmacology. Nat Rev Cancer 2010;10:130–7.
[297] Kuczynski EA, Sargent DJ, Grothey A, Kerbel RS. Drug rechallenge and treatment beyond progression-implications for drug resistance. Nat Rev Clin Oncol 2013;10:571–87.
[298] Kurata T, Tamura K, Kaneda H, Nogami T, Uejima H, Asai Go Go, et al. Effect of re-treatment with gefitinib ('Iressa', ZD1839) after acquisition of resistance. Ann Oncol 2004;15:173–4.
[299] Yano S, Nakataki E, Ohtsuka S, Inayama M, Tomimoto H, Edakuni N, et al. Retreatment of lung adenocarcinoma patients with gefitinib who had experienced favorable results from their initial treatment with this selective epidermal growth factor receptor inhibitor: a report of three cases. Oncol Res 2005;15:107–11.
[300] Wong AS, Seto KY, Chin TM, Soo RA. Lung cancer response to gefitinib, then erlotinib, then gefitinib again. J Thorac Oncol 2008;3:1077–8.

[301] Escudier B, Szczylik C, Porta C, Gore M. Treatment selection in metastatic renal cell carcinoma: expert consensus. Nat Rev Clin Oncol 2012;9:327–37.
[302] Chaft JE, Oxnard GR, Sima CS, Kris MG, Miller VA, Riely GJ. Disease flare after tyrosine kinase inhibitor discontinuation in patients with EGFR-mutant lung cancer and acquired resistance to erlotinib or gefitinib: implications for clinical trial design. Clin Cancer Res 2011;17:6298–303.
[303] Gainor JF, Shaw AT. Emerging paradigms in the development of resistance to tyrosine kinase inhibitors in lung cancer. J Clin Oncol 2013;31:3987–96.
[304] Santini D, Vincenzi B, Addeo R, Garufi C, Masi G, Scartozzi M, et al. Cetuximab rechallenge in metastatic colorectal cancer patients: how to come away from acquired resistance? Ann Oncol 2012;23:2313–8.
[305] Kantarjian HM, Fojo T, Mathisen M, Zwelling LA. Cancer drugs in the United States: justum pretium – the just price. J Clin Oncol 2013;31:3600–4.